QUANTIFYING THE BENEFIT AND MEASURING RESIDUAL UNCERTAINTIES OF MLC TRACKING DURING THE FIRST CLINICAL IMPLEMENTATION FOR LUNG CANCER RADIATION THERAPY

VINCENT CHARLES GÉRARD CAILLET

A thesis submitted to fulfil requirements
for the degree of Doctor of Philosophy

ACRF IMAGE X INSTITUTE
FACULTY OF MEDICINE AND HEALTH
UNIVERSITY OF SYDNEY December 2020

THE UNIVERSITY OF SYDNEY

« L’organisation, c’est la clé de la réussite. »
— Mes parents

Declaration of originality

I, Vincent Caillet, declare that this thesis is my own work and has not been submitted in any form for another degree or diploma at any university or other institute of tertiary education. I certify that the intellectual content of this thesis is the product of my own work and that all the assistance received in preparing this thesis and sources have been acknowledged.

13th of Decembre 2020

Sydney, Australia

Acknowledgements

It is with real gratitude that I would like to express my sincere appreciation to both my supervisors Paul Keall and Jeremy Booth for their continuous support during this PhD candidature. Paul, you have shown enormous patience, motivation and managed to successfully keep me enthusiastic for the past five years. Jeremy, it has been a pleasure to share a floor with you at RNSH for so many years. Your support and clinical knowledge managed to help me work on the LIGHT SABR clinical trial.

To the physicists, therapists, oncologists, and clinical trials staff of the Northern Sydney Cancer Centre, thank you all for welcoming me, for sharing your time and knowledge and for being patient with me. Your department is a wonderful environment to learn and work in and I am so grateful to have been part of a team which can make such great things happen. Special thanks to Adam Briggs and Nicholas Hardcastle for all those late evenings!

The ACRF Image X institute constitutes the best research environment that we wish to have as a PhD student. The women and men in this team are among the smartest and more generous colleagues I have ever worked with. You will all be missed.

No PhD can be conducted properly without its dose of caffeine, and beers. For that matter, thanks to Natasha Morton, Tess Reynolds, Brendan Whelan and many more, who have made sure that every single day requires a coffee, and that every Tuesday evening must be celebrated at the Flodge. I'm so glad you were all around!

Thanks also to the Prospection team for their moral support and encouragements, and allowing me to stay in the office to work on this thesis. Many thanks to Prab for his support.

Un grand merci à mes parents, sœur et frère de m'avoir toujours soutenu pendant cette thèse.

Last, but obviously not least. There would not be a PhD candidature without the immense help from Gema, my second half, and partner in crime. Thank you believing in me, and for keeping me afloat despite the pressure and work. It is a journey that is as much yours as mine. Our beautiful daughter was born exactly two years ago, and I hope she will also one day decide to take on the path of a PhD.

Vincent
Dec 2020

Abstract

Radiation therapy is a cancer treatment that involves the use of radiation to kill cancer cells and shrink the tumour. One of the main issues that this field is facing is that of respiratory-induced tumour motion. In the presence of motion, the radiation beam can miss the tumour and instead irradiate healthy tissues leading to radiation toxicities.

With the advent of fast computing technology, it is now feasible to treat cancer patients in a safer way, by tracking the position of their tumour and adapting the radiation beam in real-time, ensuring a better irradiation of the tumour while sparing surrounding organs.

This thesis presents the developments of frontier technology for guided lung cancer radiation therapy. More specifically, this research details the first clinical use of multi-leaf collimator (MLC) tracking for lung cancer patients, a technology that can track and adapt to the patient's breathing pattern during the irradiation. To demonstrate the feasibility and the benefits of MLC tracking, a clinical trial involving a cohort of patients diagnosed with lung cancer was conducted. This clinical trial, called LIGHT SABR, provided the context to conduct three studies as the material of this thesis.

The purpose of the first study was to evaluate the potential dosimetric impact of MLC tracking in a pre-clinical study. This study positively concluded that MLC tracking under electromagnetic guidance was feasible and safe to implement in a clinical scenario with real patients. With the positive outcomes of that pre-clinical study, the clinical trial was initiated, and seventeen patients were treated with MLC tracking with implanted electromagnetic transponders.

The second study was run post-trial and computed the geometric accuracy of the overall MLC tracking system for each source of uncertainties present at treatment. It was found that uncertainties due to MLC tracking were less than 3 mm in all directions, which brings confidence that MLC tracking for lung tumours is within acceptable uncertainties. This study brought the question of whether a faster MLC tracking optimising algorithm would be more efficient, which led to the third study.

The third study focused on understanding the output performances of two leaf-fitting algorithms, *in silico* and experimentally using a moving platform on a linear accelerator. Despite one of the algorithms being significantly faster at computing the leaves position, the results of this study showed non-significant differences in exposure errors. Instead, the MLC tracking performance is weighted towards the plan complexity and hardware limitations of the linear accelerator.

The major finding of this work is that MLC tracking can be implemented in a safe clinical environment for patients with fast and erratic tumour motion patterns.

List of publications

Chapter 3 is a review article for which I am the primary author:

> **Caillet, Vincent**, Jeremy T. Booth, and Paul Keall. "IGRT and motion management during lung SBRT delivery." *Physica Medica* 44 (2017): 113-122.

The work presented in this thesis has led to the following three publications in peer-reviewed international journals and form the major composition of **Chapter 4**, **Chapter 5,** and **Chapter 6**:

> **Caillet, Vincent**, Paul J. Keall, Emma Colvill, Nicholas Hardcastle, Ricky O'Brien, Kathryn Szymura, and Jeremy T. Booth. "MLC tracking for lung SABR reduces planning target volumes and dose to organs at risk." *Radiotherapy and Oncology* 124, no. 1 (2017): 18-24.

> **Caillet, Vincent,** Benjamin Zwan, Adam Briggs, Nicholas Hardcastle, Kathryn Szymura, Alexander Podreka, Ricky T O'Brien et al. "Geometric uncertainty analysis of MLC tracking for lung SABR." *Physics in Medicine & Biology* (2020).

> **Caillet, Vincent**, Ricky O'Brien, Douglas Moore, Per Poulsen, Tobias Pommer, Emma Colvill, Amit Sawant, Jeremy Booth, and Paul Keall. "*In silico* and experimental evaluation of two leaf-fitting algorithms for MLC tracking based on exposure error and plan complexity." *Medical physics* 46, no. 4 (2019): 1814-1820.

The following work has been published in a peer-reviewed international journal and is relevant to the body of work completed during this thesis. It appears as an appendix and I am second author:

> Booth, Jeremy, **Vincent Caillet**, Nicholas Hardcastle, Ricky O'Brien, Kathryn Szymura, Charlene Crasta, Benjamin Harris, Carol Haddad, Thomas Eade, and Paul J. Keall. "The first patient treatment of electromagnetic-guided real time adaptive radiotherapy using MLC tracking for lung SABR." *Radiotherapy and Oncology* 121, no. 1 (2016): 19-25.

The Statement of Authors' contribution can be read in the **Appendix II.**

The following works have been published during my PhD candidature that I have contributed to, listed in order of production:

Keall Paul, Jin. A. Ng, **Vincent Caillet**, Chen-Yu. Huang, Emma Colvill, Emma Simpson, Per R. Poulsen, Andrew Kneebone, Thomas Eade, and Jeremy Booth. "Sub-mm accuracy results measured from the first prospective clinical trial of a novel real-time IGRT system, Kilovoltage Intrafraction Monitoring (KIM)." *International Journal of Radiation Oncology• Biology• Physics* 93, no. 3 (2015): S192-S193.

Keall, Paul J., Jin Aun Ng, Prabhjot Juneja, Ricky T. O'Brien, Chen-Yu Huang, Emma Colvill, **Vincent Caillet** et al. "Real-time 3D image guidance using a standard LINAC: measured motion, accuracy, and precision of the first prospective clinical trial of kilovoltage intrafraction monitoring–guided gating for prostate cancer radiation therapy." *International Journal of Radiation Oncology* Biology* Physics* 94, no. 5 (2016): 1015-1021.

Juneja, Prabhjot, **Vincent Caillet**, Tom Shaw, Judith Maryland, and Jeremy T. Booth. "Kilovoltage intrafraction monitoring for real-time image guided adaptive radiotherapy reduces total dose for lung SABR." *Radiotherapy and Oncology* 121, no. 1 (2016): 15-18.

Shieh, Chun-Chien, **Vincent Caillet**, Michelle Dunbar, Paul J. Keall, Jeremy T. Booth, Nicholas Hardcastle, Carol Haddad, Thomas Eade, and Ilana Feain. "A Bayesian approach for three-dimensional markerless tumor tracking using kV imaging during lung radiotherapy." *Physics in Medicine & Biology* 62, no. 8 (2017): 3065.

Kim Jung-Ha., Doan Trang Nguyen, Chen Yu Huang, Todsaporn Fuangrod, **Vincent Caillet**, Ricky O'Brien, Per Poulsen, Jeremy Booth, and Paul Keall. "Quantifying the accuracy and precision of a novel real-time 6 degree-of-freedom kilovoltage intrafraction monitoring (KIM) target tracking system." *Physics in Medicine & Biology* 62, no. 14 (2017): 5744.

Keall, Paul J., Emma Colvill, Ricky O'Brien, **Vincent Caillet**, Thomas Eade, Andrew Kneebone, George Hruby et al. "Electromagnetic-guided MLC tracking radiation therapy for prostate cancer patients: Prospective clinical trial results." *International Journal of Radiation Oncology* Biology* Physics* 101, no. 2 (2018): 387-395.

Montanaro Tim, Doan Trang Nguyen, Paul J. Keall, Jeremy Booth, **Vincent Caillet**, Thomas Eade, Carol Haddad, and Chun-Chien Shieh. "A comparison of gantry-mounted x-ray-based real-time target tracking methods." *Medical physics* 45, no. 3 (2018): 1222-1232.

Geimer Tobias, Paul Keall, Katharina Breininger, **Vincent Caillet**, Michelle Dunbar, Christoph Bert, and Andreas Maier. "Decoupling Respiratory and Angular Variation in Rotational X-ray Scans Using a Prior Bilinear Model." In *German Conference on Pattern Recognition*, pp. 583-594. Springer, Cham, 2018.

Duncan Mitchell, Matthew K. Newall, **Vincent Caillet**, Jeremy T. Booth, Paul J. Keall, Michael Lerch, Vladimir Perevertaylo, Anatoly B. Rosenfeld, and Marco Petasecca. "Real-time high spatial resolution dose verification in stereotactic motion adaptive arc radiotherapy." *Journal of applied clinical medical physics* 19, no. 4 (2018): 173-184.

Lydiard Suzanne, **Vincent Caillet**, Svenja Ipsen, Ricky O'Brien, Oliver Blanck, Per Rugaard Poulsen, Jeremy Booth, and Paul Keall. "Investigating multi-leaf collimator tracking in stereotactic arrhythmic radioablation treatments for atrial fibrillation." *Physics in Medicine & Biology* 63, no. 19 (2018): 195008.

Steiner Elisabeth, Chun-Chien Shieh, **Vincent Caillet**, Jeremy Booth, Nicholas Hardcastle, Adam Briggs, Dasantha Jayamanne, Carol Haddad, Thomas Eade, and Paul Keall. "4-Dimensional Cone Beam Computed Tomography–Measured Target Motion Underrepresents Actual Motion." *International Journal of Radiation Oncology* Biology* Physics* 102, no. 4 (2018): 932-940.

Nguyen Doan Trang, Jeremy T. Booth, **Vincent Caillet**, Nicholas Hardcastle, Adam Briggs, Carol Haddad, Thomas Eade, Ricky O'Brien, and Paul J. Keall. "An augmented correlation framework for the estimation of tumour translational and rotational motion during external beam radiotherapy treatments using intermittent monoscopic x-ray imaging and an external respiratory signal." *Physics in Medicine & Biology* 63, no. 20 (2018): 205003.

Alnaghy Saree, Andre Kyme, **Vincent Caillet**, Doan Trang Nguyen, Ricky O'Brien, Jeremy T. Booth, and Paul J. Keall. "A six-degree-of-freedom robotic motion system for quality assurance of real-time image-guided radiotherapy." *Physics in Medicine & Biology* 64, no. 10 (2019): 105021.

Steiner Elisabeth, Chun-Chien Shieh, **Vincent Caillet**, Jeremy Booth, Ricky O'Brien, Adam Briggs, Nicholas Hardcastle et al. "Both four-dimensional computed tomography and four-dimensional cone beam computed tomography under-predict lung target motion during radiotherapy." *Radiotherapy and Oncology* 135 (2019): 65-73.

Booth, Jeremy, **Vincent Caillet**, Adam Briggs, Nicholas Hardcastle, Georgios Angelis, Dasantha Jayamanne, Meegan Shepard et al. "MLC Tracking for Lung SABR is Feasible, Efficient and Delivers High-Precision Target dose and Lower Normal Tissue Dose." *Radiotherapy and Oncology* (2020).

Zwan, Benjamin, **Vincent Caillet**, Jeremy T. Booth, Emma Colvill, Todsaporn Fuangrod, Ricky O'Brien, Adam Briggs, Daryl J. O'Connor, Paul J. Keall, Peter B. Greer "Toward real-time verification for MLC tracking treatments using time-resolved EPID imaging." *Medical Physics* (2020).

List of oral presentations

The scientific presentations listed below have been presented in conferences by me, as findings directly arising from or related to this thesis:

AAPM (American Association of Physicists in Medicine):

Denver, AAPM 59th, 2017 – Best in Physics (Therapy)

Caillet, Vincent, B. Zwan, N. Hardcastle, Ricky O. Brien, P. Poulsen, P. Greer, P. Keall, and J. Booth. "Best in Physics (Therapy): MLC Tracking for Lung SABR Reduces the Dose to Organs-at-risk and Improves the Geometric Targeting of the Tumour: mo-de-fs1-07." Medical Physics 44, no. 6 (2017): 3061.

Nashville, AAPM 60th, 2018

Caillet, Vincent, B. Swan, A. Briggs, N. Hardcastle, D. Jayamanne, T. Eade, P. Greer, R. O'Brien, P. Keall, and J. Booth. "Method to Quantify the PTV Margin Required for Patients Treated with MLC Tracking for Lung SABR." In MEDICAL PHYSICS, vol. 45, no. 6, pp. E663-E663. 111 RIVER ST, HOBOKEN 07030-5774, NJ USA: WILEY, 2018.

EPSM (Engineering and Physical Sciences in Medicine)

Wellington, 2015

Caillet, Vincent, Paul J. Keall, Emma Colvill, Nicholas Hardcastle, Ricky O'Brien, Kathryn Szymura and Jeremy T. Booth (2015). "MLC tracking during lung SABR**."**

Sydney, 2016

Caillet, Vincent, Paul J. Keall, Emma Colvill, Nicholas Hardcastle, Ricky O'Brien, Kathryn Szymura and Jeremy T. Booth (2016). "MLC tracking enables dose reduction to OARs during lung cancer SABR."

Caillet, Vincent, Jung-Ha KIM, Nicholas Hardcastle, Jeremy T. Booth, Paul J. Keall (2016). "Quantification of lung tumour translation and rotation during lung SABR."

Acronyms

4D	Four-dimensional
CBCT	Cone-beam Computed Tomography
CT	Computed Tomography
CTV	Clinical Target Volume
EPID	Electronic Portal Imaging Device
FMEA	Failure Mode and Effects Analysis
GTV	Gross Tumour Volume
IGRT	Image Guided Radiation Therapy
ITV	Internal Target Volume
kV	Kilovoltage
LIGHT SABR	Lung Intensity Guided Hypofractioned Therapy for Stereotactic Ablative Radiotherapy
Linac	Linear accelerator
MLC	Multi-Leaf Collimator
MRI	Magnetic Resonance Imaging
MV	Megavoltage
NSCLC	Non-Small Cell Lung Carcinoma
OAR	Organ-At-Risk
PET	Positron Emission Tomography
PTV	Planning Treatment Volume
QA	Quality Assurance
RPM	Real-time Position Management
SABR	Stereotactic Ablative Radiotherapy
SBRT	Stereotactic Body Radiation Therapy
TPS	Treatment Planning System
VMAT	Volumetric Modulated Arc Therapy

Contents

CHAPTER 01

Overview of this thesis

Radiation therapy is a treatment path for patients diagnosed with cancer. The patient is laid on a table in a room where radiation is then delivered to the tumour using a linear accelerator. To maximize the chances of the radiation beam hitting the target, it is important that the patient remains still underneath the radiation beam for the radiation dose to be delivered according to plan.

For patients diagnosed with lung cancer, motion can make irradiating cancer cells challenging. People are living organisms, and nobody is ever still. The heart is beating, intestines are processing food while blood is rushing to every part of the body. More importantly patients are breathing, their lungs are squeezing large volumes of air in and out of the body, causing internal displacement that is quite challenging for thoracic radiotherapy. If respiratory-induced tumour motion is not accounted for, the planned radiation dose is smeared out and displaced away from the tumour towards vital organs. This can result in undesirable doses delivered to healthy tissues leading to radiation toxicities. Possible technical solutions to prevent radiation toxicity include tracking the tumour position during treatment and shifting the radiation beam in real time.

The purpose of this research is to contribute to the development of radiation therapy by tackling the issue of internal motion for patients diagnosed with lung cancer. In this research, I detail the first clinical use of multi-leaf collimator (MLC) tracking for lung cancer patients with the purpose of evaluating the clinical feasibility of a technology that can track and adapt to the patient's breathing pattern during the irradiation.

The clinical realisation of MLC tracking for lung cancer is the product of strong collaborations between Royal North Shore hospital and the ACRF Image X institute at the University of Sydney with support from Varian Medical Systems. This collaboration led to the LIGHT SABR clinical trial. My involvement in this clinical trial lasted four years, as the main technical scientist involved in the safe and efficient clinical implementation, treatment, and post-treatment analysis of each of the seventeen patients in this clinical trial.

Chapter 2 provides general knowledge of radiation therapy for lung cancer, detailing the various challenges that tumour motion poses and how MLC tracking can solve these challenges. It is followed in **Chapter 3** by a review article, focusing on the use of Image Guided Radiation Therapy

(IGRT) for lung cancer.

Prior to the clinical trial launch, a simulation study was conducted on a linear accelerator to test MLC tracking in a real clinical scenario with a moving platform as a substitute for a real patient. This simulation study is outlined in **Chapter 4** and provides justification for the clinical use of MLC tracking.

A culmination of this project is detailed in **Chapter 5**, where a thorough analysis of MLC tracking accuracy for seventeen patients treated in the LIGHT SABR clinical trial was made to understand and compute the geometric impact of each uncertainty during treatment.

In **Chapter 6**, the output of two different MLC tracking algorithms were compared both *in silico* and under clinical conditions on a linear accelerator. The outcome of this work provided an understanding of the impact of a fast optimization algorithm for hypothetical treatment delivery.

Chapter 7 provides a summary of the project findings and includes a discussion with possible future directions for MLC tracking and motion management.

Appendix 1 details the first patient to be treated with the technology described in this thesis.

CHAPTER 02

Literature Review

This literature review provides the reader with an introductory reading in the field of medical physics. The main intent is to highlight the motivation for the implementation of a novel radiation treatment capable of accounting for tumour motion in lung cancer patients. First, this review emphasizes the importance and impact of lung cancer in our society and lists the available treatment options. Next, this review details the principles of a linear accelerator, planning techniques and treatment delivery. Following this, the importance of tumour motion in radiotherapy is described as well as its potential impact on the quality of the treatment. Finally, this literature review concludes with the motivation of this work and the compelling need for real-time tumour tracking in lung radiotherapy. **Chapter 3** tackles, in more depth, the options to correct for motion that can be realized with image-guided radiation therapy (IGRT) and motion management devices.

Lung cancer

Lung cancer and its burden on society

Lung cancer is the leading cause of cancer worldwide and accounts for 20% of all cancer deaths [1]. Its burden on society is as much psychological as financial with almost 10 million related deaths in 2018 [2] associated with the economic impact of $188 billion worldwide in 2010 [3]. In Australia, it is the fifth most common cancer diagnosis and is responsible for almost one in five cancer deaths [4]. While a large proportion of lung cancer cases can be associated with long-term tobacco smoking, about 10-15% of the cases originate from other factors such as genetic predisposition, environment exposure, or biological susceptibility [5, 6]. For that matter, lung cancer has a poor prognosis where over half of people diagnosed with the disease will die within a year of diagnosis [7].

Lung cancer treatment

Lung cancer, also known as lung carcinoma, is a malignant disease defined by uncontrolled cell growth within lung tissue. Tumour growth can spread beyond the lungs and move to other parts of the body, known as metastases. The two most common types of lung cancer are small-cell lung carcinoma (SCLC) and non-small cell lung carcinoma (NSCLC). NSCLC accounts for approximately 85% of all lung cancer.

Historically, surgery was the most common treatment for lung cancer, with substantially higher survival rates than radiotherapy [8], particularly for younger populations [9]. For advanced lung cancer cases, surgery was followed by adjuvant chemotherapy providing a 4-5% increase in 5-year overall survival [10]. An important emerging treatment is immunotherapy, which stimulates the patient's own immune system to recognize and destroy the cancerous cells. Immunotherapy has shown encouraging outcomes in Australia [11], and is currently indicated for advanced lung cancer. At present, radiation therapy for lung cancer is one of the most effective and least invasive treatment modalities. Initially, it emerged as a low comorbidity alternative of surgery and has been increasingly relied upon for the last decade [12].

Recent advances in technology and computing power have made radiation therapy an accepted and reliable treatment for early stage NSCLC [13-15]. It does not require surgery and has shown encouraging outcomes especially for patients treated with Stereotactic Ablative Radiotherapy (SABR), with similar rates of local recurrence and disease-specific survival to other treatment modalities [16, 17]. It is estimated that approximately 32% of all lung cancer patients will receive radiotherapy over the course of their treatment, accounting for 5% of the total cost of cancer care [17].

The focus of this thesis is on radiotherapy for patients with lung cancer.

Principles of radiotherapy

External beam radiotherapy

The main goal of radiotherapy is to irradiate tumour cells and deprive them of their multiplicative potential. The radiation used is *ionizing* which means that it forms electrically charged particles with the potential of single or double breaking the strand of DNA as it passes through the human body. This DNA break causes genetic mutations within the cell leading to its death. One factor that indicates the objective of the radiotherapy treatment is reflected by the amount of absorbed dose to the tumour and the sparing of the healthy tissues surrounding the tumour.

The underlying mechanism of radiotherapy relies on radiobiological traits that allow healthy cells to repair at a faster rate than cancerous cells post-irradiation. These differences in radiobiological properties between tumour and healthy cells leads to the use of fractionated treatment, whereby the radiation is delivered over multiple days or weeks, allowing the healthy tissues to repair before the next treatment fraction.

Advancements in technology have allowed the accuracy and reproducibility of radiotherapy treatment to improve. As such, the amount of radiation delivered per fraction has increased and the number of total fractions has decreased, leading to the widespread use of *hypofractionated* treatment. Stereotactic Ablative Radiotherapy (SABR) delivers an ablative treatment in an extreme hypofractionated scheme with high biological effectiveness, tumour local control and low complications [18]. Advantages of SABR over conventional fractions are multiple, such as a considerable shortened treatment length which in return improves the overall patients' quality of life [19].

Linear accelerator

Linear accelerators or *linacs*, as shown in **Figure 1,** provide the radiation used for cancer treatment. The linear accelerator accelerates electrons using an alternating microwave field. These electrons either pass through a scatter foil and exit the machine as an electron beam or hit a high Z target that creates a type of photon radiation known as *bremsstrahlung*.

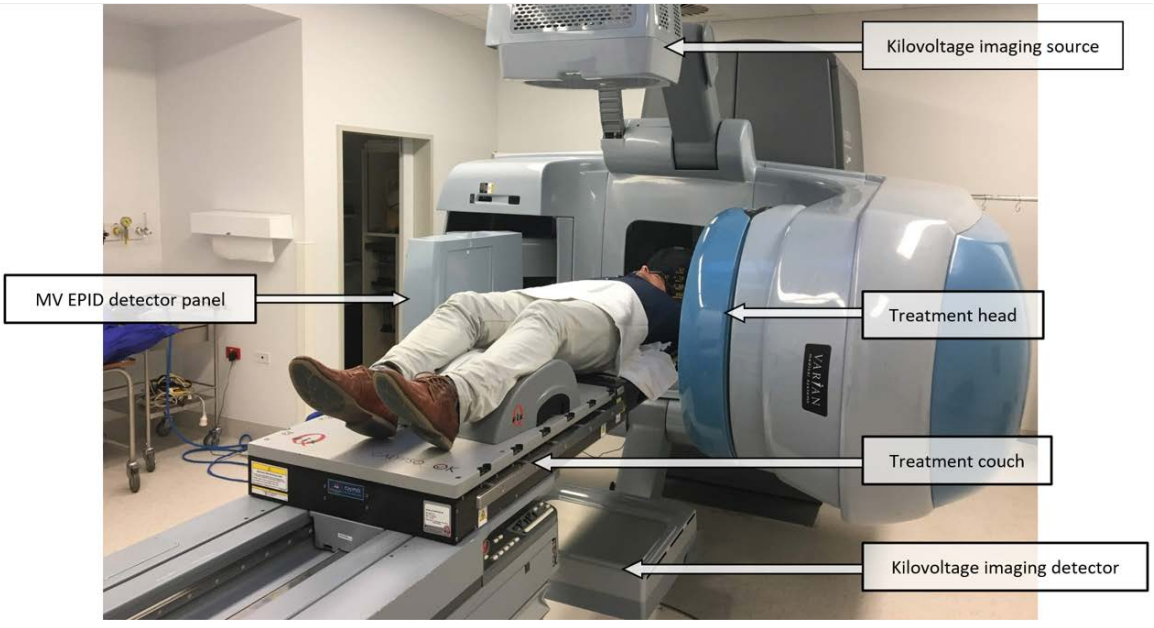

Figure 1. Varian linear accelerator with a treatment couch, EPID and kilovoltage imaging detector and source.

Linear accelerators for external beam radiotherapy produce high-energy radiation that operate in the megavoltage range.

These linear accelerators are quite versatile, with interchangeable electron and x-ray modes, adjustable energies, computer controls and isocentric mounting. The gantry is designed to rotate around the patient with the help of internal counterweights to stabilize the weight of the accelerator waveguide. The treatment couch provides five degrees of freedom, with vertical, lateral, longitudinal motion, pitch, and yaw with some couches providing roll rotation [20].

Multi-leaf collimator

Historically, accessories such as collimator jaws, blocks, virtual and dynamic wedges, were manually added to the linear accelerator to compensate for dose inhomogeneities and to shape the radiation field to the tumour. Advances in software optimization and mechanical precision have allowed these blocks and wedges to be replaced with multi-leaf collimators (MLC), now available on most clinical linacs in Australia. The MLCs are made of high density and high-atomic number material to provide conformal shaping of beams. **Figure 2** shows a picture of the head of a linac (without its cover) with the MLCs arranged into two banks of 120 leaves, arranged in pairs and closely abutting to form an arbitrary shape.

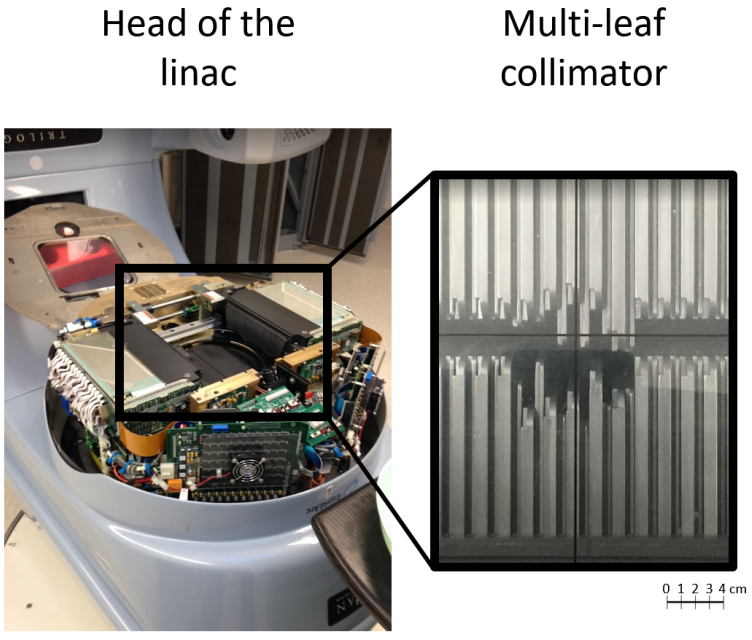

Figure 2. Head of a linac (left) with the MLC leaves (right).

The leaves within the head of the linac have the capability to move continuously during treatment along a single one-dimensional axis. The main advantage is that they do not require manual adjustment as their positions are optimized through a treatment planning system to provide the necessary dose. MLCs represent the current state of practice for shaping radiation fields during treatment.

IMRT and VMAT

Following the wide implementation of MLCs, most radiotherapy centres started using Intensity-Modulated Radiation Therapy (IMRT) as their delivery system either with static MLC or dynamic MLC treatment delivery techniques. The first option irradiates a portion of the dose at a fixed gantry position and a set shape of leaves. The beam is then interrupted, and the MLC leaves are shifted to provide a different shape used for the second dose delivery. This process is then repeated until completion of the treatment fraction. With dynamic MLC treatment, the MLC aperture is continuously shaping the treatment field during treatment delivery. IMRT *step-and-shoot* treatment utilizes the modulation of the MLC aperture to deliver a portion of the treatment, before interrupting and then rotating to another angle of irradiation. IMRT *sliding window* is another IMRT technic that continuously delivers the beam while the MLC slides across the treatment aperture.

Another type of more modern and complex IMRT is the Volumetric Modulated Arc Therapy (VMAT) that delivers intensity-modulated dose to the target volume while the gantry is continuously rotating around the patient. Studies have shown the benefit of VMAT over IMRT step-and-shoot for the treatment of thoracic tumours [21-23], with a lower dose absorbed by the organs-at-risks [24].

Thoracic motion in radiotherapy

Patient motion is a continuing challenge for radiotherapy. For thoracic cancers, respiratory and cardiac motion may have an impact on radiotherapy treatment accuracy [25]. There are also a number of unpredictable actions such as sneezing, coughing or muscle twitching [25-29] that can effect treatment delivery. For these reasons, positional uncertainty associated with motion is generally recognized as intrinsic to radiotherapy. **Figure 3** shows an example of a lung tumour moving with respiration.

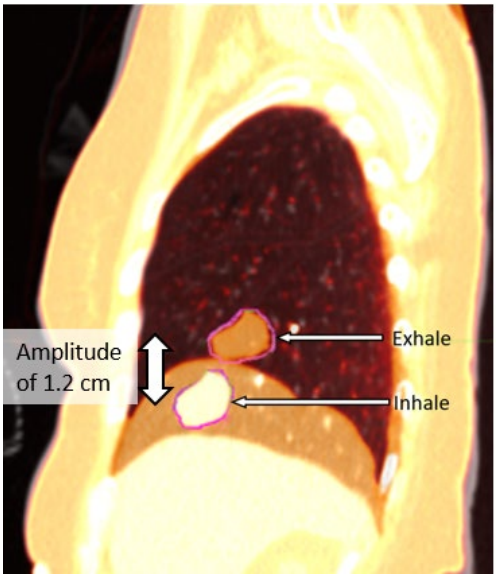

Figure 3. Registered phases from 4D-CT at end-of-exhale and end-of-inhale with a tumour amplitude of 1.2 cm located in the lateral segment of the right lower lobe.

For patients undergoing radiotherapy, thoracic motion is present at every stage of the radiation treatment pathway, from imaging and treatment planning to treatment delivery.

Motion during imaging

The first step of the radiation treatment pathway is to obtain reliable information about the patient's internal anatomy through imaging. For thoracic cancer patients, this can include a four-dimensional computed tomography (4D-CT) scan, occasionally coupled with a Positron Emission Tomography (PET) scan, that acquires 3D datasets of the patient's thorax that spans the breathing cycle. This allows the clinician to visualise the full range of tumour motion and to assess tissue deformation. Exploiting temporal-anatomic information in this way has led to huge advances in the field of lung cancer [27, 30]. These images are used for treatment planning and are now the standard of care for thoracic cancer imaging.

However, the accuracy of 4D-CT images is sensitive to changes in patient's breathing rate during the imaging process. Changes in the patient's breathing rate or depth can lead to image artefacts. Artefacts caused by irregular breathing are common during 4D-CT and despite being well known [31], they are not easily predicted or accounted for. With irregular breathing, motion induced artefacts during 4D-CT can be a major source of positional and temporal

uncertainty, causing a miss with significant dosimetric consequences. Guckenberger *et al.* [32] showed that the approximation of tumour motion from 4D-CT images is sufficient for most patients but can have detrimental effects on treatment if motion is under or over estimated.

Motion during treatment planning

Treatment planning is the second step in the patient's pathway to radiotherapy. Treatment planning is achieved using a treatment planning system (TPS) that optimizes radiation delivery based on several treatment parameters such as MLC shapes and gantry angles, and patient parameters such as the tumour location and surrounding organs-at-risk. The goal is to adequately dose the tumour while avoiding the organs-at-risk within a technically feasible framework. **Figure 4** shows an example of treatment planning for a tumour in the right middle lobe to be treated with VMAT.

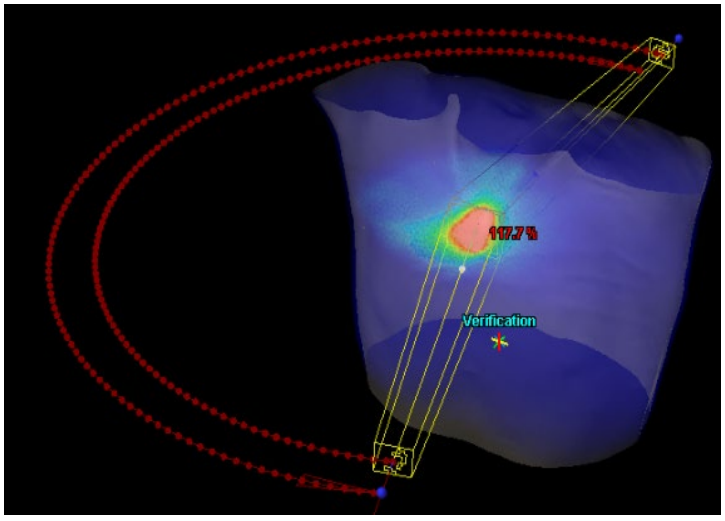

Figure 4. Example of a lung treatment plan for a tumour located in the right middle lobe, treated with VMAT.

Clinical treatment planning techniques for lung cancer define multiple target volume, with various definition, as defined by the International Commission on Radiation Units and Measurements 50, 62 and 83 [34-36], visualised in **Figure 5**. The Gross Tumour Volume (GTV) includes all clinically detectable disease and is often expanded to include sub-clinical disease into the Clinical Tumour

Volume (CTV). However, the current guidelines do not recommend the use of CTV for lung SABR planning, as the ablative dose delivered to the tumour and the flat dose profile of lung tissue are considered to provide sufficient coverage in case of sub-clinical expansion [37, 38].

The Internal Target Volume (ITV) encompasses the union of all the CTVs from the 4D-CT image set and accounts for motion through the respiratory cycle. The ITV is defined using the 4D-CT scan either by contouring on the maximum intensity projection scan, maximum inspiratory and expiratory scans or contoured on registered 4D-CT phases. The Planning Target Volume (PTV) encloses the ITV with anisotropic margins to account for possible uncertainties in beam alignment, patient positioning, organ motion, or organ deformation. The absorbed dose to the CTV, PTV and abutting organs-at-risk are reported as part of the radiotherapeutic process to assess the quality of the planning.

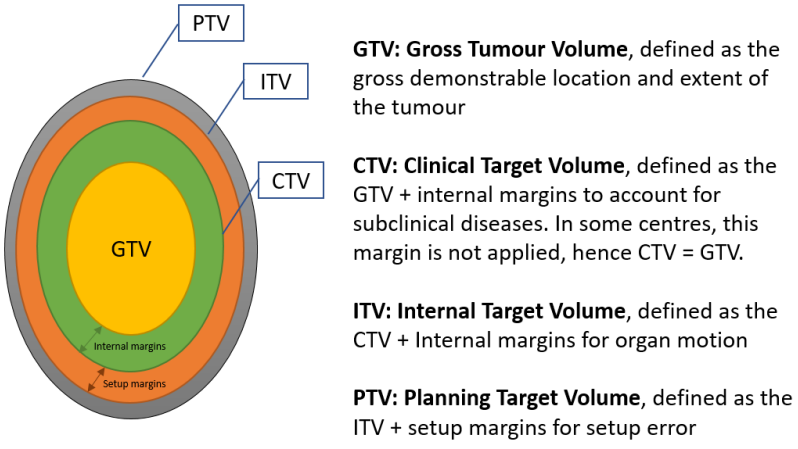

Figure 5. Schematic showing ICRU defined volumes and their relative sizes.

Motion on treatment day

Motion not only affects pre-treatment imaging but also the treatment itself. This motion can be categorized as *inter-fractional motion*, due to variations in day-to-day patient set up during treatment, and/or *intra-fractional motion*, due to motion during treatment.

Typical inter-fraction motion may be due to weight loss, tumour shrinkage or inflation. A large number of studies have investigated the characteristics of inter-fractional motion, such as Sonke *et al.* [39] showing day-to-day motion variations in thoracic bronchi. While inter-fractional motion can be hard to account for, it is generally easy to detect using Image Guided Radiation Therapy (IGRT) which

images the patient on the treatment table directly before treatment.

IGRT is the use of imaging to obtain the position of the patient's internal anatomy, either in two dimensions or three dimensions using planar imaging or Cone Beam Computer Tomography (CBCT). The latter requires the acquisition of multiple 2D planar images, reconstructed into a 3D dataset and manual alignment with the planned dataset. The main purposes of the CBCT before treatment are to align the anatomy to the treatment beam and verify the degree of soft tissue deformation within the thoracic cage. If the anatomical changes exceeded a given margin threshold, the clinician in charge could make the decision of pausing the treatment, continuing, or replanning.

Intra-fractional motion on the other hand is challenging to detect as it requires constant monitoring of the tumour position during treatment, either via imaging or other methods of detection detailed in the following **Chapter 3**. Intra-fractional motion for lung cancer treatment is generally related to changes in the patient's breathing magnitude and pattern. The magnitude of tumour motion is correlated to its position within the lung, with tumours in the lower lung lobe close to the diaphragm exhibiting greater motion than those located in an upper lobe [40-42]. **Figure 6** shows an example of varying lung tumour motion during radiotherapy treatment, with its baseline position shown in red, starting at -3 mm in the inferior direction and finishing after ~200s at +5 mm.

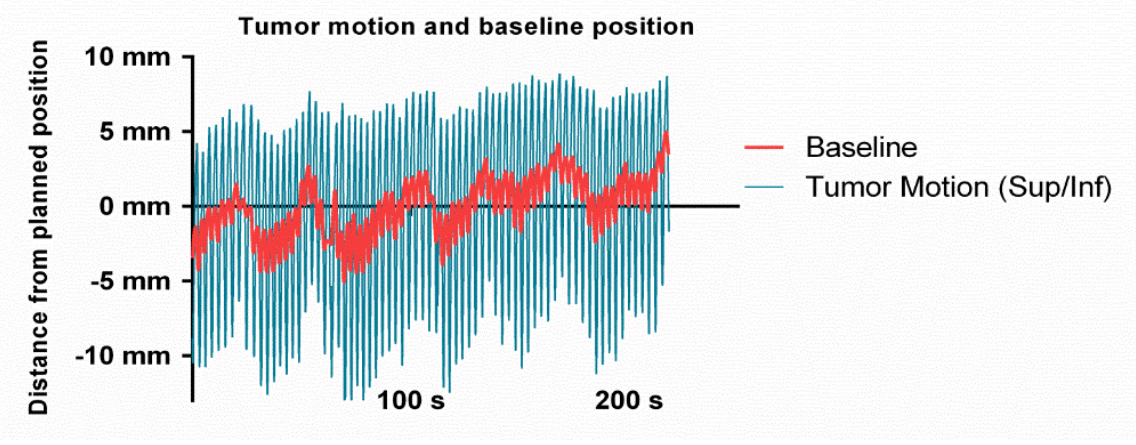

Figure 6. Example of tumour motion (blue) during treatment with a baseline shift.

Multi-leaf collimator tracking

Multi-leaf collimator (MLC) tracking is one of several techniques that permits real-time adaptation, accounting for intra-fractional tumour motion. MLC tracking is a beam adaptation technique that relies on the MLC leaves to adapt to tumour motion in real-time using the optimized leaf positions combined with the tumour motion input. To our knowledge, MLC tracking is the only beam adaptation technique that has been implemented on a linear accelerator with a rotating gantry, as opposed to the dedicated commercialized linear accelerator for motion management, such as the CyberKnife system (Accuray Inc. Sunnyvale, USA), the Accuray Radixact (Accuray, Sunnyvale, CA) or the Vero system (Brainlab AG, Feldkirchen, Germany).

Proof-of-concept and early developments

MLC tracking emerged as a proof-of-concept in 2001, published by Keall *et al.* [43]. It was originally implemented for translational motion with an *a priori* knowledge of the tumour motion, whereby the MLC leaves were shifted along their translational axis with its geometric accuracy investigated [44]. With promising results, theoretical investigations of MLC tracking began, following a target moving in one dimension [45], two dimensions [46, 47] and three dimensions [48]. MLC tracking was then experimentally implemented for IMRT [48] and VMAT [49-52]. As a final step towards clinical implementation, patient workflow was tested *in vivo* on pigs , showing the potential clinical benefits of MLC tracking for SABR [53].

Clinical Implementation

The first clinical implementation of MLC tracking was published by Keall *et al.* [54]. Twenty-eight patients with prostate cancer were treated on a conventional linear accelerator (Varian Trilogy), tracking implanted electromagnetic transponders. The reported geometric and dosimetric results were published in Colvill *et al.* [55] and Keall *et al.* [56]. Following the success of this clinical trial, seventeen patients with lung implanted electromagnetic transponders were treated as part of the LIGHT SABR trial with the primary objective to test whether MLC tracking is feasible, and the secondary objective to evaluate transponder implantation safety/migration and potential dosimetric benefits of MLC tracking over ITV-based treatment. The dosimetric benefits of the first patient was published by Booth *et al.* [57] with substantial geometric benefits reported for some patients [58]. MLC tracking using the KIM technology (Kilovoltage Intrafraction Monitoring) [59, 60] was clinically tested as part of the TROG 15.01 SPARK clinical trial for prostate patients. KIM employs the kilovoltage mounted x-ray imagers, common to most linacs, to visualise

during treatment the implanted beacons within the prostate. This allows MLC tracking to be implemented on a linac without relying on additional hardware for tracking the moving tumour. The reported geometric and dosimetric results of this clinical trial are encouraging for further centres to adopt this technology [59, 61].

Target detection devices used in MLC tracking

Several devices have been used to detect and track the target for MLC tracking, implemented generally as an "add-on" onto the current linear accelerator, the only two devices that have been used clinically being the electromagnetic transponders, and the use of the KIM technology.

Electromagnetic transponders are potentially the most advanced and clinically available technique for providing continuous and reliable tumour position in real-time. Electromagnetic transponders rely on electromagnetic signal detected by an electromagnetic panel. It is generally considered safe to use since EM waves have little effect on the body, but these transponders do require an invasive procedure that is not without risk. The positional accuracy of EM transponders was investigated by Willoughby *et al.* [62], Keall *et al.* [50], Krauss *et al.* [63] and Ravkilde *et al.* [64] who reported error in positioning of < 1 mm.

The use of kV imagers for MLC tracking has been tested by Poulsen *et al*. [65] and Keall *et al.* [60] using the KIM technology. This showed promising results as it would allow MLC tracking to be available with a software upgrade on most linacs with a rotating gantry and fluoroscopic imagers. Despite the well-known limitation that imaging is responsible for additional dose to the patient, this technology has been heavily relied upon to treat patients with MLC tracking for prostate cancer [59, 60, 66].

Markerless EPID imaging guided MLC tracking for lung tumours has been investigated by Poulsen *et al.* [53], Zhang *et al.* [67], Rottmann *et al.* [68, 69] and Cho *et al.* [70, 71]. This technology is promising as it relies on available linear accelerator technology but suffers from a lack of tissue contrast on MV images.

MLC tracking has been tested with ultrasound systems by Fast *et al.* [72] and Ipsen *et al.* [73] with reported latencies equivalent to dedicated devices for motion management. Ultrasound is an attractive modality for real-time and radiation-free imaging but suffers from a serious limitation related to the speed-of-sound error that can mis-interpret distances and the range of motion during tumour tracking.

With the advent of MRI-linac, the notion of MLC tracking using MRI guidance has garnered interest where Menten *et al.* [74] and Paganelli *et al.* [75] have proposed the potential benefits of combining the two technologies. Recently, Glitzner *et al.* [76] demonstrated the feasibility of implementing MLC tracking on a commercially available MRI-linac system, reporting capability of the MLC control system to follow targets with a latency of around 20 ms. Borman *et al.* [96] studied the image acquisition latency, and concluded that this latency is highly sequence-dependent, and therefore can be greatly improved when the appropriate sequence is selected.

Some optical systems have shown to be usable with MLC tracking, such as the Real-time position management (RPM) that tracks the movement of the chest using an infrared camera. Being an external tracking system, the RPM is a poor surrogate for tumour motion and was mostly relied on as proof-of-concepts [48], rather than actual reliable tracking devices.

Quality assurance in place

The clinical translation of MLC tracking from bench-to-bedside requires new quality assurance processes. Current quality assurance for radiotherapy delivery assumes static patients and unaltered MLC shapes that match the treatment planning. As such, protocols and tools have been developed to monitor the delivered dose during MLC tracking. One such protocol includes a failures mode and effect analysis-based quality assurance (FMEA) of the MLC tracking system, developed by Sawant *et al.* [77]. This study identified specific failure mode for MLC tracking with a calculated probability of occurrence, severity of effect and the degree of detectability of the failure. This FMEA quality assurance procedure was used for the MLC tracking for prostate and lung [54, 57] clinical trials at our institution.

Multiple quality assurance techniques were developed to ensure reliable and safe treatment delivery. Poulsen *et al.* [78] developed an isocentre shift method to compute, post-treatment, the dose delivered to the target and surrounding organs based on the detected tumour position and the leaf pattern. Fast *et al.* [79] developed an online algorithm for fast dose reconstruction for prostate SABR calculated on pre-calculated fluences and leaf patterns. Woodruff *et al.* [80] also demonstrated that the MV imagers can be successfully used for dose reconstruction that could potentially be used for MLC tracking treatment delivery. Kamerling *et al*. [81, 82] implemented a real-time 4D dose reconstruction method by connecting the MLC tracking software to the treatment planning system. Skouboe *et al.* [83] implemented, clinically, for the first time, a real-time motion-including tumour dose reconstruction [84].

The use of real-time adaptation to account for inter-fractional motion and intra-fractional motion is detailed in the following chapter.

Limitations of MLC tracking

MLC tracking suffers from several shortcomings that are worth highlighting.

A key limitation is due to hardware and software restrictions on linear accelerators. The finite leaf width, the direction of leaf motion along one single axis and the leaf speed, hinder the performance of MLC tracking. To correct for a target shift perpendicular to the axis of motion, the MLC must adapt by collectively shifting the aperture, which due to the finite leaf width and leaf speed, is not always possible and never instantaneous. **Figure 7** illustrates the case of an ideal aperture restricted by the leaf width. Pommer *et al.* [85] explored the relationship between the leaf width, speed and the ability of MLC tracking to deliver the planned dose within given margins. They found that aligning the MLC leaves to the major axis of motion, lowering the plan complexity, and using thinner leaves, are all potential solutions to reduce the amount of exposure errors during MLC tracking. A really interesting study from Toftegaard *et al.* [86] found that a hybrid of MLC tracking and couch-tracking has the capability to correct for tumour motion perpendicular to the leaves axis of motion, therefore reducing exposure errors.

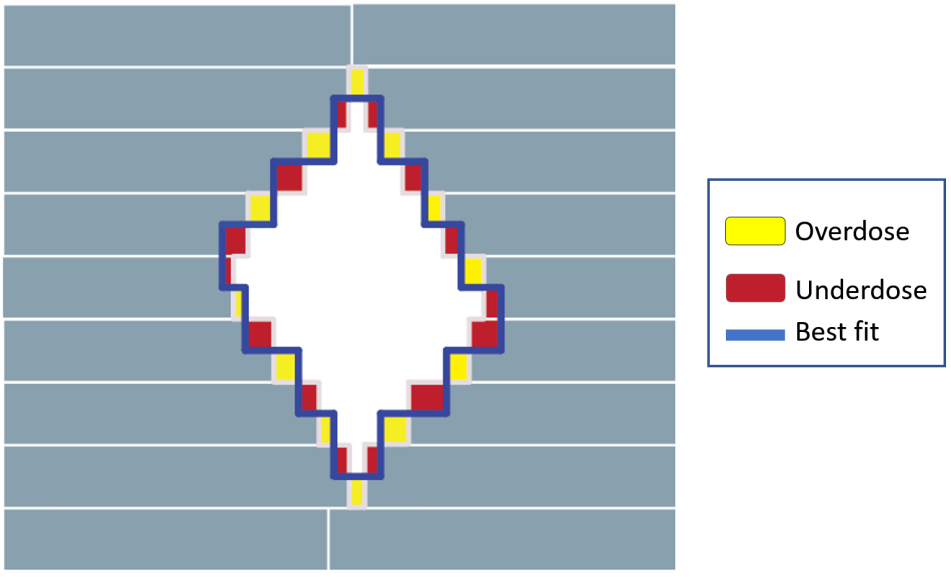

Figure 7. Ideal aperture (red contours) as compared to the actual aperture during MLC tracking. The ideal aperture cannot always be fit during MLC tracking due to the finite leaf-width, leading to organs being overdosed (yellow) or underdosed (brown).

Another limitation to the success of MLC tracking is the system's latency. Latency can deteriorate the performance of the treatment due to a lag between the tumour motion and the MLC mechanical shift. The effect of latency can be mitigated by using a prediction algorithm that aims to predict the tumour position ahead of time. The majority of prediction algorithms rely on linear prediction models based on an auto-regressive moving averages [87, 88], Kalman filters [89-91] and machine learning with neural networks [92, 93]. These models all perform well when predicting regular motion. Unfortunately, tumour motion is often erratic, causing several standard prediction approaches to perform poorly. Ultimately, reducing the system's latency could be achieved, similarly to the CyberKnife and Vero, by coupling the tumour motion detection system (e.g. ExacTrac) with a motion detection system with a faster input (e.g. thoracic belt, vest) and building a correlation model to help reduce the overall system's latency. Despite using fluoroscopic images for beacon segmentation sporadically (Yang *et al.* [94] reported on fluoroscopic images obtained every 40 seconds), CyberKnife studies [95] report latencies of 115 ms, while for MLC tracking for lung SABR, we reported 230 ms [57].

The use of MLC collimator for beam shaping suffers from several shortcomings. One of them is related to the use of fixed collimator positions that only allow discrete adaption to motion perpendicular to the leaves. Potential solutions could be to align the MLC along the major motion axis, restrict the complexity of the treatment plan or use thinner leaves. Another shortcoming is that MLC tracking requires a wider jaw opening than standard delivery to allow the leaves to travel during tracking, thereby increasing the risks of inter-leaf leakage. To minimize the leakage, jaw tracking has been tested during MLC tracking as a potential solution for future MLC tracking treatments [86].

Motivation for this work

With the development of IGRT and tumour detection techniques, more detailed in **Chapter 3**, a very natural step in the field of radiotherapy was to combine these detection techniques within a beam adaptation modality. The first MLC tracking implementation occurred for the treatment of prostate cancer, with the treatment of twenty-eight patients.

With the success of the prostate clinical trial, the motivation for this work was to tackle an even more challenging task and treat patients with lung cancer.

As detailed in this review, lung tumours are fast moving structures, potentially exhibiting large and highly variable amplitudes, and surrounding radiosensitive critical structures. It is therefore not surprising that lung tumours pose a challenge in radiotherapy as their intrinsic breathing-induced motion cannot be easily suppressed and therefore require beam adaptation. The goal of this work is to show whether MLC tracking will improve the accuracy of the treatment delivery as well as providing higher tumour dose coverage.

This thesis focuses on the first clinical implementation of MLC tracking for lung SABR using electromagnetic transponders implanted around the tumour.

Chapter 3 provides details about motion management in radiation therapy, particularly in relation to lung SABR. **Chapter 4** in this thesis describes a study on the pre-clinical trial potential dosimetric benefits of MLC tracking for lung SABR. **Chapter 5** provides a geometric analysis of the uncertainty of MLC tracking for lung SABR using the data of seventeen patients treated with this technology. To understand the impact of the algorithms for MLC tracking, **Chapter 6** compares two different optimizing algorithms, both *in silico*, and experimentally on a linear accelerator. **Appendix 1** provides a detail dosimetric analysis of the first patient treated with MLC tracking for lung SABR.

References

1. Bray, F., et al., *Global cancer statistics 2018: GLOBOCAN estimates of incidence and mortality worldwide for 36 cancers in 185 countries.* CA: a cancer journal for clinicians, 2018. **68**(6): p. 394-424.
2. Torre, L.A., R.L. Siegel, and A. Jemal, *Lung cancer statistics*, in *Lung cancer and personalized medicine*. 2016, Springer. p. 1-19.
3. John, R. and H. Ross, *The global economic cost of cancer.* Atlanta, GA: American Cancer Society and LIVESTRONG, 2010.
4. Council, C., *Lung Cancer.* 2020.
5. Samet, J.M., et al., *Lung cancer in never smokers: clinical epidemiology and environmental risk factors.* Clinical Cancer Research, 2009. **15**(18): p. 5626-5645.
6. Cruz, C.S.D., L.T. Tanoue, and R.A. Matthay, *Lung cancer: epidemiology, etiology, and prevention.* Clinics in chest medicine, 2011. **32**(4): p. 605-644.
7. Howlader, N., A. Noone, and M. Krapcho, *National Cancer Institute. SEER Cancer Statistics Review: 1975-2011*. 2015.
8. Mountain, C.F. *The international system for staging lung cancer*. in *Seminars in surgical oncology*. 2000. Wiley Online Library.
9. Yazgan, S., et al., *Outcome of surgery for lung cancer in young and elderly patients.* Surgery today, 2005. **35**(10): p. 823-827.
10. Cortés, Á.A., L.C. Urquizu, and J.H. Cubero, *Adjuvant chemotherapy in non-small cell lung cancer: state-of-the-art.* Translational lung cancer research, 2015. **4**(2): p. 191.
11. Doroshow, D.B., et al., *Immunotherapy in non–small cell lung cancer: facts and hopes.* Clinical Cancer Research, 2019. **25**(15): p. 4592-4602.
12. Corso, C.D., et al., *Stage I lung SBRT clinical practice patterns.* American journal of clinical oncology, 2017. **40**(4): p. 358-361.
13. Simone, C.B. and J.F.D. II, *Additional data in the debate on stage I non-small cell lung cancer: surgery versus stereotactic ablative radiotherapy.* Annals of translational medicine, 2015. **3**(13).
14. Deng, H.-Y., et al., *Radiotherapy, lobectomy or sublobar resection? A meta-analysis of the choices for treating stage I non-small-cell lung cancer.* European Journal of Cardio-Thoracic Surgery, 2017. **51**(2): p. 203-210.
15. Onishi, H., et al., *Stereotactic Body Radiotherapy (SBRT, BED≥ 100 Gy) for Operable Stage I Non-Small Cell Lung Cancer: Is SBRT Comparable to Surgery?* International Journal of Radiation Oncology• Biology• Physics, 2007. **69**(3): p. S86-S87.
16. Crabtree, T.D., et al., *Stereotactic body radiation therapy versus surgical resection for stage I non–small cell lung cancer.* The Journal of thoracic and cardiovascular surgery, 2010. **140**(2): p. 377-386.
17. Cheng, M., et al., *Modern radiation further improves survival in non-small cell lung cancer: an analysis of 288,670 patients.* Journal of Cancer, 2019. **10**(1): p. 168.
18. Joseph, N. and A. Choudhury, *SABR versus conventional fractionation regimens in NSCLC.* The Lancet Oncology, 2019. **20**(5): p. e231.

19. Ball, D., et al., *Stereotactic ablative radiotherapy versus standard radiotherapy in stage 1 non-small-cell lung cancer (TROG 09.02 CHISEL): a phase 3, open-label, randomised controlled trial.* The Lancet Oncology, 2019. **20**(4): p. 494-503.
20. Schmidhalter, D., et al., *Evaluation of a new six degrees of freedom couch for radiation therapy.* Medical physics, 2013. **40**(11): p. 111710.
21. Rao, M., et al., *Comparison of Elekta VMAT with helical tomotherapy and fixed field IMRT: plan quality, delivery efficiency and accuracy.* Medical physics, 2010. **37**(3): p. 1350-1359.
22. Yu, C.X., *Intensity-modulated arc therapy with dynamic multileaf collimation: an alternative to tomotherapy.* Physics in Medicine & Biology, 1995. **40**(9): p. 1435.
23. Li, Y., et al., *Dosimetric comparison between IMRT and VMAT in irradiation for peripheral and central lung cancer.* Oncology letters, 2018. **15**(3): p. 3735-3745.
24. Wu, Q.J., et al., *Volumetric arc intensity–modulated therapy for spine body radiotherapy: comparison with static intensity-modulated treatment.* International Journal of Radiation Oncology* Biology* Physics, 2009. **75**(5): p. 1596-1604.
25. Seppenwoolde, Y., et al., *Precise and real-time measurement of 3D tumor motion in lung due to breathing and heartbeat, measured during radiotherapy.* International Journal of Radiation Oncology* Biology* Physics, 2002. **53**(4): p. 822-834.
26. Kitamura, K., et al., *Three-dimensional intrafractional movement of prostate measured during real-time tumor-tracking radiotherapy in supine and prone treatment positions.* International Journal of Radiation Oncology* Biology* Physics, 2002. **53**(5): p. 1117-1123.
27. Shirato, H., et al. *Intrafractional tumor motion: lung and liver*. in *Seminars in radiation oncology*. 2004. Elsevier.
28. Schild, S.E., H.E. Casale, and L.P. Bellefontaine, *Movements of the prostate due to rectal and bladder distension: implications for radiotherapy.* Medical dosimetry, 1993. **18**(1): p. 13-15.
29. Lin, Y., et al., *Respiratory-induced prostate motion using wavelet decomposition of the real-time electromagnetic tracking signal.* International Journal of Radiation Oncology* Biology* Physics, 2013. **87**(2): p. 370-374.
30. Ford, E., et al., *Respiration-correlated spiral CT: a method of measuring respiratory-induced anatomic motion for radiation treatment planning.* Medical physics, 2003. **30**(1): p. 88-97.
31. Yamamoto, T., et al., *Retrospective analysis of artifacts in four-dimensional CT images of 50 abdominal and thoracic radiotherapy patients.* International Journal of Radiation Oncology* Biology* Physics, 2008. **72**(4): p. 1250-1258.
32. Guckenberger, M., et al., *Is a single respiratory correlated 4D-CT study sufficient for evaluation of breathing motion?* International Journal of Radiation Oncology* Biology* Physics, 2007. **67**(5): p. 1352-1359.
33. Wu, A.J.-C., *Safety of stereotactic ablative body radiation for ultracentral stage I non-small cell lung cancer.* Translational lung cancer research, 2019. **8**(Suppl 2): p. S135.
34. Units, I.C.o.R., *Prescribing, recording, and reporting photon beam therapy*. Vol. 50. 1993: International Commission on Radiation.
35. Prescribing, I., *recording and reporting photon beam therapy (supplement to ICRU Report 50).* ICRU report, 1999. **62**.
36. Units, I.C.o.R. and Measurements, *ICRU Report 83 Prescribing, Recording, and Reporting Photon-beam Intensity-modulated Radiation Therapy (IMRT)-Journal of the ICRU-Vol 10 No 1 2010*. 2010: Oxford University Press.
37. Potters, L., et al., *American Society for Therapeutic Radiology and Oncology (ASTRO) and American College of Radiology (ACR) practice guideline for the performance of stereotactic*

body radiation therapy. International Journal of Radiation Oncology• Biology• Physics, 2010. **76**(2): p. 326-332.
38. De Ruysscher, D., et al., *European Organisation for Research and Treatment of Cancer recommendations for planning and delivery of high-dose, high-precision radiotherapy for lung cancer.* Journal of Clinical Oncology, 2010. **28**(36): p. 5301-5310.
39. Sonke, J.-J., J. Lebesque, and M. Van Herk, *Variability of four-dimensional computed tomography patient models.* International Journal of Radiation Oncology* Biology* Physics, 2008. **70**(2): p. 590-598.
40. Stevens, C.W., et al., *Respiratory-driven lung tumor motion is independent of tumor size, tumor location, and pulmonary function.* International Journal of Radiation Oncology* Biology* Physics, 2001. **51**(1): p. 62-68.
41. Knybel, L., et al., *Analysis of lung tumor motion in a large sample: patterns and factors influencing precise delineation of internal target volume.* International Journal of Radiation Oncology* Biology* Physics, 2016. **96**(4): p. 751-758.
42. Sarudis, S., et al., *Systematic evaluation of lung tumor motion using four-dimensional computed tomography.* Acta Oncologica, 2017. **56**(4): p. 525-530.
43. Keall, P., et al., *Motion adaptive x-ray therapy: a feasibility study.* Physics in Medicine & Biology, 2001. **46**(1): p. 1.
44. Keall, P.J., et al., *Geometric accuracy of a real-time target tracking system with dynamic multileaf collimator tracking system.* International Journal of Radiation Oncology* Biology* Physics, 2006. **65**(5): p. 1579-1584.
45. Papiez, L., D. Rangaraj, and P. Keall, *Real-time DMLC IMRT delivery for mobile and deforming targets.* Medical physics, 2005. **32**(9): p. 3037-3048.
46. McClelland, J., et al., *Tracking 'differential organ motion'with a 'breathing'multileaf collimator: magnitude of problem assessed using 4D CT data and a motion-compensation strategy.* Physics in Medicine & Biology, 2007. **52**(16): p. 4805.
47. McQuaid, D. and S. Webb, *IMRT delivery to a moving target by dynamic MLC tracking: delivery for targets moving in two dimensions in the beam's eye view.* Physics in Medicine & Biology, 2006. **51**(19): p. 4819.
48. Sawant, A., et al., *Management of three-dimensional intrafraction motion through real-time DMLC tracking.* Medical physics, 2008. **35**(5): p. 2050-2061.
49. Zimmerman, J., et al., *DMLC motion tracking of moving targets for intensity modulated arc therapy treatment–a feasibility study.* Acta oncologica, 2009. **48**(2): p. 245-250.
50. Keall, P.J., et al., *Electromagnetic-guided dynamic multileaf collimator tracking enables motion management for intensity-modulated arc therapy.* International Journal of Radiation Oncology* Biology* Physics, 2011. **79**(1): p. 312-320.
51. Davies, G., et al., *An experimental evaluation of the Agility MLC for motion-compensated VMAT delivery.* Physics in Medicine & Biology, 2013. **58**(13): p. 4643.
52. Bedford, J.L., et al., *Effect of MLC tracking latency on conformal volumetric modulated arc therapy (VMAT) plans in 4D stereotactic lung treatment.* Radiotherapy and Oncology, 2015. **117**(3): p. 491-495.
53. Poulsen, P.R., et al., *Megavoltage image-based dynamic multileaf collimator tracking of a NiTi stent in porcine lungs on a linear accelerator.* International Journal of Radiation Oncology* Biology* Physics, 2012. **82**(2): p. e321-e327.

54. Keall, P.J., et al., *The first clinical implementation of electromagnetic transponder-guided MLC tracking.* Medical physics, 2014. **41**(2).
55. Colvill, E., et al., *Multileaf collimator tracking improves dose delivery for prostate cancer radiation therapy: results of the first clinical trial.* International Journal of Radiation Oncology* Biology* Physics, 2015. **92**(5): p. 1141-1147.
56. Keall, P.J., et al., *Electromagnetic-guided MLC tracking radiation therapy for prostate cancer patients: Prospective clinical trial results.* International Journal of Radiation Oncology* Biology* Physics, 2018. **101**(2): p. 387-395.
57. Booth, J.T., et al., *The first patient treatment of electromagnetic-guided real time adaptive radiotherapy using MLC tracking for lung SABR.* Radiotherapy and Oncology, 2016. **121**(1): p. 19-25.
58. Caillet, V., et al., *Geometric uncertainty analysis of MLC tracking for lung SABR.* Physics in Medicine & Biology, 2020.
59. Hewson, E.A., et al., *The accuracy and precision of the KIM motion monitoring system used in the multi-institutional TROG 15.01 Stereotactic Prostate Ablative Radiotherapy with KIM (SPARK) trial.* Medical Physics, 2019. **46**(11): p. 4725-4737.
60. Keall, P.J., et al., *The first clinical implementation of real-time image-guided adaptive radiotherapy using a standard linear accelerator.* Radiotherapy and Oncology, 2018. **127**(1): p. 6-11.
61. Wolf, J., et al., *Dosimetric impact of intrafraction rotations in stereotactic prostate radiotherapy: a subset analysis of the TROG 15.01 spark trial.* Radiotherapy and Oncology, 2019. **136**: p. 143-147.
62. Willoughby, T.R., et al., *Target localization and real-time tracking using the Calypso 4D localization system in patients with localized prostate cancer.* International Journal of Radiation Oncology* Biology* Physics, 2006. **65**(2): p. 528-534.
63. Krauss, A., et al., *Electromagnetic real-time tumor position monitoring and dynamic multileaf collimator tracking using a Siemens 160 MLC: Geometric and dosimetric accuracy of an integrated system.* International Journal of Radiation Oncology* Biology* Physics, 2011. **79**(2): p. 579-587.
64. Ravkilde, T., et al., *Geometric accuracy of dynamic MLC tracking with an implantable wired electromagnetic transponder.* Acta Oncologica, 2011. **50**(6): p. 944-951.
65. Poulsen, P.R., et al., *Implementation of a new method for dynamic multileaf collimator tracking of prostate motion in arc radiotherapy using a single kV imager.* International Journal of Radiation Oncology* Biology* Physics, 2010. **76**(3): p. 914-923.
66. Keall, P.J., et al., *The first clinical treatment with kilovoltage intrafraction monitoring (KIM): a real-time image guidance method.* Medical physics, 2015. **42**(1): p. 354-358.
67. Zhang, X., et al., *Tracking tumor boundary in MV-EPID images without implanted markers: A feasibility study.* Medical physics, 2015. **42**(5): p. 2510-2523.
68. Rottmann, J., P. Keall, and R. Berbeco, *Markerless EPID image guided dynamic multi-leaf collimator tracking for lung tumors.* Physics in Medicine & Biology, 2013. **58**(12): p. 4195.
69. Rottmann, J., et al., *A multi-region algorithm for markerless beam's-eye view lung tumor tracking.* Physics in Medicine & Biology, 2010. **55**(18): p. 5585.
70. Cho, B., et al., *Real-time target position estimation using stereoscopic kilovoltage/megavoltage imaging and external respiratory monitoring for dynamic multileaf collimator tracking.* International Journal of Radiation Oncology* Biology* Physics, 2011. **79**(1): p. 269-278.

71. Cho, B., et al., *First demonstration of combined kV/MV image-guided real-time dynamic multileaf-collimator target tracking.* International Journal of Radiation Oncology* Biology* Physics, 2009. **74**(3): p. 859-867.
72. Fast, M.F., et al., *First evaluation of the feasibility of MLC tracking using ultrasound motion estimation.* Medical Physics, 2016. **43**(8Part1): p. 4628-4633.
73. Ipsen, S., et al., *Online 4D ultrasound guidance for real-time motion compensation by MLC tracking.* Medical physics, 2016. **43**(10): p. 5695-5704.
74. Menten, M.J., et al., *Lung stereotactic body radiotherapy with an MR-linac–Quantifying the impact of the magnetic field and real-time tumor tracking.* Radiotherapy and Oncology, 2016. **119**(3): p. 461-466.
75. Paganelli, C., et al., *MRI-guidance for motion management in external beam radiotherapy: current status and future challenges.* Physics in Medicine & Biology, 2018. **63**(22): p. 22TR03.
76. Glitzner, M., et al., *MLC-tracking performance on the Elekta unity MRI-linac.* Physics in Medicine & Biology, 2019. **64**(15): p. 15NT02.
77. Sawant, A., et al., *Failure mode and effect analysis-based quality assurance for dynamic MLC tracking systems.* Medical physics, 2010. **37**(12): p. 6466-6479.
78. Poulsen, P.R., et al., *A method of dose reconstruction for moving targets compatible with dynamic treatments.* Medical physics, 2012. **39**(10): p. 6237-6246.
79. Fast, M., et al., *Assessment of MLC tracking performance during hypofractionated prostate radiotherapy using real-time dose reconstruction.* Physics in Medicine & Biology, 2016. **61**(4): p. 1546.
80. Woodruff, H.C., et al., *First experience with real-time EPID-based delivery verification during IMRT and VMAT sessions.* International Journal of Radiation Oncology* Biology* Physics, 2015. **93**(3): p. 516-522.
81. Kamerling, C.P., et al., *Real-time 4D dose reconstruction for tracked dynamic MLC deliveries for lung SBRT.* Medical physics, 2016. **43**(11): p. 6072-6081.
82. Kamerling, C.P., et al., *Online dose reconstruction for tracked volumetric arc therapy: Real-time implementation and offline quality assurance for prostate SBRT.* Medical physics, 2017. **44**(11): p. 5997-6007.
83. Skouboe, S., et al., *First clinical real-time motion-including tumor dose reconstruction during radiotherapy delivery.* Radiotherapy and Oncology, 2019. **139**: p. 66-71.
84. Ravkilde, T., et al., *First online real-time evaluation of motion-induced 4D dose errors during radiotherapy delivery.* Medical physics, 2018. **45**(8): p. 3893-3903.
85. Pommer, T., et al., *The impact of leaf width and plan complexity on DMLC tracking of prostate intensity modulated arc therapy.* Medical physics, 2013. **40**(11): p. 111717.
86. Toftegaard, J., et al., *An experimentally validated couch and MLC tracking simulator used to investigate hybrid couch-MLC tracking.* Medical physics, 2017. **44**(3): p. 798-809.
87. McCall, K. and R. Jeraj, *Dual-component model of respiratory motion based on the periodic autoregressive moving average (periodic ARMA) method.* Physics in Medicine & Biology, 2007. **52**(12): p. 3455.
88. Ren, Q., et al., *Adaptive prediction of respiratory motion for motion compensation radiotherapy.* Physics in Medicine & Biology, 2007. **52**(22): p. 6651.
89. Sharp, G.C., et al. *Plastimatch-an open source software suite for radiotherapy image processing*. in *Proceedings of the XVI'th International Conference on the use of Computers in Radiotherapy (ICCR), Amsterdam, Netherlands*. 2010.

90. Kalet, A., et al., *A state-based probabilistic model for tumor respiratory motion prediction.* Physics in Medicine & Biology, 2010. **55**(24): p. 7615.
91. Hong, S., B. Jung, and D. Ruan, *Real-time prediction of respiratory motion based on a local dynamic model in an augmented space.* Physics in Medicine & Biology, 2011. **56**(6): p. 1775.
92. Cheong, K.-H., et al., *A proof-of-concept study for the real-time prediction of respiratory patterns: a simple Bayesian approach.* Journal of the Korean Physical Society, 2018. **73**(3): p. 368-376.
93. Ernst, F. and A. Schweikard, *Forecasting respiratory motion with accurate online support vector regression (SVRpred).* International journal of computer assisted radiology and surgery, 2009. **4**(5): p. 439-447.
94. Yang, Z.-Y., et al., *Target margin design for real-time lung tumor tracking stereotactic body radiation therapy using CyberKnife Xsight Lung Tracking System.* Scientific Reports, 2017. **7**(1): p. 10826.
95. Pepin, E.W., et al., *Correlation and prediction uncertainties in the cyberknife synchrony respiratory tracking system.* Medical physics, 2011. **38**(7): p. 4036-4044.
96. Borman, P.T.S., Tijssen, R.H.N., Bos, C., Moonen, C.T.W., Raaymakers, B.W. and Glitzner, M., 2018. *Characterization of imaging latency for real-time MRI-guided radiotherapy*. Physics in Medicine & Biology, 63(15), p.155023.

CHAPTER 03

IGRT and motion management during lung SBRT delivery

This review article was published in *Physica Medica* edited by Paolo Russo. This article was written by me at the invitation of the editors and co-authors.

This chapter is a follow-up from **Chapter 2** and provides background on the use of IGRT and motion management during lung SBRT delivery. This includes techniques that are available in room, prior to treatment delivery, and those that are used during the treatment delivery. It explores the various devices, commercial or still at the research stage, that are currently available to detect, correct and adapt for motion for lung SBRT.

Physica Medica 44 (2017) 113–122

Contents lists available at ScienceDirect

Physica Medica

journal homepage: http://www.physicamedica.com

REVIEW PAPER

IGRT and motion management during lung SBRT delivery

Vincent Caillet [a,b,*], Jeremy T. Booth [a,b], Paul Keall [c]

[a] Northern Sydney Cancer Centre, Royal North Shore Hospital, Sydney, Australia
[b] School of Physics, University of Sydney, Sydney, Australia
[c] School of Medicine, University of Sydney, Sydney, Australia

ARTICLE INFO

Article history:
Received 5 February 2017
Received in Revised form 4 June 2017
Accepted 9 June 2017
Available online 21 June 2017

Keywords:
Stereotactic radiotherapy
Lung cancer
IGRT
Motion management

ABSTRACT

Patient motion can cause misalignment of the tumour and toxicities to the healthy lung tissue during lung stereotactic body radiation therapy (SBRT). Any deviations from the reference setup can miss the target and have acute toxic effects on the patient with consequences onto its quality of life and survival outcomes. Correction for motion, either immediately prior to treatment or intra-treatment, can be realized with image-guided radiation therapy (IGRT) and motion management devices. The use of these techniques has demonstrated the feasibility of integrating complex technology with clinical linear accelerator to provide a higher standard of care for the patients and increase their quality of life.

© 2017 Associazione Italiana di Fisica Medica. Published by Elsevier Ltd. All rights reserved.

Contents

* Corresponding author at: Room 475, Blackburn Building D06, The University of Sydney, NSW 2006, Australia.
E-mail address: vcai6204@uni.sydney.edu.au (V. Caillet).

http://dx.doi.org/10.1016/j.ejmp.2017.06.006
1120-1797/© 2017 Associazione Italiana di Fisica Medica. Published by Elsevier Ltd. All rights reserved.

1. Introduction

Lung Stereotactic Body Radiation Therapy (SBRT), or stereotactic ablative body radiotherapy (SABR), is a radiation therapy technique that delivers large ablative doses to the tumour with fewer fractions than conventional radiation therapy. The high biological dose delivered to patients requires a high conformal dose distribution around the tumour with minimal exposure of surrounding healthy tissues. However, lung tumours are subjected to motion, which complicates the provision of high accuracy targeting during treatment delivery. Failure to adequately account for uncertainties due to motion can cause geographic miss and inaccurate dose coverage, such as underdosing the target and/or overdosing surrounding organs-at-risk (OAR) [1–4]. For these reasons, it is a desideratum of modern radiotherapy to manage tumour motion, trajectory irregularities, deformation and patient repositioning during lung radiation therapy.

Image-guided radiation therapy (IGRT) is the image-based guidance of radiotherapy delivery and a sub-set of the motion management strategies clinically implemented to help mitigate motion-related errors [5]. The scope of this chapter is narrowly defined to IGRT and motion management during SBRT delivery of photon beam therapy. The novelty of Magnetic Resonance Imaging (MRI) combined with linear accelerators is detailed in another chapter [6] and will not be extensively mentioned here. We presuppose that a patient scan has been acquired (e.g. 4D-CT, MRI), and a treatment plan appropriate to the delivery method has been developed. This chapter is then organised into IGRT and motion management technologies that are used in room but prior to the treatment delivery (section II) and those that are used during the treatment (section III).

2. In room pre-treatment IGRT and motion management

Pre-treatment IGRT and motion management techniques available either commercially or in the research phase are summarised below in Fig. 1. Each of these devices are compartmentalised into four domains; kV imaging, MV imaging, optical imaging and treatment couch.

2.1. KV imaging

2.1.1. Conventional kV-imagers and 3D-CBCT

Fluoroscopic imaging devices are offered as standard components for nearly all linear accelerators (linacs). Most C-arm shaped linacs are made available with retractable kilovoltage (kV) source and a detector panel that provide a radiographic image of the patient's anatomy with submillimetre resolution enabling highly accurate positioning relative to a reference setup. The visibility of internal anatomy using kilovoltage x-rays is largely imposed by the Compton cross sections of the targeted tissue in the patient. For that reason, bone and metal (implanted fiducials) are high

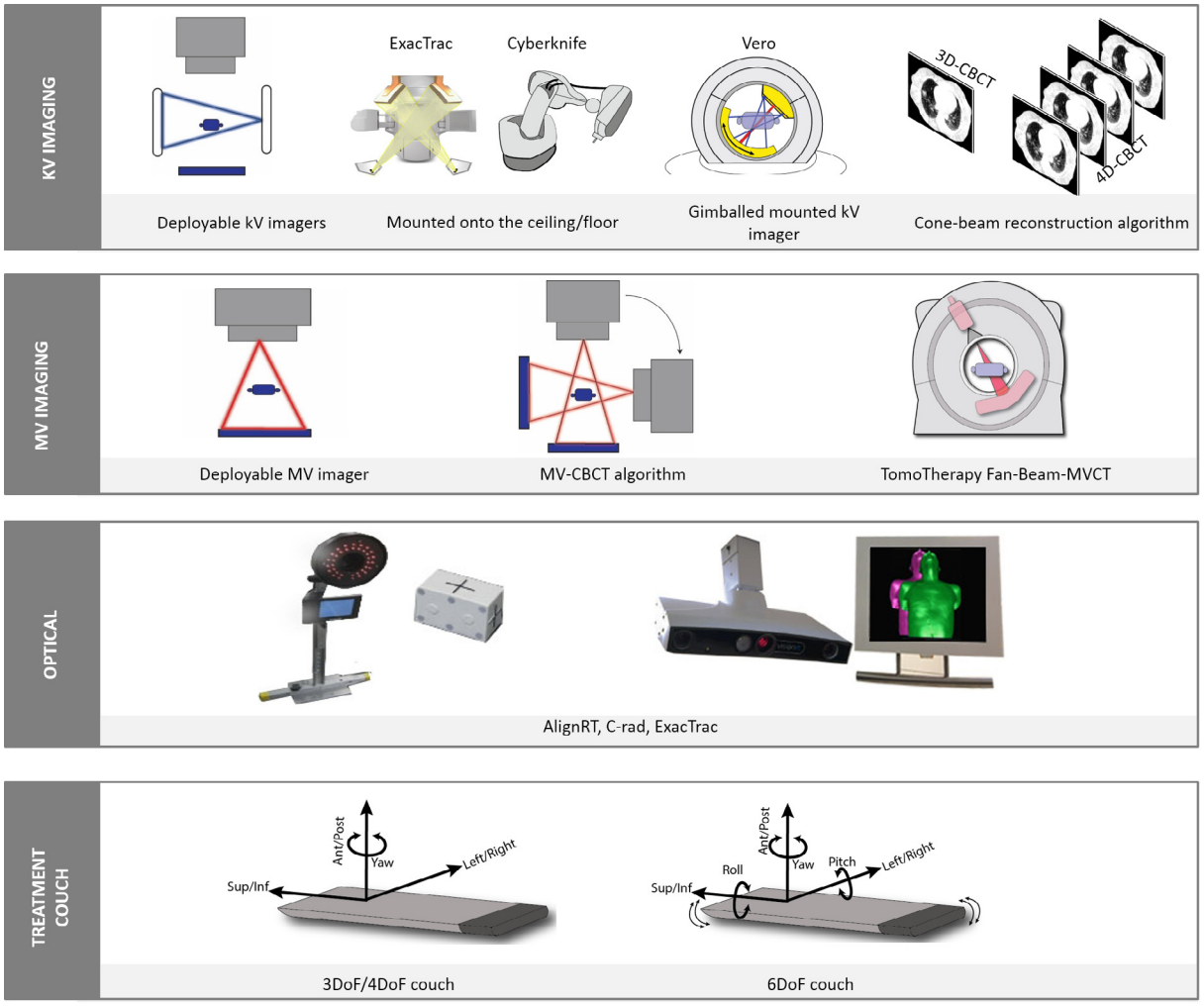

Fig. 1. Summary of motion management techniques available prior to treatment.

contrast due to their high attenuation coefficient and can be used as landmarks for patient's positioning, as opposed to soft tissue that have a low visibility contrast.

Another system, the Vero system (Brainlab AG, Feldkirchen, Germany) uses gimballed X-ray sources and imager. The Cyberknife system (Accuray Inc. Sunnyvale, USA) and the ExacTrac X-ray system (ExacTrac optical-tracking system, Brainlab, Heimstetten, Germany) are both systems that entail the use of mounted X-ray imagers and in-floor built detectors.

For rotating X-ray gantry, the 2D images can be reconstructed in three dimensions (cone-beam-computed-tomography, 3D-CBCT). Compared with kV planar images, CBCT provides offers a more complete assessment of patient deformation, rotation, tumour to OAR distances [7,8] and more importantly, a higher contrast visibility of soft tissue. AAPM Task-group 179 recommends quality assurance and iso-calibration tests monthly, to ensure that geometric and image quality remain within tolerance, and daily, for safety (collision check) and laser/image/treatment isocentre coincidence [9]. 3D-CBCT entails the use of fluoroscopic images and gantry rotation to calculate a three dimensional image showing the patient's internal anatomy prior to each fraction and allows visualisation of a range of geometric deviations such as motion-related uncertainties [10]. The main drawback of 3D-CBCT for lung imaging is that the projections from breathing phases are averaged to reconstruct a single 3D scan. Average projection yields blurred regions of interest or multiple diaphragm artefacts [11], potentially providing misinformation regarding actual tumour amplitude and its relative position to the OAR during breathing [12]. These artefacts complicate the task of the clinician to assess the degree of internal motion, deformation and the repositioning of the patient according to the reference set up

2.1.2. 4D-CBCT

4D-CBCT is the reconstruction of time-resolved 2D projections in phase or amplitude bins. Online 4D-CBCT has the advantage over 3D-CBCT of providing daily motion information such as visualising lesions that are near the ribs or diaphragm that might be inside 3D-CBCT blur and identifying baseline shift [13]. Compared with 3D-CBCT, the 4D-CBCT supplementary information on the trajectory-of-the-day keeps the margins around the target small [14] and reduces inter-observer variability for patient positioning [15]. 4D-CBCT was first developed and implemented on a linac by Tagushi et al. [16] and Sonke et al. [17]. Elekta released the first commercially available 4D-CBCT followed by Varian with the Truebeam 2.0.

The image quality of 4D-CBCT is dependent on the binning strategies and the type of CBCT reconstruction algorithm. Binning strategies are grouped either by phase or by displacement. Phase binning divides the breathing cycle into discrete phases relative to an arbitrary origin (i.e. end of exhalation), while displacement uses the magnitude of displacement to discretise the breathing signal. Phase binning was shown to be more clinically relevant, with a more accurate and clearer representation of small moving structures but the method is weakened in the presence of baseline shift [18]. On the other hand, displacement binning has the advantage to be less sensitive to variation in breathing patterns during the acquisition but the quality of reconstruction is influenced by inter-bin image quality variation and large projection angular gaps [18]. The reconstruction of CBCT is also heavily dependent on the reconstruction algorithm clinically in use. The current clinical reconstruction algorithm is the Feldkamp-Davis-Kress (FKD) algorithm or the McKinnon-Bates (MKB) algorithm, the latter mostly used for fast reconstruction. Both algorithms suffer from streak artefacts and a considerable amount of noise [18]

There is active research towards an enhanced version of 4D-CBCT to decrease the imaging dose per acquisition and reduce the streak artefacts. Dose reductions are obtained with hardware enhancement by varying the gantry speed [19,20], acquisition and imaging frequency [21] on a patient-specific basis in response to the patient's respiratory signal, with reported ~50% reduction of image dose. Streak artefacts can be reduced by implementing an iterative reconstruction algorithm [22]. Iterative algorithms are limited clinically by their requirements for long and intensive computation. However, they provide a higher image quality when constraints are applied to the similarity between the image to be reconstructed and higher quality prior image.

2.2. MV imaging

2.2.1. Electronic Portal imaging device (EPID)

The EPID was developed to provide a fast and accessible tool to replace film dosimetry. For most C-shaped linear accelerators, the EPID is a retractable panel that can be deployed at different distances and is typically used as a quality assurance tool on modern linacs for verification of modulated deliveries. For older linacs without on-board imagers, the EPID remains the go-to tool for pre-treatment patient setup. Its use in the beam-eye-view is particularly well appreciated by clinicians since both the image and the therapeutic MV beam share the same isocentre with projection having less distortion from metal artefacts compared with kV imaging. The inconvenience of MV X-ray imaging is that high energy photons have low tissue-density differentiation, resulting in 2D images with lower contrast-to-noise ratio than kV images. Average dose per image is as high as 3–7 cGy, compared with the kV system of 0.1–0.3 cGy per images. Better image quality will improve the potential for patient positioning prior to treatment using the MV frames. For that reason, efforts have been made to investigate the detectors' response using high efficiency materials [23–26] and enhancing reconstruction algorithms with MV-CT and MV-CBCT [27–29].

2.2.2. Fan beam MV-CT with tomotherapy

As part of the IGRT techniques utilised before treatment, fan beam MV-CT is available in the helical Tomotherapy Hi-ART system (Madison, Wisconsin, USA, HI-ART II). The MV beam rotates around the patient in a fast and helical manner, much like a third-generation helical CT would (i.e. both X-ray tube and detector rotate). Tomotherapy is the only commercial product that currently utilises the MV imaging device in the narrow beam geometry as a computed tomographic device. Length in the cranio-caudal (CC) direction is user dependent but the field-of-view in the other directions is restricted to ~40 cm. The fan-beam MVCT imaging dose is typically in the range of 1–3 cGy per scan [30] depending on the length of the patient to be imaged. We like to utilise.

2.2.3. MV-CBCT

MV-CBCT utilises the EPID to provide reconstructed 3D images prior to treatment. Lower energy settings than treatment MV is commonly used, 2.5 MV on the Varian Truebeam linac and 1 MV for the Siemens linear accelerators. Acquisition and reconstruction are performed in less than 2 min with a typical dose between 2 and 9 cGy but motion blur and low density differentiation can reduce the image quality. Studies aiming to enhance the image quality utilised the MV-CBCT on thoracic scan in a gated rotation acquisition method, where the gantry rotations are stopped and started when the tumour reaches the gating threshold [31], or fast acquisition, by combining kV and MV projections during approximately 15 s breath-holds [32]. For the latter, the gantry needs to rotate only 90 degrees and reduces the acquisition time to ~15 s, achievable throughout one breath-hold. This has been automated to be performed clinically [33], with patient positioning set up shown to be equivalent to conventional IGRT techniques [34]. Additionally,

MV-CBCT was shown to be feasible for rapid dose planning in urgent palliative situations [35].

2.3. Optical verification

Optical IGRT systems dedicated to guidance of patient setup have also been developed, such as AlignRT (Vision RT, London, United Kingdom), Catalyst (C-Rad AB, Uppsala, Sweden) and ExacTrac optical-tracking system (BrainLab AG, Munich, Germany). These devices rely on room-mounted optical cameras that verify the patient position and detect gross alignment errors. AlignRT and Catalyst use an infra-red camera that maps the patient surface contours in 6 degrees of freedom without the need of markers while the ExacTrac relies on external markers placed on the patient's chest. The ExacTrac also offers the advantage of integration with a kV radiographic imaging system to verify the internal markers' position prior to treatment for building a correlation model between external and internal markers.

2.4. Robotic couch

Treatment couch re-positioning is an important intervention made prior to treatment and is closely intertwined with the use of image guidance. The patient is positioned on the couch and aligned manually according to landmarks, tattoo or indexed to immobilisation devices. Following imaging, the couch can be re-aligned in 3 translations and a couch rotation about the anterior-posterior axis (yaw) to match current patient positioning with reference set up. Optimal alignment requires 6D correction including the roll and pitch to account for patient internal movement and rotation [29,30] to facilitate isocentre shifts. Commercially available 6 degrees of freedom couches include the Brainlab's Robotics 6D couch HexaPOD evo RT (integrated with Exactrac X-ray 6D system), Protura Robotic Patient Positioning System (via Civco Medical Solution, Kalona, USA), and the PerfectPitch couch system (Varian, Palo Alto, USA).

3. Intra-treatment IGRT and motion management

During treatment, a range of devices are available for correction of errors related to motion. Motion compensation intra-treatment is paramount either by tracking the tumour or monitoring and adapting to its position. Fig. 2 summarises the commercial and research applications of the IGRT and non-IGRT motion management techniques available during treatment, from beam-on until end of treatment. In this section, we restrict the analysis to *during treatment* as offline review can also be processed as an *a posteriori* treatment quality assurance.

3.1. Dedicated devices for motion management

Several motion management devices have been clinically implemented as therapeutic tools to ensure a safer and more accurate radiation therapy treatment. These devices rely on motion correction in real-time either by adapting the position of the beam, its shape, or the patient couch position. The motion input may vary depending on the specific machine, using kV (with or without radio-opaque markers), electromagnetic transponders or surface markers for the motion of the thorax.

The most prevalent device for motion management with lung tumour tracking is the Cyberknife system commercialised and clinically implemented since 2006 [36]. The Cyberknife is comprised of a six degree-of-freedom robotic arm capable of compensating for the thoracic motion and internal anatomy movement in real-time [37]. Two orthogonal fluoroscopic systems are mounted onto the ceiling with the flat panel in-built into the floor around the treatment couch. The other commercialised device specifically designed for real-time adaptation is the gimballed linac Vero. The Vero linear accelerator is mounted on a ring gantry that rotates both around the patient and on its vertical axis (±60 degrees) with two gimbals that enable the treatment beam to pan and tilt, a feature particularly useful for tumour tracking [38,39]. For the Vero, two kV sources and the flat panel imagers are directly located on the rotating gantry. Both the Cyberknife and the Vero tracking system are supplied with a correlation model, initially built before treatment, based on the detection motion system of an internal (measured using kV imaging) and external (measured using optical imaging) surrogate motion of the chest wall. The measured external chest motion combined with the correlation model predicts the tumour position, allowing the treatment beam to be shifted accordingly in real-time. For the Cyberknife, the correlation model is frequently verified (typically 30–60 s) and updated using marker segmentation on a single kV image. For the Vero system, the correlation model is verified more frequently than the Cyberknife (1 Hz) but requires treatment interruption to be updated [40]. Studies show that patient survival of the Cyberknife and the Vero are equivalent to standard SABR [41–45]. These studies also confirm that tumour tracking result in lower toxicity issues when compared with standard SABR, with significant increase in dose conformity.

A third technique is dynamic Multi-Leaf Collimator (MLC) tracking for standard linear accelerators. MLC tracking takes a tumour position signal and integrates it with the MLC to reconfigure the aperture in real-time in response to detected motion. MLC tracking is not available commercially but has been demonstrated on Varian [46,47], Elekta [48,49] and Siemens [50,51] linear accelerators. One unique possibility presented by MLC tracking is the ability to adapt to deformation of a target, which might be best utilised within the MR-linac framework.

Couch tracking is another real-time adaptation modality available for the standard linear accelerator where a tumour localisation signal is fed back to re-align the treatment couch [52]. Couch tracking has not been clinically implemented but has been demonstrated as a proof of concept with electromagnetic beacons [53], a topometrical device (Topos, Cyber Technologies, Germany), the respiratory gating system RPM (Varian) and a laser triangulation system (Micro Epsilon, Ortenburg, Germany) [54]. Couch tracking requires a high-precision couch motion system and was shown to be feasibly implemented on most linear accelerators. MLC tracking and couch tracking stand as potentially highly accessible modalities to enable increased utilisation of real-time adaptive radiotherapy [55].

3.2. Tracking or monitoring the tumour motion

kV imagers are an emerging tool for motion management to offer image guidance solutions during treatment. Gating or triggered imaging are available on certain linear accelerators (e.g. Varian Truebeam) with the capacity to monitor the tumour position, either to deliver the therapeutic beam at a specific phage during the patient's respiratory cycle or for real-time quality assurance and treatment accuracy.

The Cyberknife and the Vero systems take advantage of the set of orthogonal kV-imagers and optical tracking of external markers. The Cyberknife system includes the Synchrony Respiration Tracking System [56,57], a tracking system that reads the Light-Emitting Diodes (LED) chest motion input, correlates it with internal motion, and synchronises the beam accordingly with a latency of approximately 115 ms [58]. For the Vero, the correlation model is similarly built with a system latency for the infra-red markers of approximately 50 ms [39]. This is a much faster response time than

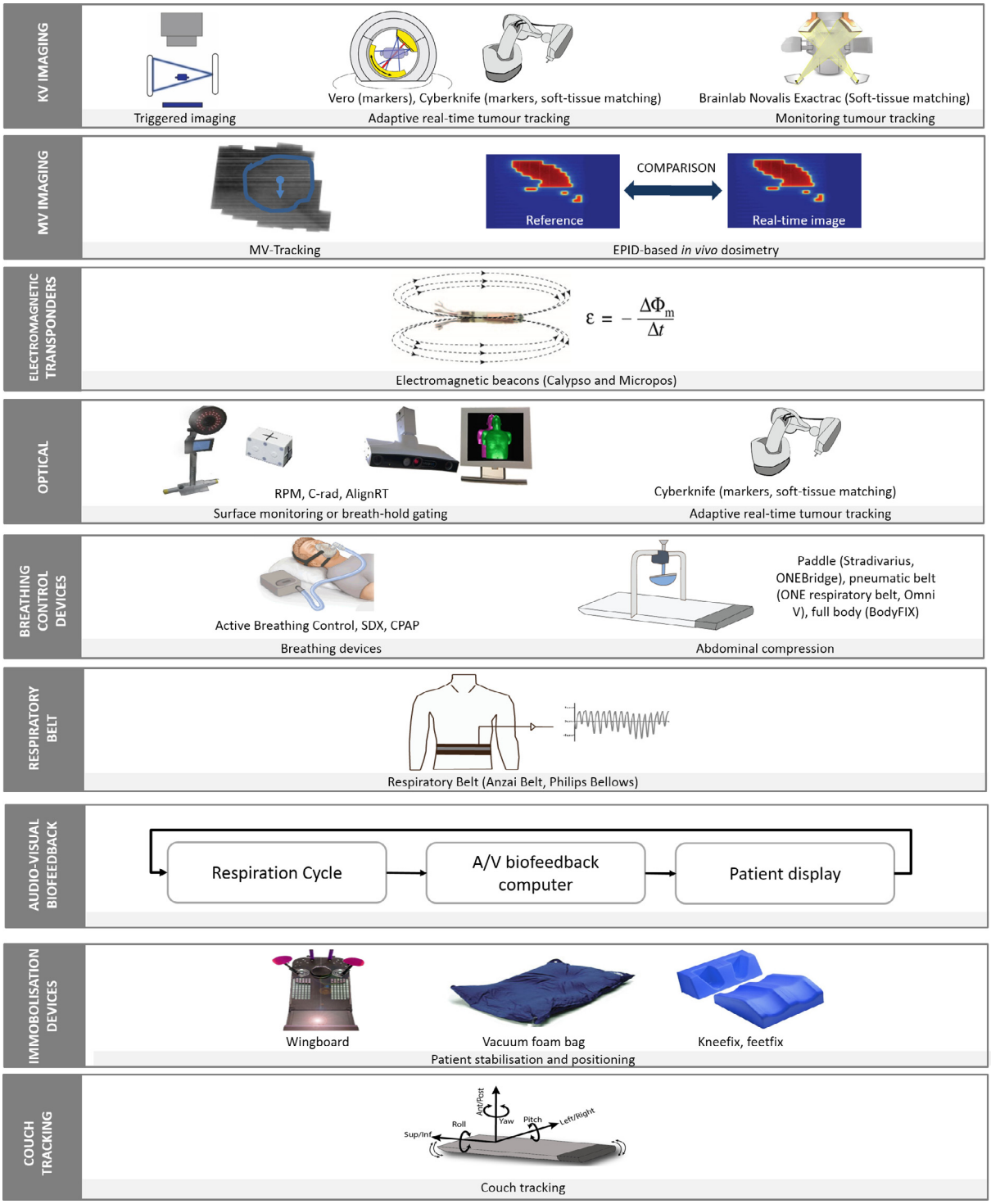

Fig. 2. Summary of IGRT and non-IGRT motion management techniques available during treatment.

any other devices because the beam is mounted on gimbals that provide a fast mechanical response of the therapeutic beam to be re-oriented. Both the Cyberknife and Vero rely on the high contrast of implanted gold markers, like the coiled gold Visicoils (IBA, Louvain-la-neuve, Belgium) to guide adaptation.

The Brainlab Exactrac Adaptive Gating system is a device used for patient positioning and intra-treatment tumour motion monitoring. Its principle is similar to the Cyberknife and Vero as it takes advantage of a kV imaging system and chest motion to build a correlation model. Instead of tracking the tumour, it monitors the tumour position and irradiates at a selected cycle of respiration, during free breathing or deep inhale breath hold (DIBH) [59,60]. Compared with continuous tumour tracking, the Exactrac gating system has the disadvantage of increased treatment duty cycle, treatment time and imaging. The kV-imagers are mounted on the ceiling and floor and work independently from the on-board imaging device of the linear accelerators. The system is compatible with Vero and most Varian linear accelerators as an integrated platform.

kV-based tracking generally relies on *in vivo* implanted markers as a surrogate to track tumours within kV images acquired during treatment. There are several challenges limiting the utilisation of kV marker based tracking for lung SABR including the potential of marker-induced toxicity [61–63], marker migration [64] and surrogacy errors between tumour and markers (external or internal markers) [65]. Markerless tumour tracking, where automated soft tissue matching is performed without implanted markers, has the potential to negate these issues. It must operate under the conditions of adequate internal landmark visualisation and surrogacy by the kV-imaging system or a correlation model coupled with a robust prediction algorithm. For patient not amenable for fiducial placement, Cyberknife proposes alternative registration landmarks such as spine tracking [66], carina [67,68] or direct tumour tracking [69] with the Xsight lung tracking system. Soft-tissue matching using MLC tracking has been tested in a feasibility study using offline kilovoltage projections based on a Bayesian approach [70]. Quality assurance for markerless tumour tracking may also pose some challenges and require specialist and possibly patient specific motion phantoms.

3.3. MV imaging

3.3.1. MV tumour tracking

Lung megavoltage tumour tracking is predominantly a type of markerless tracking, based on the tumour or surrogate landmarks featured onto the EPID. To our knowledge, MV tracking has never been clinically implemented on linear accelerators. It was tested as a proof-of-concept using the "STiL" algorithm combined with MLC tracking to visualise and adapt the conformal MLC that is shaped according to a 3D printed tumour inside a deformable thoracic phantom [71]. With SBRT and modulated plans, one problem is that the tumour is not continuously visible on the images and its visibility can be obstructed by the diaphragm, ribs or heart. Also, the use of modulated fields complicates the tasks where the lesions are often obscured by the MLC.

3.3.2. EPID-based Intra-treatment dose verification

EPID-based *in vivo* dosimetry is the verification of the cumulative dose by comparison with the reference planned dose. EPID-based *in vivo* dosimetry is a system that flags major errors resulting from large clinical deviations such as machine fault, human error or large and unnoticed patient movement during treatment. A recent study from the Netherlands showed the effectiveness of this system [72] claiming that 1 in 300 plans required the inspection of a medical physicist to address clinical relevant deviations. Several countries have now integrated EPID-based *in vivo* dosimetry as part of their compulsory protocols. Commercial products currently available are the EPIDose (Sun Nuclear Corporation, Melbourne, FL), Portal Dosimetry system (Varian Medical Systems, Palo Alto, CA), EPIgray (DOSIsoft, Cachan, France), and Dosimetry Check (Math Resolutions LLC, USA). However, with the current increase in biological dose used for SBRT fractionation, post-delivery analysis is not suitable for avoiding radiation-induced toxicities. Real-time EPID-based dose verification can mitigate these issues. Although never implemented for the lung, the use of the EPID for real-time dose verification ("WatchDog") has been clinically tested on a cohort of 28 patients with head-and-neck and prostate cancer [73] allowing for both real-time dosimetric and geometric quality control.

3.4. Electromagnetic transponders

As a non-imaging based motion management technique, the use of electromagnetic transponders for lung tumour tracking is potentially the most advanced. This system uses non-ionising alternating current electromagnetic radiation to locate and continuously track small devices. It relies on a set of electromagnetic transponders (bronchoscopically or percutaneously) inserted in the vicinity of the lung tumour to be wirelessly detected by a detector placed above the patient chest during treatment (Fig. 3). Electromagnetic beacons for real-time tumour tracking in radiation therapy are commercialised by RayPilot (Micropos Medical AB, Gothenburg, Sweden) and the Calypso Anchored Beacons System (Calypso, Varian Medical system). Both products are suited for use on conventional linac. Micropos rely on wired beacons that are intended to be retracted after treatment. Although this technique has demonstrated its feasibility for prostate, the use of Micropos for lung has never been tested. The Calypso beacons are permanently implanted near the tumour. For lung insertion, Varian provides an improved version of regular prostate beacons with a five legged nitinol stability feature to facilitate anchoring within small airways [74]. The Calypso beacons for lung are approved for gated lung SABR and motion monitoring for data acquisition and analysis by numerous Government Regulatory bodies, such as the TGA in Australia and FDA in the USA. The use of the Calypso beacons is also conceivable for lung SBRT gating and couch tracking [75].

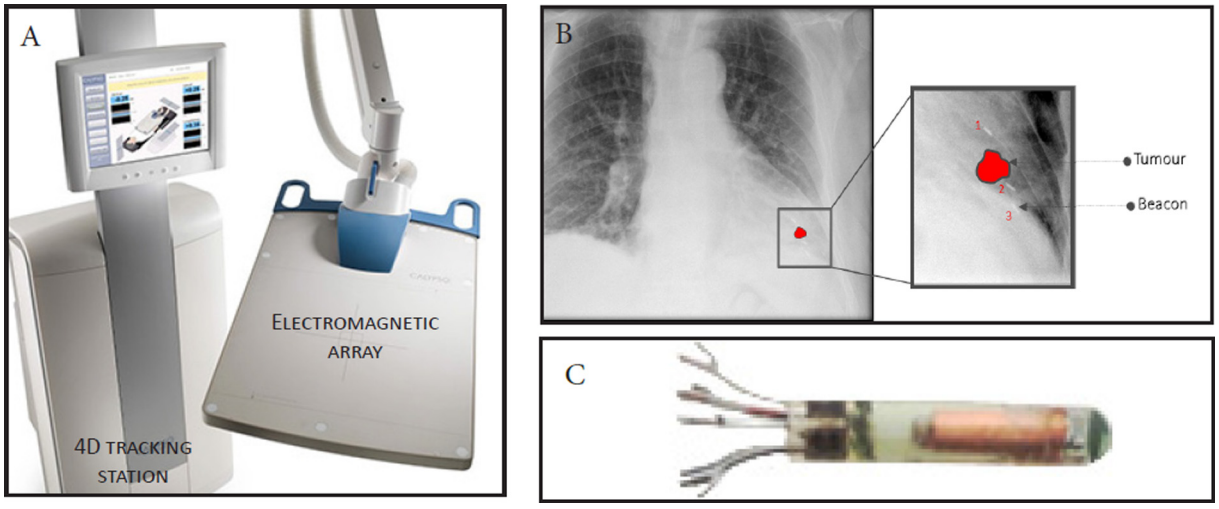

Fig. 3. A) Calypso tracking station with the electromagnetic arm B) fluoroscopic images of implanted beacons within vicinity of the tumour C) lung calypso beacons with the nitinol legs.

Our current clinical trial treats patients with lung tumours on a Trilogy Varian linac (Varian Medical Systems, Palo Alto, CA) using electromagnetic beacons inserted around the lesions [47]. Other groups have integrated the use of Calypso on a Siemens linac as a proof-of-concept but not to treat patients as yet [51]. The beacons are tracked in real-time with sub-2 mm position accuracy [76] and the beam is adapted using MLC tracking. This is the first and only institution treating patients with MLC tracking for lung SABR [47]. Patients (7/7) were successfully implanted, each with three beacons placed around the tumour, with positive dosimetric impact [77]. The underlying system latency of the MLC tracking system is approximately 220 ms [78] and is balanced with a kernel density-based method to predict the future target position [79].

3.5. Optical imaging

Optical imaging can be used to monitor the patient's abdomen or thorax for the patient's positioning, therapeutic beam gating or real-time monitoring of lung SBRT. Although it has the advantage of being non-ionising and non-invasive, its main challenge is to provide an accurate correlation between external markers and internal motion despite potential tumour hysteresis.

Optical imaging gating devices like the RPM system entail the use of an infra-red camera that illuminates a block covered with reflective markers positioned onto the patient's abdomen. AlignRT (Vision RT, London, UK) and Catalyst (C-Rad AB, Uppsala, Sweden) map the patient surface contours. Other devices using reflective markers are the Cyberknife, Vero and ExacTrac, all described in an earlier section as they require regular fluoroscopic images to update the correlation model. The combination of optical imaging and kV imaging can improve this correlation with regular model updates during monitoring of the chest motion. All of these devices are used to monitor the patient's abdomen or chest motion during DIBH, free-breathing gating or tumour tracking and detect unwanted patient movement like coughing and sneezing. It has been shown that DIBH combined with optical imaging decreases the dose to mediastinal structures as the inflated lung is caudally displaced away from the heart [80,81].

3.6. Breathing control devices

Breathing control devices aim to manipulate the patient's breathing pattern. They directly interact with the patient's airflow with facial masks or restrict thoracic motion using devices to block the motion of the abdomen. Commercialised products that interact directly with the patient's airflow through the mouth or nose are the Active Breathing Coordinator (ABC) device (Elekta AB, Stockholm, Sweden) and the SDX (Dyn'R, Toulouse, France). The ABC is a spirometer device dedicated to the practice of semi-voluntary breath-hold. It is connected to a balloon valve that blocks the patient air flow in several DIBH until the field is delivered, usually requiring two or three breath holds for the entire delivery. The SDX is also a spirometer device, however the patient is expected to perform breath-hold on their own with a pair of goggles providing instructions as a visual aid. The volume of air intakes is recorded from a flow sensor and converted into analogue signals. The signals are analysed by the SDX software that triggers the linac beam when the patient breathing curves reaches the breath-hold zone.

A large clinical trial (STIC 2003) with 403 patients demonstrated significant dose reduction for patients that were treated with ABC or SDX compared with free-breathing or RPM gating technique [80]. Study showed that significant increase in lung volume were found with breathing control devices which resulted in noticeable higher dosimetric benefits compared with RPM gating techniques [82].

Another device, the Continuous Positive Air Pressure (CPAP device), is currently being tested for its potential clinical use in lung radiation therapy [83,84]. The original clinical use of the CPAP device was to avert blockage of upper airways for patients suffering from sleep apnoea. A continuous pressurised air flow is delivered to the patient's airway by pumping air into the patient's mouth or nose. The hypothesis is that continuous pressurised air results in a hyper-inflated lung which stabilises the diaphragm and increases the distance between the tumour target and OAR (e.g. Heart).

Other types of breathing control devices employ abdominal compression. Abdominal compression may be applied with several devices to mechanically restrict the motion of the abdomen during respiration. Since forced shallow breathing reduces the respiratory motion, dose escalation is permitted and beneficial for SBRT treatment. Compared with others forms of tracking or patient monitoring, the use of abdominal compression retains the advantages that its implementation is easy and accessible on linear accelerators and significantly reduces the cranio-caudal motion. Abdominal compression is increasingly popular. A survey in 2013 showed that abdominal compression was used in 51% of clinical centres in the USA [85].

One form of abdominal compression is a paddle pressed against the patient's abdomen, just below the ribs, using an arch system with screws to regulated the force of the paddle [86]. For this type of system, commercialised products are the Stradivarius abdominal compression paddle system (Qfix Systems, Avondale, PA), or the ONEBridge (Civco Medical Solutions, Kalona, IA) that comes in various sizes of respiratory plates. Another type of abdominal compression device, the pneumatic belt, applies pressure uniformly against the abdomen using an inflated belt controlled by a pump and a gauge. Commercialised products are the Stradivarius compression belt (Qfix), ONE Respiratory Belt (Civco Medical Solutions, Kalona, IA) and Omni V SBRT solution system (Bionix Radiation Therapy, Toledo, Ohio, US). It is worth noting that clinical centres have also designing their own custom-built external compression devices either for research purpose or to answer for their own specific needs [87,88].

Despite abdominal compression, patients may still experience upper body motion. Full thoracic motion restriction can be utilised to mitigate this problem. The BodyFIX system (Elekta, Medical Intelligence, Schwabmuenchen, Germany) is a dual-vacuum whole-body immobilisation device in which the patient is placed in a vacuum bag and the patient's lower body, abdomen and thorax are wrapped in clear plastic. The air between the plastic, patient and the vacuum cushions is then evacuated [89,90]. Compared with the abdominal compression paddle, both techniques performed equivalently, although applying uniform compression to the body of the patient with the BodyFIX system was reported to be more comfortable [90]. Another type of body immobilisation is used with the Orfit SBRT body mask (Orfit Industries Nv, Wijnegem, Belgium). The body mask helps to immobilise the patient and is attached along specifically made slots. This technique is reported to be effective for treating patients with spinal metastases [91].

Objectives and implementation differ between centres depending on the strategies in place, clinical objectives of the centres and the type of patients treated. Forced shallow breathing with abdominal compression was shown to be most effective for patients with tumour motion exceeding 5 mm in free-breathing [92], or 13 mm for gating [93,94], with significant reduction in the cranio-caudal direction with the paddle compared with free-breathing [95] specially for lower lobe lesions [96]. However the reported residual excursion with the compression belt raises concerns about the tumour amplitude reproducibility [95].

3.7. Respiratory belt

The use of a respiratory belt wrapped around the patient's abdomen for monitoring or gating has also been tested. The most widely available systems are the Anzai belt (AZ-733V Anzai) manufactured by Siemens and the Bellows belt (Philips Medical System, Cleveland, OH). Respiratory belts are equipped with a strain gauge coupled with a sensor to record pressure variation induced by the chest stretching during breathing. The two-dimensional data is sent to the controller that triggers the beam according to the patient's amplitude. Small groups of patients were treated with the respiratory belt [97,98] with evidence that gating provides a constant treatment quality control, depth dose and beam profile [99,100]. Respiratory gating with a belt or optical imaging remains a popular motion management technique with approximately 31% of centres in USA using this with lung radiotherapy treatment [85].

3.8. Audio-visual biofeedback

Coaching the patient to breathe regularly and/or showing them their respiratory trace for active patient control is known as Audio-visual feedback. The use of audio-visual biofeedback from monitoring devices to the patient allows the patient to actively participate in the treatment. The patient directly addresses irregular tumour motion by remaining within a threshold during DIBH or following a regular and predictable breathing pattern that is beneficial for tumour tracking devices. Breathing signals can be obtained from the RPM, belt, optical cameras or other devices providing an analogue output that can be redirected back to the patient. In a systematic review, most studies reported beneficial effects of the use of audio, visual or audio-visual biofeedback compared with free breathing [101].

3.9. Immobilisation devices

Immobilisation of the patient is evidently paramount and can be obtained by locking the patient in a vacuum-lock foam bag, stereotactic frame with wingboard and alpha-cradle, and immobilising their feet and knees. These steps minimise motion or wobbling during CBCT couch shift after the 3D/3D match.

4. Conclusion and outlook

This chapter is a review of the current use of IGRT and motion management techniques available in radiation therapy. It explores the various devices, commercial or still at the research stage, that are currently available for patients treated with lung SBRT. The use of IGRT and motion management prior to treatment are established standardised techniques and their dissemination in clinical practice is ongoing [85]. However, the clinical benefits of motion management during radiation therapy are hard to interpret. Clinical trials generally involve small cohorts of patients, and the treatment strategies between radiotherapy centres cover a large range of fractionations, lung staging or tumour lobe location as well as different treatment techniques (VMAT, IMRT). Also, comparison of motion management against the absence of motion management is difficult because of the lack of randomised controlled trials. For that reason, stronger clinical data for a large cohort of patients is needed to fully claim the benefits of motion management for lung SBRT.

The rise of MRI-guided linear accelerators may provide a paradigm shift in the way lung SBRT is currently performed. Because of its high tissue contrast, MRI-guided capabilities are far superior to kV-based imaging, with better target and OAR delineations [6]. In addition, it does not require ionising radiation to image the internal anatomy and is therefore safer for the patient.

Funding

The MLC tracking trial with electromagnetic beacons mentioned in this review is partially-funded by Varian Medical Systems.

References

[1] Timmerman R, McGarry R, Yiannoutsos C, Papiez L, Tudor K, DeLuca J, et al. Excessive toxicity when treating central tumors in a phase II study of stereotactic body radiation therapy for medically inoperable early-stage lung cancer. J Clin Oncol 2006;24:4833–9.
[2] Baumann P, Nyman J, Hoyer M, Wennberg B, Gagliardi G, Lax I, et al. Outcome in a prospective phase II trial of medically inoperable stage I non–small-cell lung cancer patients treated with stereotactic body radiotherapy. J Clin Oncol 2009;27:3290–6.
[3] Stephans KL, Djemil T, Tendulkar RD, Robinson CG, Reddy CA, Videtic GM. Prediction of chest wall toxicity from lung stereotactic body radiotherapy (SBRT). Int J Radiat Oncol Biol Phys 2012;82:974–80.
[4] Ong CL, Palma D, Verbakel WF, Slotman BJ, Senan S. Treatment of large stage I-II lung tumors using stereotactic body radiotherapy (SBRT): planning considerations and early toxicity. Radiother Oncol 2010;97:431–6.
[5] Keall PJ, Mageras GS, Balter JM, Emery RS, Forster KM, Jiang SB, et al. The management of respiratory motion in radiation oncology report of AAPM Task Group 76. Med Phys 2006;33:3874–900.
[6] Menten MJ, Wetscherek A, Fast MF. MRI-guided lung SBRT: present and future developments. Physica Med 2017.
[7] Bujold A, Craig T, Jaffray D, Dawson LA. Image-guided radiotherapy: has it influenced patient outcomes? Seminars in radiation oncology. Elsevier; 2012. p. 50–61.
[8] Jaffray DA, Drake DG, Moreau M, Martinez AA, Wong JW. A radiographic and tomographic imaging system integrated into a medical linear accelerator for localization of bone and soft-tissue targets. Int J Radiat Oncol Biol Phys 1999;45:773–89.
[9] Bissonnette J-P, Balter PA, Dong L, Langen KM, Lovelock DM, Miften M, et al. Quality assurance for image-guided radiation therapy utilizing CT-based technologies: a report of the AAPM TG-179. Med Phys 2012;39:1946–63.
[10] Purdie TG, Bissonnette J-P, Franks K, Bezjak A, Payne D, Sie F, et al. Cone-beam computed tomography for on-line image guidance of lung stereotactic radiotherapy: localization, verification, and intrafraction tumor position. Int J Radiat Oncol Biol Phys 2007;68:243–52.
[11] Schulze R, Heil U, Groβ D, Bruellmann D, Dranischnikow E, Schwanecke U, et al. Artefacts in CBCT: a review. Dentomaxillofacial Radiol 2014.
[12] Shah C, Grills IS, Kestin LL, McGrath S, Ye H, Martin SK, et al. Intrafraction variation of mean tumor position during image-guided hypofractionated stereotactic body radiotherapy for lung cancer. Int J Radiat Oncol Biol Phys 2012;82:1636–41.
[13] Thengumpallil S, Smith K, Monnin P, Bourhis J, Bochud F, Moeckli R. Difference in performance between 3D and 4D CBCT for lung imaging: a dose and image quality analysis. J Appl Clin Med Phys 2016;17.
[14] Sonke J-J, Rossi M, Wolthaus J, van Herk M, Damen E, Belderbos J. Frameless stereotactic body radiotherapy for lung cancer using four-dimensional cone beam CT guidance. Int J Radiat Oncol Biol Phys. 2009;74:567-74.
[15] Sweeney RA, Seubert B, Stark S, Homann V, Müller G, Flentje M, et al. Accuracy and inter-observer variability of 3D versus 4D cone-beam CT based image-guidance in SBRT for lung tumors. Radiat Oncol 2012;7:1.
[16] Taguchi K. Temporal resolution and the evaluation of candidate algorithms for four-dimensional CT. Med Phys 2003;30:640–50.
[17] Sonke J, Remeijer P, Van Herk M. Respiration-correlated cone beam CT: obtaining a four-dimensional data set. Med Phys 2003;30:1415.
[18] OBrien R, Shieh C, Kipritidis J, Keall P. TH-E-17A-05: Optimizing Four Dimensional Cone Beam Computed Tomography Projection Allocation to Respiratory Bins. Med Phys. 2014;41:573.
[19] Li T, Xing L. Optimizing 4D cone-beam CT acquisition protocol for external beam radiotherapy. Int J Radiat Oncol Biol Phys 2007;67:1211–9.
[20] Lu J, Guerrero TM, Munro P, Jeung A, Chi P-CM, Balter P, et al. Four-dimensional cone beam CT with adaptive gantry rotation and adaptive data sampling. Med Phys 2007;34:3520–9.
[21] T O'Brien R, Cooper BJ, Shieh C-C, Stankovic U, Keall PJ, Sonke J-J. The first implementation of respiratory triggered 4DCBCT on a linear accelerator. Phys Med Biol 2016;61:3488.
[22] Bergner F, Berkus T, Oelhafen M, Kunz P, Pan T, Grimmer R, et al. An investigation of 4D cone-beam CT algorithms for slowly rotating scanners. Med Phys 2010;37:5044–53.
[23] Chen H, Rottmann J, Yip SS, Morf D, Füglistaller R, Star-Lack J, et al. Super-resolution imaging in a multiple layer EPID. Biomed Phys Eng Express 2017;3:025004.
[24] Star-Lack J, Shedlock D, Swahn D, Humber D, Wang A, Hirsh H, et al. A piecewise-focused high DQE detector for MV imaging. Med Phys 2015;42:5084–99.

[25] Wang Y, Antonuk LE, Zhao Q, El-Mohri Y, Perna L. High-DQE EPIDs based on thick, segmented BGO and CsI: Tl scintillators: performance evaluation at extremely low dose. Med Phys 2009;36:5707–18.
[26] Kirvan P, Monajemi T, Fallone B, Rathee S. Performance characterization of a MVCT scanner using multislice thick, segmented cadmium tungstate-photodiode detectors. Med Phys 2010;37:249–57.
[27] Hardie RC, Barnard KJ, Armstrong EE. Joint MAP registration and high-resolution image estimation using a sequence of undersampled images. IEEE Trans Image Process 1997;6:1621–33.
[28] Bannore V. Iterative-interpolation super-resolution image reconstruction: a computationally efficient technique: Springer Science & Business Media; 2009.
[29] Xia D, Paysan P, Zhang Z, Seghers D, Brehm M, Munro P, et al. Optimization-based Reconstruction from Megavoltage Cone-beam CT Data in Image Guided Radiation Therapy.
[30] Shah AP, Langen KM, Ruchala KJ, Cox A, Kupelian PA, Meeks SL. Patient dose from megavoltage computed tomography imaging. Int J Radiat Oncol Biol Phys 2008;70:1579–87.
[31] Chang J, Sillanpaa J, Ling CC, Seppi E, Yorke E, Mageras G, et al. Integrating respiratory gating into a megavoltage cone-beam CT system. Med Phys 2006;33:2354–61.
[32] Chang J, Mageras GS, Yorke E, De Arruda F, Sillanpaa J, Rosenzweig KE, et al. Observation of interfractional variations in lung tumor position using respiratory gated and ungated megavoltage cone-beam computed tomography. Int J Radiat Oncol Biol Phys 2007;67:1548–58.
[33] Blessing M, Arns A, Wertz H, Stsepankou D, Boda-Heggemann J, Lohr F, et al. Image guided radiation therapy using ultrafast kV-MV CBCT: End-to-End test results of the finalized implementation. Int J Radiat Oncol Biol Phys 2014;90:S828–9.
[34] Arns A, Blessing M, Fleckenstein J, Stsepankou D, Boda-Heggemann J, Simeonova-Chergou A, et al. Towards clinical implementation of ultrafast combined kV-MV CBCT for IGRT of lung cancer. Strahlenther Onkol 2016;192:312–21.
[35] Held M, Cremers F, Sneed PK, Braunstein S, Fogh SE, Nakamura J, et al. Assessment of image quality and dose calculation accuracy on kV CBCT, MV CBCT, and MV CT images for urgent palliative radiotherapy treatments. J Appl Clin Med Phys 2016;17.
[36] Kamino Y, Takayama K, Kokubo M, Narita Y, Hirai E, Kawawda N, et al. Development of a four-dimensional image-guided radiotherapy system with a gimbaled X-ray head. Int J Radiat Oncol Biol Phys 2006;66:271–8.
[37] Kuo JS, Yu C, Petrovich Z, Apuzzo ML. The CyberKnife stereotactic radiosurgery system: description, installation, and an initial evaluation of use and functionality. Neurosurgery 2003;53:1235–9.
[38] Shirato H, Shimizu S, Kitamura K, Nishioka T, Kagei K, Hashimoto S, et al. Four-dimensional treatment planning and fluoroscopic real-time tumor tracking radiotherapy for moving tumor. Int J Radiat Oncol Biol Phys 2000;48:435–42.
[39] Depuydt T, Verellen D, Haas O, Gevaert T, Linthout N, Duchateau M, et al. Geometric accuracy of a novel gimbals based radiation therapy tumor tracking system. Radiother Oncol 2011;98:365–72.
[40] Sothmann T, Blanck O, Poels K, Werner R, Gauer T. Real time tracking in liver SBRT: comparison of CyberKnife and Vero by planning structure-based γ-evaluation and dose-area-histograms. Phys Med Biol 2016;61:1677.
[41] Shen Z-T, Wu X-H, Li B, Zhu X-X. Clinical outcomes of CyberKnife stereotactic body radiotherapy for peripheral stage I non-small cell lung cancer. Med Oncol 2015;32:1–8.
[42] Orecchia R, Surgo A, Muto M, Ferrari A, Piperno G, Gerardi M, et al. VERO® radiotherapy for low burden cancer: 789 patients with 957 lesions. ecancermedicalscience. 2016;10.
[43] Wang Z, Kong Q-T, Li J, Wu X-H, Li B, Shen Z-T, et al. Clinical outcomes of cyberknife stereotactic radiosurgery for lung metastases. J Thorac Dis 2015;7:407.
[44] Brown WT, Wu X, Fayad F, Fowler JF, Amendola BE, García S, et al. CyberKnife® radiosurgery for stage I lung cancer: results at 36 months. Clin Lung Cancer 2007;8:488–92.
[45] Jung I-H, Song SY, Jung J, Cho B, Kwak J, Je HU, et al. Clinical outcome of fiducial-less CyberKnife radiosurgery for stage I non-small cell lung cancer. Radiat Oncol J 2015;33:89.
[46] Keall PJ, Colvill E, O'Brien R, Ng JA, Poulsen PR, Eade T, et al. The first clinical implementation of electromagnetic transponder-guided MLC tracking. Med Phys 2014;41.
[47] Booth JT, Caillet V, Hardcastle N, O'Brien R, Szymura K, Crasta C, et al. The first patient treatment of electromagnetic-guided real time adaptive radiotherapy using MLC tracking for lung SABR. Radiother Oncol 2016;121:19–25.
[48] Davies G, Poludniowski G, Webb S. MLC tracking for Elekta VMAT: a modelling study. Phys Med Biol 2011;56:7541.
[49] Fast MF, Nill S, Bedford JL, Oelfke U. Dynamic tumor tracking using the Elekta Agility MLC. Med Phys 2014;41.
[50] Tacke MB, Nill S, Krauss A, Oelfke U. Real-time tumor tracking: automatic compensation of target motion using the Siemens 160 MLC. Med Phys 2010;37:753–61.
[51] Krauss A, Nill S, Tacke M, Oelfke U. Electromagnetic real-time tumor position monitoring and dynamic multileaf collimator tracking using a Siemens 160 MLC: geometric and dosimetric accuracy of an integrated system. Int J Radiat Oncol Biol Phys 2011;79:579–87.
[52] D'Souza D, Naqvi SA, Cedric XY. Real-time intra-fraction-motion tracking using the treatment couch: a feasibility study. Phys Med Biol 2005;50:4021.
[53] Hansen R, Ravkilde T, Worm ES, Toftegaard J, Grau C, Macek K, et al. Electromagnetic guided couch and multileaf collimator tracking on a TrueBeam accelerator. Med Phys 2016;43:2387–98.
[54] Lang S, Zeimetz J, Ochsner G, Schmid Daners M, Riesterer O, Klöck S. Development and evaluation of a prototype tracking system using the treatment couch. Med Phys 2014;41.
[55] Toftegaard J, Hansen R, Ravkilde T, Macek K, Poulsen PR. An experimentally validated couch and MLC tracking simulator used to investigate hybrid couch-MLC tracking. Med Phys 2017.
[56] Gibbs IC, Loo BW. CyberKnife stereotactic ablative radiotherapy for lung tumors. Technol Cancer Res Treat 2010;9:589–96.
[57] Soldà F, Lodge M, Ashley S, Whitington A, Goldstraw P, Brada M. Stereotactic radiotherapy (SABR) for the treatment of primary non-small cell lung cancer; systematic review and comparison with a surgical cohort. Radiother Oncol 2013;109:1–7.
[58] Pepin EW, Wu H, Zhang Y, Lord B. Correlation and prediction uncertainties in the cyberknife synchrony respiratory tracking system. Med Phys 2011;38:4036–44.
[59] Willoughby TR, Forbes AR, Buchholz D, Langen KM, Wagner TH, Zeidan OA, et al. Evaluation of an infrared camera and X-ray system using implanted fiducials in patients with lung tumors for gated radiation therapy. Int J Radiat Oncol Biol Phys 2006;66:568–75.
[60] Wurm R, Gum F, Erbel S, Schlenger L, Scheffler D, Agaoglu D, et al. Image guided respiratory gated hypofractionated Stereotactic Body Radiation Therapy (H-SBRT) for liver and lung tumors: initial experience. Acta Oncol 2006;45:881–9.
[61] Whyte RI, Crownover R, Murphy MJ, Martin DP, Rice TW, DeCamp MM, et al. Stereotactic radiosurgery for lung tumors: preliminary report of a phase I trial. Ann Thorac Surg 2003;75:1097–101.
[62] Nabavizadeh N, Zhang J, Elliott DA, Tanyi JA, Thomas Jr CR, Fuss M, et al. Electromagnetic navigational bronchoscopy-guided fiducial markers for lung stereotactic body radiation therapy: analysis of safety, feasibility, and interfraction stability. J Bronchol Interventional Pulmonol 2014;21:123–30.
[63] Harley DP, Krimsky WS, Sarkar S, Highfield D, Aygun C, Gurses B. Fiducial marker placement using endobronchial ultrasound and navigational bronchoscopy for stereotactic radiosurgery: an alternative strategy. Ann Thorac Surg 2010;89:368–74.
[64] Hong JC, Eclov NC, Yu Y, Rao AK, Dieterich S, Le Q-T, et al. Migration of implanted markers for image-guided lung tumor stereotactic ablative radiotherapy. J Appl Clin Med Phys 2013;14.
[65] Hardcastle N, Booth J, Caillet V, O'Brien R, Haddad C, Crasta C, et al. MO-FG-BRA-06: electromagnetic beacon insertion in lung cancer patients and resultant surrogacy errors for dynamic MLC tumour tracking. Med Phys 2016;43:3710–1.
[66] James J, Swanson C, Lynch B, Wang B, Dunlap NE. Quantification of planning target volume margin when using a robotic radiosurgery system to treat lung tumors with spine tracking. Pract Radiat Oncol 2015;5:e337–43.
[67] Higgins J, Bezjak A, Franks K, Le LW, Cho B, Payne D, et al. Comparison of spine, carina, and tumor as registration landmarks for volumetric image-guided lung radiotherapy. Int J Radiat Oncol Biol Phys 2009;73:1404–13.
[68] Lavoie C, Higgins J, Bissonnette J-P, Le LW, Sun A, Brade A, et al. Volumetric image guidance using carina vs spine as registration landmarks for conventionally fractionated lung radiotherapy. Int J Radiat Oncol Biol Phys 2012;84:1086–92.
[69] Fu D, Kahn R, Wang B, Wang H, Mu Z, Park J, et al. Xsight lung tracking system: a fiducial-less method for respiratory motion tracking. Treating Tumors that Move with Respiration: Springer; 2007. p. 265-82.
[70] Shieh C-C, Keall PJ, Kuncic Z, Huang C-Y, Feain I. Markerless tumor tracking using short kilovoltage imaging arcs for lung image-guided radiotherapy. Phys Med Biol 2015;60:9437.
[71] Rottmann J, Keall P, Berbeco R. Markerless EPID image guided dynamic multi-leaf collimator tracking for lung tumors. Phys Med Biol 2013;58:4195.
[72] Mijnheer B, Olaciregui-Ruiz I, Rozendaal R, Spreeuw H, van Herk M, Mans A. Current status of 3D EPID-based in vivo dosimetry in The Netherlands Cancer Institute. Journal of Physics: Conference Series: IOP Publishing; 2015. p. 012014.
[73] Woodruff HC, Fuangrod T, Van Uytven E, McCurdy BM, van Beek T, Bhatia S, et al. First experience with real-time EPID-based delivery verification during IMRT and VMAT sessions. Int J Radiat Oncol Biol Phys 2015;93:516–22.
[74] Shah AP, Kupelian PA, Waghorn BJ, Willoughby TR, Rineer JM, Mañon RR, et al. Real-time tumor tracking in the lung using an electromagnetic tracking system. Int J Radiat Oncol Biol Phys 2013;86:477–83.
[75] Wilbert J, Baier K, Hermann C, Flentje M, Guckenberger M. Accuracy of real-time couch tracking during 3-dimensional conformal radiation therapy, intensity modulated radiation therapy, and volumetric modulated arc therapy for prostate cancer. Int J Radiat Oncol Biol Phys 2013;85:237–42.
[76] Sawant A, Smith RL, Venkat RB, Santanam L, Cho B, Poulsen P, et al. Toward submillimeter accuracy in the management of intrafraction motion: the integration of real-time internal position monitoring and multileaf collimator target tracking. Int J Radiat Oncol Biol Phys 2009;74:575–82.
[77] Caillet V, Colvill E, Szymura K, Stevens M, Booth J, Keall P. SU-G-JeP1-05: Clinical Impact of MLC Tracking for Lung SABR. Med Phys 2016;43:3648–9.
[78] Colvill E, Poulsen PR, Booth J, O'brien R, Ng J, Keall P. DMLC tracking and gating can improve dose coverage for prostate VMAT. Med Phys. 2014;41.
[79] Ruan D. Kernel density estimation-based real-time prediction for respiratory motion. Phys Med Biol 2010;55:1311.

[80] Giraud P, Morvan E, Claude L, Mornex F, Le Pechoux C, Bachaud J-M, et al. Respiratory gating techniques for optimization of lung cancer radiotherapy. J Thorac Oncol 2011;6:2058–68.
[81] D'Ambrosio DJ, Bayouth J, Chetty IJ, Buyyounouski MK, Price RA, Correa CR, et al. Continuous localization technologies for radiotherapy delivery: report of the American Society for Radiation Oncology Emerging Technology Committee. Pract Radiat Oncol 2012;2:145–50.
[82] Barnes EA, Murray BR, Robinson DM, Underwood LJ, Hanson J, Roa WH. Dosimetric evaluation of lung tumor immobilization using breath hold at deep inspiration. Int J Radiat Oncol Biol Phys 2001;50:1091–8.
[83] Goldstein JD, Lawrence YR, Appel S, Landau E, Ben-David MA, Rabin T, et al. Continuous positive airway pressure for motion management in stereotactic body radiation therapy to the lung: a controlled pilot study. Int J Radiat Oncol Biol Phys 2015;93:391–9.
[84] T Eade JB, P Keall. Lung Cancer Radiotherapy Using Realtime Dynamic Multileaf Collimator (MLC) Adaptation And Radiofrequency Tracking (LIGHTSABR). ClinicalTrials.gov2015.
[85] Daly ME, Perks JR, Chen AM. Patterns-of-care for thoracic stereotactic body radiotherapy among practicing radiation oncologists in the United States. J Thorac Oncol 2013;8:202–7.
[86] Heinzerling JH, Anderson JF, Papiez L, Boike T, Chien S, Zhang G, et al. Four-dimensional computed tomography scan analysis of tumor and organ motion at varying levels of abdominal compression during stereotactic treatment of lung and liver. Int J Radiat Oncol Biol Phys 2008;70:1571–8.
[87] Baker R, Han G, Sarangkasiri S, DeMarco M, Turke C, Stevens CW, et al. Clinical and dosimetric predictors of radiation pneumonitis in a large series of patients treated with stereotactic body radiation therapy to the lung. Int J Radiat Oncol Biol Phys 2013;85:190–5.
[88] Heerkens H, Reerink O, Intven M, Hiensch R, van den Berg C, Crijns S, et al. Pancreatic tumor motion reduction by use of a custom abdominal corset. Phys Imaging Radiat Oncol 2017;2:7–10.
[89] Baba F, Shibamoto Y, Tomita N, Ikeya-Hashizume C, Oda K, Ayakawa S, et al. Stereotactic body radiotherapy for stage I lung cancer and small lung metastasis: evaluation of an immobilization system for suppression of respiratory tumor movement and preliminary results. Radiat Oncol 2009;4:15.
[90] Han K, Cheung P, Basran PS, Poon I, Yeung L, Lochray F. A comparison of two immobilization systems for stereotactic body radiation therapy of lung tumors. Radiother Oncol 2010;95:103–8.
[91] Chao ST, Koyfman SA, Woody N, Angelov L, Soeder SL, Reddy CA, et al. Recursive partitioning analysis index is predictive for overall survival in patients undergoing spine stereotactic body radiation therapy for spinal metastases. Int J Radiat Oncol Biol Phys 2012;82:1738–43.
[92] Negoro Y, Nagata Y, Aoki T, Mizowaki T, Araki N, Takayama K, et al. The effectiveness of an immobilization device in conformal radiotherapy for lung tumor: reduction of respiratory tumor movement and evaluation of the daily setup accuracy. Int J Radiat Oncol Biol Phys 2001;50:889–98.
[93] Korreman S, Persson G, Nygaard D, Brink C, Juhler-Nøttrup T. Respiration-correlated image guidance is the most important radiotherapy motion management strategy for most lung cancer patients. Int J Radiat Oncol Biol Phys 2012;83:1338–43.
[94] Guckenberger M, Krieger T, Richter A, Baier K, Wilbert J, Sweeney RA, et al. Potential of image-guidance, gating and real-time tracking to improve accuracy in pulmonary stereotactic body radiotherapy. Radiother Oncol 2009;91:288–95.
[95] Wunderink W, Romero AM, De Kruijf W, De Boer H, Levendag P, Heijmen B. Reduction of respiratory liver tumor motion by abdominal compression in stereotactic body frame, analyzed by tracking fiducial markers implanted in liver. Int J Radiat Oncol Biol Phys 2008;71:907–15.
[96] Bouilhol G, Ayadi M, Rit S, Thengumpallil S, Schaerer J, Vandemeulebroucke J, et al. Is abdominal compression useful in lung stereotactic body radiation therapy? A 4DCT and dosimetric lobe-dependent study. Physica Med 2013;29:333–40.
[97] Otani Y, Fukuda I, Tsukamoto N, Kumazaki Y, Sekine H, Imabayashi E, et al. A comparison of the respiratory signals acquired by different respiratory monitoring systems used in respiratory gated radiotherapy. Med Phys 2010;37:6178–86.
[98] Bradley JD, Nofal AN, El Naqa IM, Lu W, Liu J, Hubenschmidt J, et al. Comparison of helical, maximum intensity projection (MIP), and averaged intensity (AI) 4D CT imaging for stereotactic body radiation therapy (SBRT) planning in lung cancer. Radiother Oncol 2006;81:264–8.
[99] Weibert K, Biller S, Wendt TG, Wiezorek T. Dosimetry of a linear accelerator under respiratory gating. Zeitschrift für Medizinische Physik 2009;19:136–41.
[100] Li XA, Stepaniak C, Gore E. Technical and dosimetric aspects of respiratory gating using a pressure-sensor motion monitoring system. Med Phys 2006;33:145–54.
[101] Pollock S, Keall R, Keall P. Breathing guidance in radiation oncology and radiology: a systematic review of patient and healthy volunteer studies. Med Phys 2015;42:5490–509.

CHAPTER 04

MLC tracking for lung SABR reduces planning target volumes and dose to organs-at-risk

This chapter was published in *Radiotherapy and Oncology* and written by me.

The purpose of this chapter was to estimate the potential benefits of implementing MLC tracking in a clinical environment for patients diagnosed with lung cancer. For that purpose, a dose reconstruction study was used to assess the dosimetric benefits of MLC tracking and compare these dosimetric outcomes with mid-ventilation and ITV-based planning and delivery methods.

This manuscript is the first of its kind to compare a clinically implemented MLC tracking techniques with ITV-based planning and mid-ventilation planning using real tumour motion. In the grand scheme of this thesis, these experiments estimate the feasibility and potential benefits of this frontier technology and laid the foundations for understanding the clinical procedures required to treat actual patients as part of the MLC tracking for lung SABR clinical trial.

Radiotherapy and Oncology 124 (2017) 18–24

Contents lists available at ScienceDirect

Radiotherapy and Oncology

journal homepage: www.thegreenjournal.com

MLC tracking in lung cancer

MLC tracking for lung SABR reduces planning target volumes and dose to organs at risk

Vincent Caillet [a,b], Paul J. Keall [b], Emma Colvill [a,b], Nicholas Hardcastle [a], Ricky O'Brien [b], Kathryn Szymura [a], Jeremy T. Booth [a,b,*]

[a] Northern Sydney Cancer Centre, Level 1 Royal North Shore Hospital; and [b] University of Sydney, Schools of Physics or Medicine, Australia

ARTICLE INFO

Article history:
Received 7 July 2016
Received in revised form 8 June 2017
Accepted 9 June 2017
Available online 24 June 2017

Keywords:
Lung cancer
Real time adaptive radiotherapy
MLC tracking
Radiation pneumonitis

ABSTRACT

Purpose: Assess the dosimetric impact of multi-leaf collimator (MLC) tracking and mid-ventilation (midV) planning compared with the internal target volume (ITV)-based planning approach for lung Stereotactic Ablative Body Radiotherapy (SABR).
Method: Ten lung SABR patients originally treated with an ITV-based plan were re-planned according to MLC tracking and midV planning schemes. All plans were delivered on a linac to a motion phantom in a simulated treatment with real lung motions. Delivered dose was reconstructed in patient planning scans. ITV-based, tracking and midV regimes were compared at the planning and delivered stages based on PTV volume and dose metrics for the GTV and OAR.
Results: MLC tracking and midV schemes yielded favourable outcomes compared with ITV-based plans. Average reduction in PTV volume was (MLC tracking/MidV) 33.9%/22%. GTV dose coverage performed better with MLC tracking than the other regimes. Reduction in dose to OAR were for the lung (mean lung dose, 0.8 Gy/0.2 Gy), oesophagus (D3 cc, 1.9 Gy/1.4 Gy), great vessels (D10 cc, 3.2 Gy/1.3 Gy), trachea (D4 cc, 1.1 Gy/0.9 Gy), heart (D1 cc, 2.0 Gy/0.5 Gy) and spinal cord (D0.03 cc, 0.5 Gy/−0.1 Gy).
Conclusion: MLC tracking showed reduction in PTV volume, superior GTV dose coverage and organ dose sparing than MidV and ITV-based strategies.
© 2017 Elsevier B.V. All rights reserved. Radiotherapy and Oncology 124 (2017) 18–24

Stereotactic Ablative Body Radiotherapy (SABR) delivering hypofractionated doses to the tumour is increasing in use due to the encouraging local control rates with minimal toxicity [1,2]. Lung SABR treatments require careful treatment planning and extensive pre-treatment image guidance to ensure the high dose is correctly placed in the lung [3]. In the presence of motion, this task becomes challenging. The prevalent approach, recommended by the ICRU 83, is to apply the Internal Treatment Volume (ITV)-based motion-inclusive method that enlarges the treatment fields to account for motion and uncertainty. Since dose to organs-at-risk (OAR) generally shows a relationship with toxicity [4], numerous strategies have been deployed to moderate unnecessary dose spillage such as treatment beam gating [5], adaptive couch tracking [6], adaptive real-time tumour tracking [7–9] and passive strategies such as the mid-ventilation (midV) planning treatment volume (PTV)-based approach [10].

Multi-leaf collimator (MLC) tracking for lung tumours is an active motion management technique that utilizes the MLC leaves within the head of the linac. During tracking, the radiation beam is shifted to correct for tumour motion from respiration. This strategy has the potential to increase the dose distribution conformity despite fast moving tumours or baseline shifts. The midV approach for lung SABR is a planning approach that accounts for the population-based statistical uncertainties to define the set of margins used for the PTV [11,12].

The purpose of this study is to investigate potential clinical benefits of MLC tracking compared against midV and ITV-based planning for lung SABR in end-to-end clinically realistic planning and delivery scenarios. We performed a dosimetric comparison between motion management strategies using real patient motion traces to allow comparison between the three techniques. This study supported the implementation of a current prospective clinical trial (NCT02514512) to evaluate the use of MLC tracking for lung SABR to meet requirements of practicability in a clinical environment and its operability at meeting dosimetric constraints.

Methods and material

Treatment planning

Ten consecutive patients were previously treated with ITV-based SABR-VMAT (Volumetric Modulated Arc Therapy) in

* Corresponding author at: Northern Sydney Cancer Centre, Level 1 Royal North Shore Hospital, Reserve Rd, St Leonards NSW 2065, Australia.
E-mail address: Jeremy.Booth@health.nsw.gov.au (J.T. Booth).

http://dx.doi.org/10.1016/j.radonc.2017.06.016
0167-8140/© 2017 Elsevier B.V. All rights reserved.

the period 2014–2015 at our institution. Patients were diagnosed with non-small cell lung carcinoma (NSCLC) stage I or oligometastatic lung metastases. The original treatments were based on a conventional ITV-based plan. Patients were planned based on the dose constraints from RTOG 0813 and 0915 with 100% of the Gross Tumour Volume (GTV) receiving no less than 100% of the dose and at least 97% of the PTV receiving 100% of the dose [13,14]. Three patients received 48 Gy in 4 fractions and seven patients received 50 Gy in 5 fractions. Planning was performed in the Eclipse treatment planning system (v. 11.3, Varian Medical Systems, Palo Alto) using the analytical anisotropic algorithm (AAA). The ITV was contoured using the maximum intensity projection from a 4D-CT dataset. The planning treatment volume ($PTV_{ITV\text{-}BASED}$) was created as a uniform 5 mm expansion of the ITV. Collimator angles of 40°/50° were used.

The first step was for each patient to be replanned following an adaptive tracking protocol. The GTV was defined on the end-of-exhale phase, namely the GTV_{TRACK}, to assure a proper localization and delineation of the tumour [7,15–17]. Collimators were angled to have the leaf trajectory parallel to the superior–inferior motion (85/95°) [18]. Around the GTV_{TRACK}, a 5 mm uniform margin was applied to create the PTV_{TRACK}. This PTV_{TRACK} accounts for motion-related errors from a range of sources including motion prediction errors, Calypso positioning system uncertainties, MLC leaf width, and beacon-to-tumour centroid surrogacy errors. The prediction algorithm was tested on 110 lung traces from 22 patients [19] with an accuracy estimated to be ±0.8 mm (95% confidence interval). Calypso tracking system positioning errors were reported to be ±0.56 mm [20]. Motion along the MLC leaves translates with sub-millimetre accuracy but the perpendicular motion can misalign the target, contributing to the maximum possible error of ±2.5 mm (i.e. ± half a leaf width on a Varian Trilogy linac). The maximum error was implemented into the margins calculation to accommodate for the worst-case scenario. Surrogacy between markers and tumour positions were found to be ±1.0 mm [21,22]. These uncertainties add in quadrature to 2.9 mm. The decision to keep 5 mm is therefore more conservative than needed but offered reassurance for the start of the clinical trial.

The second step was for the original patients' plans to be adjusted for the mid-ventilation passive strategy. Margins were defined based on the work of Van Herk [11]. Parameters were obtained from Sonke et al. [12] while the method applied for selecting the mid-ventilation phase was done following the work of Peulen et al. [10]. The same collimator angle as the ITV-based plans was used to respect planning consistency. For all patients, the margins calculated for the left–right and anterior–posterior amplitude were 6 mm. In the superior–inferior direction, the margins were also 6 mm when the motion was less than 7 mm, or the margins were extended to 7 mm otherwise. The margin recipe calculates with high accuracy the margin necessary but the TPS discretizes the margins values to the nearest millimetre.

The target structures were all contoured by a single experienced radiation oncologist and optimized by a single senior radiation therapist to ensure that the plans were optimized comparably between each other. Dose to OARs was optimized to be as low as possible following our strict in-house regulation conforming to the RTOG guidelines.

Treatment plan delivery

For each motion management strategy, the treatment plans were delivered to a moving phantom (Fig. 1) to generate MLC tracking logs from which simulated delivered doses can be reconstructed. Respiratory motion for each patient was estimated from the 4D-CT motion extent and matched with the closest trace available in a Synchrony (Accuray Inc., Sunnyvale, CA) motion database [13]. Each patient plan was matched with the first fraction of a Cyberknife patient based on both the 3D Peak to Trough (PTT) distance and the most dominant tumour motion direction. The motion in the next fraction for that same Synchrony patient was used as the clinically realistic target trajectory input for a programmable motion phantom for simulated treatment. Table 1 provides details of the PTT distance of each patient and their respective match in the synchrony database.

The 30 plans were delivered to a programmable motion phantom as shown in Fig. 1. Three electromagnetic beacon transponders were placed onto the HexaMotion 6D platform (Scandidos, Uppsala) programmed with the selected lung motion traces moving in three dimensions. The in-house MLC tracking software is integrated with the Calypso real-time position monitoring system and a Varian linear accelerator. Real-time positions are fed to the MLC tracking software which calculates the new leaf positions and sends them to the MLC controller. MLC log files (Dynalog) and target trajectory files were collected for use in dose reconstruction.

Dose reconstruction

Two strategies were deployed for dose reconstruction to differentiate organs that move with respiration and static organs, with separate reconstructions for each summarized in Fig. 2. The GTV and lung were considered structures moving equivalently with breathing cycle while spinal cord, heart, oesophagus, great vessels and trachea were simulated as static (Fig. 3).

To evaluate the dose that would have been delivered for each motion management strategy, the MLC positions and target trajectory files were inputted into the dose reconstruction software. The software provided the dose distribution post-treatment for moving structures by binning the treatment arc into multiple isocentre shifts according to the detected tumour motions. The target motion was divided into 1 mm bins so that a series of sub-arcs, each corresponding to motion within that 1 mm bin was created with the isocentre at the centre of the bin. The multiple sub-arc plan was then imported into Eclipse for dose calculation. With this method, the sum of the arcs in the bins equal the angle spanned for the original treatment arcs. Further details on the dose reconstruction framework can be found in Poulsen et al. [23]. For the evaluation of the dose distribution for static organs, tumour motion trajectory files were not used and a single treatment isocentre was used instead (using delivered MLC and no motion).

For dose reconstruction of the ITV-based plan, the GTV dose coverage is simulated by the dose reconstruction method above. However the OARs are considered static, so the dose to static organs during ITV-based treatment therefore equated to the planned dose (MLC and no motion).

Data analysis

The analysis to determine the potential role of each motion management strategy was assessed based on the target dose coverage and the OAR dose reductions comparatively from ITV-based to MLC tracking or midV approaches. The statistical differences between strategies was assessed using a Wilcoxon signed-rank non-parametric statistical test (one-tail).

Assessment of target dose coverage

To validate the delivered target doses for the motion management strategies, the reconstructed GTV_{TRACK}, GTV_{MidV} and $GTV_{ITV\text{-}BASED}$ D98% (the dose received by 98% of the volume, i.e. near-minimum dose), D95% and D2% (i.e. near-maximum dose) were compared to their planned equivalent dose metric values.

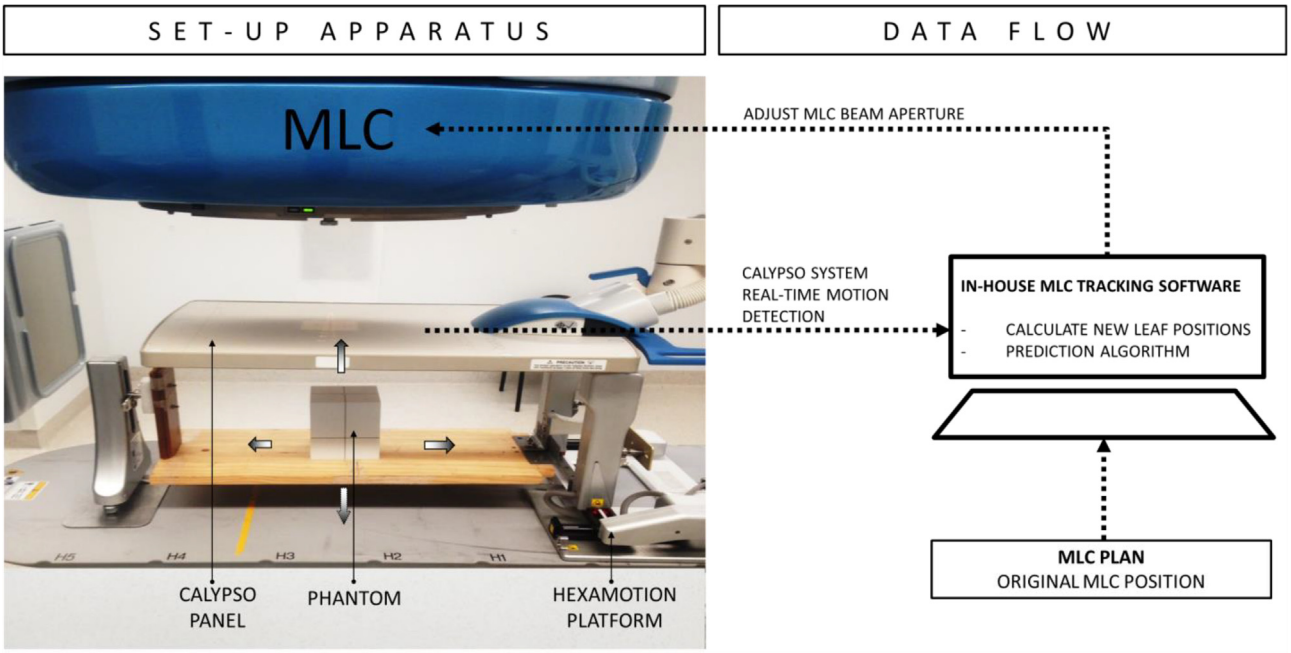

Fig. 1. Experimental set-up and data flow of the MLC tracking system. Motion of the phantom containing electromagnetic transponders on the HexaMotion platform was detected by the Calypso tracking system and sent to an in-house tracking software to calculate and reshape the MLC leaves in real-time.

Table 1
Summary of patient motion evaluated at 4D-CT compared with the motion used during physical experiments. 4D-CT motion was evaluated and matched with the first fraction obtained from a synchrony database. Fraction 2 of that same synchrony patient was used as the tumour motion input into the motion platform.

Patient #	4DCT PTT	PTT Delivered Tumour Motion	PTV ITV-based	PTV Tracking	PTVMidV	Lobe	PTV Characteristics	Baseline shift*	PTV Excursion**
1	0.31 cm	0.24 cm	23 cm^3	14 cm^3	18 cm^3	Right UL	Overlaps with the bronchi; ultra-central tumour	1 mm lateral toward periphery	No
2	0.67 cm	0.68 cm	49 cm^3	32 cm^3	39 cm^3	Right ML	Overlaps with the heart	No	No
3	0.05 cm	0.02 cm	17 cm^3	13 cm^3	11 cm^3	Left UL	Sitting right above the heart in transverse plan – transverse plan of trachea and bronchi	No	No
4	0.18 cm	0.23 cm	15 cm^3	10 cm^3	12 cm^3	Right UL	Overlaps with upper chestwall	No	No
5	0.25 cm	0.23 cm	13 cm^3	7 cm^3	9 cm^3	Right ML	Superior to the heart – dose out of range of the OAR	No	No
6	0.56 cm	0.16 cm	68 cm^3	62 cm^3	71 cm^3	Right ML	Tumour very large – no motion – close proximity to the spinal cord	No	No
7	0.34 cm	0.33 cm	19 cm^3	13 cm^3	16 cm^3	Left UL	Relatively distant from any OAR	No	No
8	0.18 cm	0.81 cm	116 cm^3	51 cm^3	52 cm^3	Right ML	Relatively distant from any OAR	No	No
9	1.10 cm	0.88 cm	41 cm^3	28 cm^3	35 cm^3	Right LL	Overlaps with posterior chestwall	No	No
10	0.42 cm	0.85 cm	36 cm^3	23 cm^3	29 cm^3	Right LL	Overlaps with posterior chestwall	1 mm lateral 2 mm anterior	No

Abv: PTT = Peak-to-trough.
* Baseline shift detected when maximum to minimum position exceeded 0.5 mm. Taken over an averaging window of 10 s.
** PTV excursion occurs during ITV-based treatment when GTV position is outside the PTV. PTV excursion was estimated using the detected tumour motion and calculating the time the GTV within the ITV would have spent outside the $PTV_{ITV\text{-}BASED}$.

OAR exposure in the presence of motion

For both planned and reconstructed dose, a set of statistical comparisons of dose-metrics was used to report the dose difference for both target and OAR structures from ITV-based plans. This scheme provides the dose difference as positive values to reflect a dose reduction) compared to ITV-based planning. Mean lung dose and V20 are commonly used as a metric for dose reporting and were shown to be correlated with pulmonary toxicities [24–27]. We report mean lung dose reduction (bilateral lung volume minus the GTV) and V20 reduction (percentage of the bilateral lung volume minus the GTV receiving 20 Gy). Further, OAR dose–volume metrics, as prescribed by the ICRU 83 [28], were reported for the spinal cord (D0.3 cc), heart (D1 cc), oesophagus (D3 cc), trachea (D4 cc) and great vessels (D10 cc).

Uncertainties of dose reconstruction

The dose reconstruction method utilized in this study relies on assumptions regarding relative motion and dose accumulation

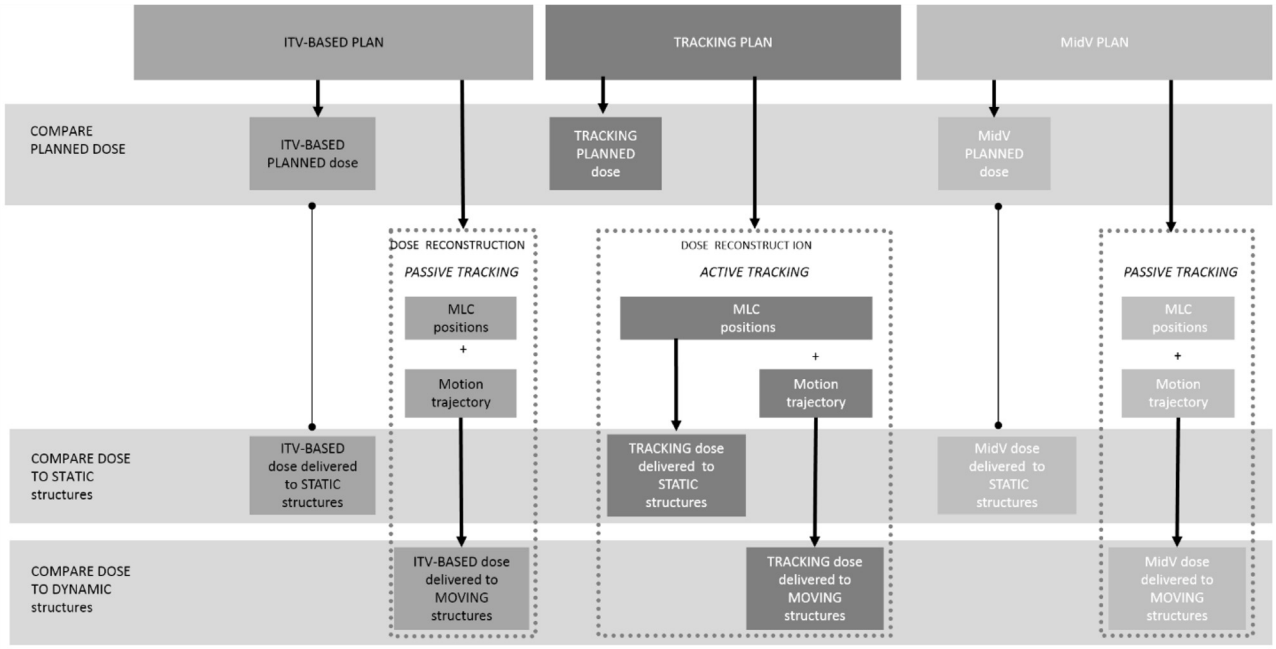

Fig. 2. Overview of the planned and reconstructed dose comparisons for ITV-based, MLC tracking and mid-ventilation. The estimation of the delivered doses during ITV-based, MLC tracking, and midV treatments to static (spinal cord, heart, oesophagus, trachea and great vessels) and moving targets (lung and target) required different inputs acquired through delivery of the two treatment plans: the MLC positions for static organs and both the MLC positions and the trajectory positions for the moving structures. Dose–Volume Histogram metrics of the motion management strategies were then compared.

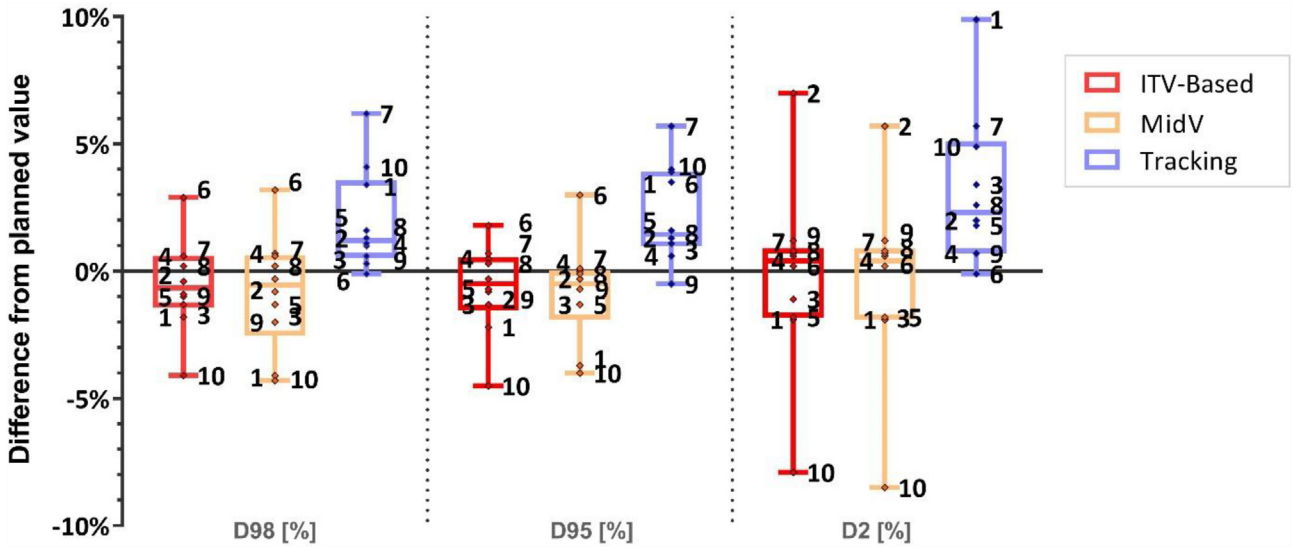

Fig. 3. Reconstructed GTV dose coverage (D98%, D95% and D2%) for ITV-based (red), midV (orange) and tracking (red) delivery. Individual patient numbers are shown on the boxplots. The box plots depict the minimum and maximum values, the upper and lower quartiles and the median (line).

across moving/deforming organs that lead to uncertainty in the reported dose metrics. Specifically, the MLC tracking and midV plans were set on one specific reference phase. A sensitivity analysis method was developed to provide the range in dose metric values as an uncertainty estimate across the full 4D-CT phases for each OAR. The first step in this sensitivity analysis was to transfer the reference plan to the other phases of the 4D-CT. The isocentre was shifted according to the GTV position for each phase, and each OAR was re-contoured. The second step was to calculate the dose on each phase and calculate the dose metrics (i.e. mean lung dose, D3 cc etc.) associated with each OAR. The standard deviation of each dose metric across phases then constitutes the sensitivity to motion and the uncertainty in dose reconstruction. The average of standard deviations was calculated for each organ to indicate the magnitude of error and estimate the errors during the dose reconstruction of both static and moving organs.

Results

PTV reduction

The mean PTV of the ITV-based plans (39.6 cm^3), was reduced with MLC tracking (24.8 cm^3) representing a mean percentage reduction of 37.3% (range 9–56%). The mean PTV was also reduced with the midV plans (29.3 cm^3) compared to the ITV-based plans with a mean percentage reduction of 26% (range −5–33%).

As expected, the magnitude of the PTV percentage reduction for midV plans was smaller than MLC tracking. The margins for MLC tracking are set to 5 mm for all patients, whereas with midV plans the PTV margins start at ~6 mm for GTV without motion and increase with motion. In one instance, the PTV_{MidV} was larger than its $PTV_{ITV\text{-}BASED}$ comparator due to small motion and artefacts in the mid-ventilation phase planned (See Table 1, patient 6).

Assessment of target dose coverage

For each motion management strategy, the reconstructed dose to the target is consistently higher or closer to planned dose using MLC tracking than the other motion management strategies. The GTV_{TRACK} dose coverage across patients were all superior and statistically different ($p < 0.01$, one sided) than the midV and ITV-based dose coverage.

Comparing MLC tracking planned against delivered, the GTV dose metrics D95%, D98% and D2% obtained during treatment were larger than the equivalent planned dose metrics with the percentage changes of 1.8% (±2.0%, $p < 0.01$), 2.1% (±1.8%, $p < 0.01$) and 2.8% (±2.8%, $p < 0.01$) respectively. The increase in dose metric values is thought to be contributed to by errors in prediction algorithm and MLC tracking errors.

For the midV regime, the delivered GTV D95%, D98% and D2% is different from midV planned by −0.5% (±1.6%, $p > 0.2$), −0.6% (±1.6%, $p > 0.2$), and −0.2% (±3.1%, $p > 0.2$) respectively. The average delivered dose to the target is close to zero, whereas variation between patients (i.e. standard deviation) is larger than without tracking.

For the ITV-based regime, the GTV dose metrics of D95%, D98% and D2% being −0.4% (±2.1%, $p = 0.3$), −0.65% (±1.6%, $p = 0.3$) and −0.4% (±3.2%, $p = 0.3$) compared with their planned values. No significant differences were seen between planned and delivered in these cases.

OAR exposure in the presence of motion

Using MLC tracking and midV, dose reductions to the OAR for both planned and dose reconstruction dose metrics suggest benefit over the ITV-based planning method. Differences in dose metrics are shown in Fig. 4. Every organ shows a positive average dose reduction implying that, for this cohort of patients, midV and MLC tracking regimes both improve the treatment quality over the ITV-based planning method. For the delivered treatment, reduction in dose to OAR were (MLC Tracking/MidV) for the lung (mean lung dose, 0.8 Gy/0.2 Gy and V20 Gy, 1.6/0.3%), oesophagus (D3 cc, 1.9 Gy/1.4 Gy), great vessels (D10 cc, 3.2 Gy/1.3 Gy), trachea (D4 cc, 1.1 Gy/0.9 Gy), heart (D1 cc, 2.0 Gy/0.5 Gy) and spinal cord (D0.03 cc, 0.5 Gy/−0.1 Gy). Using MLC tracking, the dose distribution was shown to be significantly different from the ITV-based plan for the lung, oesophagus, heart and trachea (only the delivered data for trachea). However, no statistical differences were found for the mean lung dose, V20 and spinal cord. Similarly, the mid-ventilation approach demonstrated that on average the dose was reduced using mid-ventilation planning, however the dose distributions were not significantly different than the ITV-based plan.

The accuracy of the dose reconstruction is reported as the range in dose metrics across all phases for each patient. Using the 4D-CT, the mean lung dose exported for each 10 phases of each patient showed a mean lung dose range of ±0.2 Gy across all phases. Similarly, it was calculated a range of ±0.2% for the V20, ±0.3 Gy for the oesophagus, ±0.2 Gy for the great vessels, ±0.6 Gy for the trachea, ±0.4 Gy for the heart and ±0.2 Gy for the spinal cord.

For both MLC tracking and midV strategies, individual large dose reductions were shown. Heart D1 cc shows reduction up to 17.6 Gy for Patient 2 (See Supplementary Fig. 1 for an example of dose distribution) where the original $PTV_{ITV\text{-}BASED}$ overlaps with the heart, while the reduction in target defined by the PTV_{TRACK} avoids this overlap. Similar dose reductions for other OAR (expressed as delivered dose metrics reduction for Tracking/MidV) were observed for oesophagus (Patient 3, 6.5/4.8 Gy for D3 cc), great vessels (Patient 3, 10.8/8.4 Gy for D10 cc), trachea (Patient 1, 6.0/4.0 Gy for D4 cc), heart (Patient 2, 17.6 Gy/5.5 Gy) and spinal cord (Patient 10, 3.2/2.0 Gy for D0.3 cc). These individual cases all had in common the position of the OAR either close to the target or at the same superior–inferior level as the treatment field.

Discussion

MLC tracking dosimetric performance

Potential dosimetric benefits for lung SABR with MLC tracking and midV have been shown by quantifying a reduction in dose delivered to the OAR while maintaining the target dose coverage. For tracking, the 30% reduction in PTV found in this study is consistent in magnitude with the PTV reduction of 30.2% and 36% reported with the Cyberknife experience [29] and the Vero gimbal linac [7], respectively. This study was conducted in a clinically realistic scenario, in that the treatment workflow was followed and real patient motion trajectories applied, supporting clinical translation from benchtop to bedside of a prospective clinical trial for MLC tracking with implanted electromagnetic transponders (NCT02514512).

This study underlines and refocuses on the purposes of MLC tracking for lung. For this cohort of patients, the use of motion management mildly influenced the delivered target dose coverage, showing for all 10 patients acceptable doses even without using MLC tracking or mid-ventilation. The strength of MLC tracking was found in its ability to significantly reduce the dose spillage to the OAR. This study also showed that MLC tracking in this context offers greater benefits not only for tumours with large motion, but also tumours located in close vicinity with OARs.

Mid-ventilation planning was tested along with MLC tracking to investigate any potential differences between passive and active motion management strategies. Although the dose reductions were not statistically different from the ITV-based plan in this study, other studies evaluating mid-ventilation have found significant differences [30] based on film dosimetry.

This study illustrated that MLC tracking reduces doses to surrounding organs in Radiotherapy treatments specifically for stage I or oligometastatic metastases. It is hypothesized that a similar effect will be seen in other lung tumour sites such as node-negative large tumours (>5 cm) or tumours adjacent to critical structures [31]. These sites pose a challenge due to the difficulty of sparing adjacent structures with ablative doses which lead to the formulation of a more conservative dose escalation and lower biological equivalent dose (RTOG 0813). While this prescription spares surrounding structures, it could also reduce local control and overall survival. Motion management techniques, like MLC tracking, can help maximize the clinical outcomes of these patients by reducing the margins and delivering a most accurate treatment. This could allow increased dose escalation to the tumour while still sparing surrounding structures and thereby improve the clinical outcomes of these patients.

Dose reconstruction limitations

The dose reconstruction method relies on the assumption that the patient is subjected to no OAR motion and deformation, with the exception of the lung assumed to move rigidly with the tumour. The impact of this assumption is estimated with our sen-

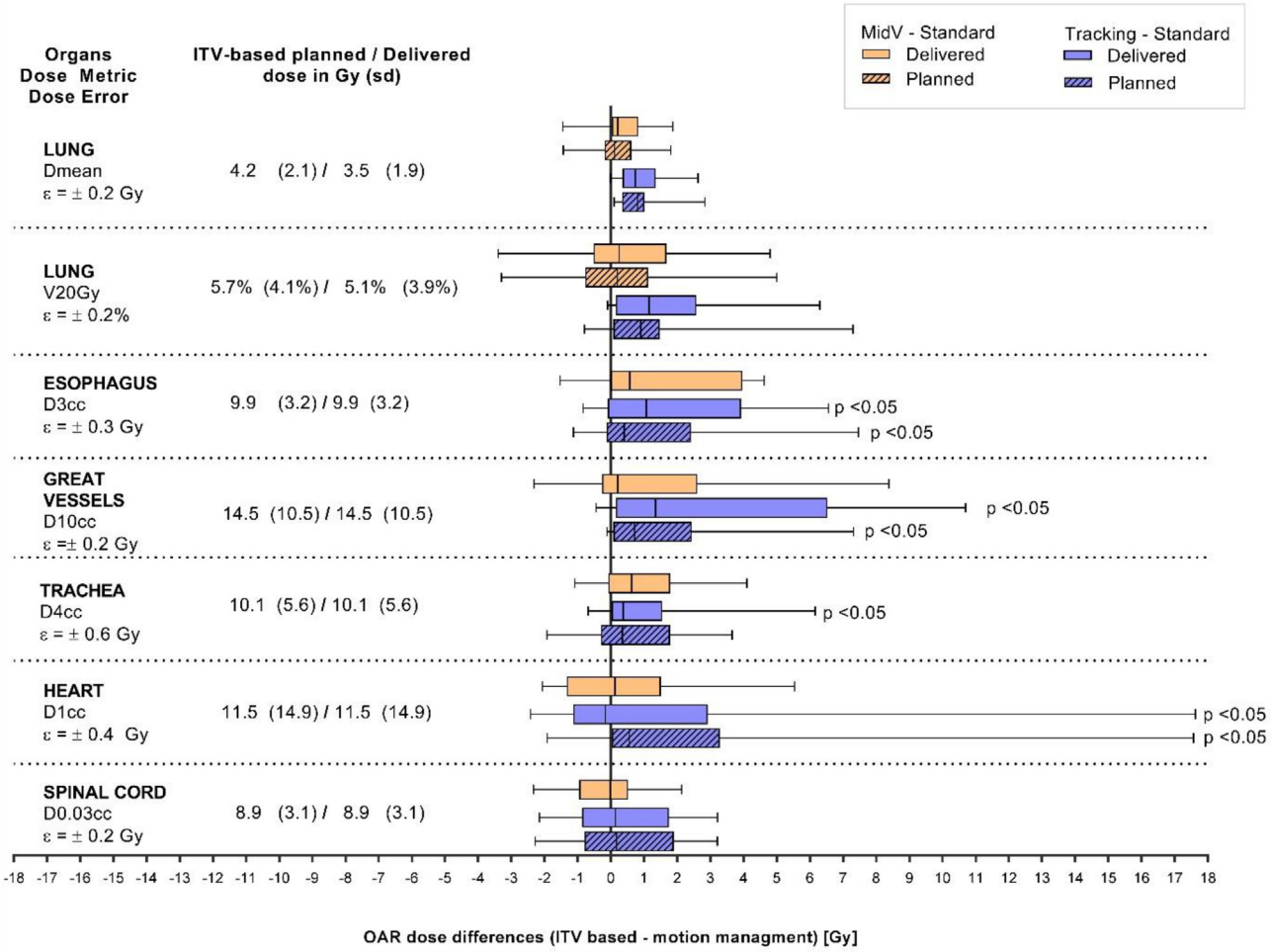

Fig. 4. OAR dose differences for midV and tracking strategies compared with ITV-based planning for the given dose metrics. The doses planned or delivered with the midV or tracking strategies were subtracted from the ITV-planned doses to obtain the OAR dose difference. Positive values signify a dose reduction during tracking or mid-ventilation based on specific dose metric. The horizontal boxplots show the minimum and maximum values, the upper and lower quartiles and the mean. Average values from the tracking plan at end-of-inhale to show the range of dose seen from the 4D-CT plan. OAR dose differences that were significantly different to the ITV-planned doses are denoted by $p < 0.05$.

sitivity analysis that showed errors in the range of ±0.2 Gy for most organs and up to ±0.6 Gy for small organs. Fig. 4 shows that given the magnitude of some dose reductions during tracking and midV, errors for not accounting for 4D motion is mostly outweighed for the majority of organs. A fully developed dose reconstruction algorithm would account for deformation (organs stretching and/or organ rotation). However, deformation, even at the best of times is not a guaranteed technology, and would also require its own quality assurance which is beyond the scope of this paper, as seen in the AAPM TG132.

Relationship between mean lung dose and pulmonary toxicity

SABR techniques are increasingly used in the oligometastatic setting where local recurrence and retreatment to nearby lesions within the lung is not uncommon. Application of compact dose distributions with accurate targeting will be advantageous in this setting to keep lung dose, and potential toxicity, as low as reasonably achievable. Mean lung dose has been correlated with the risk of radiation induced pneumonitis; a study of 251 patients [32] showed a cut-off point for toxicity with grade 2 to grade 4 toxicities reported in 4.3% of patients with MLD < 4 Gy and 17.6% of patients with MLD > 4 Gy. For our cohort, the average MLD presented was estimated to be above this 4 Gy cut-off value with ITV-based planning, and was lowered below 4 Gy with MLC tracking (3.5 Gy). A recent study simulated the effect of MLC tracking during MR-LINAC treatment and showed a mean lung dose reduction of 0.3 Gy, against our study with 0.8 Gy [33].

Conclusion

MLC tracking and mid-ventilation have the potential to provide dosimetric benefits compared to conventional lung treatments by reducing the PTV and subsequent normal lung dose. Delivered MLC tracking plans showed PTV reduction of more than 30%, full GTV dose coverage and reduction in the OAR dose spillage, supporting full clinical implementation of the technology.

Funding

This work is funded by the Australian National Health and Medical Research Council and a Collaborative Research Agreement with Varian Medical Systems.

Conflict of interest

This work is funded by a Collaborative Research Agreement with Varian Medical Systems.

Acknowledgments

The authors acknowledge funding from the Australian National Health and Medical Research Council and Varian Medical Systems.

Appendix A. Supplementary data

Supplementary data associated with this article can be found, in the online version, at http://dx.doi.org/10.1016/j.radonc.2017.06.016.

References

[1] Lagerwaard FJ, Verstegen NE, Haasbeek CJ, Slotman BJ, Paul MA, Smit EF, et al. Outcomes of stereotactic ablative radiotherapy in patients with potentially operable stage I non-small cell lung cancer. Int J Radiat Oncol Biol Phys 2012;83:348–53.
[2] Haasbeek CJ, Lagerwaard FJ, Slotman BJ, Senan S. Outcomes of stereotactic ablative radiotherapy for centrally located early-stage lung cancer. J Thor Oncol. 2011;6:2036–43.
[3] Potters L, Kavanagh B, Galvin JM, Hevezi JM, Janjan NA, Larson DA, et al. American Society for Therapeutic Radiology and Oncology (ASTRO) and American College of Radiology (ACR) practice guideline for the performance of stereotactic body radiation therapy.. Int J Radiat Oncol Biol Phys 2010;76:326–32.
[4] Chang JY, Liu H, Balter P, Komaki R, Liao Z, Welsh J, et al. Clinical outcome and predictors of survival and pneumonitis after stereotactic ablative radiotherapy for stage I non-small cell lung cancer. Radiat Oncol. 2012;7:1.
[5] Verstegen N, Oosterhuis J, Palma D, Rodrigues G, Lagerwaard F, van der Elst A, et al. Stage I-II non-small-cell lung cancer treated using either stereotactic ablative radiotherapy (SABR) or lobectomy by video-assisted thoracoscopic surgery (VATS): outcomes of a propensity score-matched analysis. Ann Oncol 2013;24:1543–8.
[6] Wilbert J, Baier K, Hermann C, Flentje M, Guckenberger M. Accuracy of real-time couch tracking during 3-dimensional conformal radiation therapy, intensity modulated radiation therapy, and volumetric modulated arc therapy for prostate cancer.. Int J Radiat Oncol Biol Phys. 2013;85:237–42.
[7] Depuydt T, Poels K, Verellen D, Engels B, Collen C, Buleteanu M, et al. Treating patients with real-time tumor tracking using the Vero gimbaled linac system: implementation and first review. Radiother Oncol 2014;112:343–51.
[8] Nuyttens J, Prevost J-B, Praag J, Hoogeman M, Van Klaveren R, Levendag P, et al. Lung tumor tracking during stereotactic radiotherapy treatment with the CyberKnife: marker placement and early results. Acta Oncol 2006;45:961–5.
[9] D'Souza D. W, Naqvi SA, Cedric XY. Real-time intra-fraction-motion tracking using the treatment couch: a feasibility study. Phys Med Biol 2005;50:4021.
[10] Peulen H, Belderbos J, Rossi M, Sonke J-J. Mid-ventilation based PTV margins in Stereotactic Body Radiotherapy (SBRT): a clinical evaluation. Radiother Oncol 2014;110:511–6.
[11] van Herk M, Remeijer P, Rasch C, Lebesque JV. The probability of correct target dosage: dose-population histograms for deriving treatment margins in radiotherapy. Int J Radiat Oncol Biol Phys 2000;47:1121–35.
[12] Sonke J-J, Rossi M, Wolthaus J, van Herk M, Damen E. Belderbos J. Frameless stereotactic body radiotherapy for lung cancer using four-dimensional cone beam CT guidance. Int J Radiat Oncol Biol Phys 2009;74:567–74.
[13] Radiation Therapy Oncology Group. RTOG 0813: Seamless phase I/II study of stereotactic lung radiotherapy (SBRT) for early stage, centrally located, non-small cell lung cancer (NSCLC) in medically inoperable patients; 2010.
[14] Radiation Therapy Oncology Group. RTOG 0915. A Randomized Phase II Study Comparing 2 Stereotactic Body Radiation Therapy (SBRT) Schedules for Medically Inoperable Patients with Stage I Peripheral Non-Small Cell Lung Cancer. Philadelphia (PA): RTOG; 2009.
[15] Berbeco RI, Nishioka S, Shirato H, Chen GT, Jiang SB. Residual motion of lung tumours in gated radiotherapy with external respiratory surrogates. Phys Med Biol 2005;50:3655.
[16] Accuray. Accuray achieves milestone of 150th CyberKnife system installed worldwide. Accuray California; 2008.
[17] Zhang T, Orton NP, Tomé WA. On the automated definition of mobile target volumes from 4D-CT images for stereotactic body radiotherapy. Med Phys 2005;32:3493–502.
[18] Sawant A, Smith RL, Venkat RB, Santanam L, Cho B, Poulsen P, et al. Toward submillimeter accuracy in the management of intrafraction motion: the integration of real-time internal position monitoring and multileaf collimator target tracking.. Int J Radiat Oncol Biol Phys. 2009;74:575–82.
[19] Suh Y, Dieterich S, Cho B, Keall PJ. An analysis of thoracic and abdominal tumour motion for stereotactic body radiotherapy patients. Phys Med Biol 2008;53:3623.
[20] Ravkilde T, Keall PJ, Højbjerre K, Fledelius W, Worm E, Poulsen PR. Geometric accuracy of dynamic MLC tracking with an implantable wired electromagnetic transponder. Acta Oncol 2011;50:944–51.
[21] Booth JT, Caillet V, Hardcastle N, O'Brien R, Szymura K, Crasta C, et al. The first patient treatment of electromagnetic-guided real time adaptive radiotherapy using MLC tracking for lung SABR. Radiother Oncol 2016;121:19–25.
[22] Hardcastle N, Booth J, Caillet V, O'Brien R, Haddad C, Crasta C, et al. MO-FG-BRA-06: electromagnetic beacon insertion in lung cancer patients and resultant surrogacy errors for dynamic MLC tumour tracking. Med Phys 2016;43:3710–1.
[23] Poulsen PR, Schmidt ML, Keall P, Worm ES, Fledelius W, Hoffmann L. A method of dose reconstruction for moving targets compatible with dynamic treatments. Med Phys 2012;39:6237–46.
[24] Wang W, Xu Y, Schipper M, Matuszak MM, Ritter T, Cao Y, et al. Effect of normal lung definition on lung dosimetry and lung toxicity prediction in radiation therapy treatment planning.. Int J Radiat Oncol Biol Phys 2013;86:956–63.
[25] Seppenwoolde Y, Lebesque JV, De Jaeger K, Belderbos JS, Boersma LJ, Schilstra C, et al. Comparing different NTCP models that predict the incidence of radiation pneumonitis. Int J Radiat Oncol Biol Phys 2003;55:724–35.
[26] Kwa SL, Lebesque JV, Theuws JC, Marks LB, Munley MT, Bentel G, et al. Radiation pneumonitis as a function of mean lung dose: an analysis of pooled data of 540 patients. Int J Radiat Oncol Biol Phys 1998;42:1–9.
[27] Hernando ML, Marks LB, Bentel GC, Zhou S-M, Hollis D, Das SK, et al. Radiation-induced pulmonary toxicity: a dose-volume histogram analysis in 201 patients with lung cancer.. Int J Radiat Oncol Biol Phys. 2001;51:650–9.
[28] DeLuca PM. The international commission on radiation units and measurements. J ICRU 2007;7:v–vi.
[29] Hoogeman M, Prévost J-B, Nuyttens J, Pöll J, Levendag P, Heijmen B. Clinical accuracy of the respiratory tumor tracking system of the cyberknife: assessment by analysis of log files. Int J Radiat Oncol Biol Phys 2009;74:297–303.
[30] Ehrbar S, Perrin R, Peroni M, Bernatowicz K, Parkel T, Pytko I, et al. Respiratory motion-management in stereotactic body radiation therapy for lung cancer–a dosimetric comparison in an anthropomorphic lung phantom (LuCa). Radiother Oncol 2016;121:328–34.
[31] Chi A, Nguyen NP, Komaki R. The potential role of respiratory motion management and image guidance in the reduction of severe toxicities following stereotactic ablative radiation therapy for patients with centrally located early stage non-small cell lung cancer or lung metastases. Front Oncol 2014;4:151.
[32] Barriger RB, Forquer JA, Brabham JG, Andolino DL, Shapiro RH, Henderson MA, et al. A dose-volume analysis of radiation pneumonitis in non-small cell lung cancer patients treated with stereotactic body radiation therapy. Int J Radiat Oncol Biol Phys 2012;82:457–62.
[33] Menten MJ, Fast MF, Nill S, Kamerling CP, McDonald F, Oelfke U. Lung stereotactic body radiotherapy with an MR-linac–Quantifying the impact of the magnetic field and real-time tumor tracking. Radiother Oncol 2016;119:461–6.

CHAPTER 05

Geometric uncertainty analysis of MLC tracking for lung SABR

This chapter was published in *Physics in Medicine and Biology* and written by me.

While the previous chapter estimates the feasibility and potential benefits of MLC tracking, this chapter reports on the actual clinical performances of the technology following the LIGHT SABR clinical trial.

The novelty of this work is that it relies on real patients' data to inform on the geometric accuracy of MLC tracking and therefore helps putting into context the range of uncertainties that may be expected during treatment.

To compute the geometric uncertainty, we relied on a convolution method that combines the multiple probability density function of individual uncertainty into a total uncertainty for each patient, and for the entire cohort of patients. This convolution method allowed to utilize the entirety of the probability density functions without making any assumptions about its shape.

IOP Publishing Phys. Med. Biol. 0 (2020) xxxxxx https://doi.org/10.1088/1361-6560/abb0c6

Physics in Medicine & Biology

IPEM Institute of Physics and Engineering in Medicine

RECEIVED
29 February 2020

REVISED
3 August 2020

ACCEPTED FOR PUBLICATION
19 August 2020

PUBLISHED
xx xx xxxx

PAPER

Geometric uncertainty analysis of MLC tracking for lung SABR

Vincent Caillet[1,2], Benjamin Zwan[1,5], Adam Briggs[1], Nicholas Hardcastle[3,4], Kathryn Szymura[1], Alexander Prodreka[1], Ricky O'Brien[2], Ben E Harris[7,8], Peter Greer[5,6], Carol Haddad[1], Dasantha Jayamanne[1], Thomas Eade[1], Jeremy Booth[1,4] and Paul Keall[2]

1 Northern Sydney Cancer Centre, Royal North Shore Hospital, St Leonards, NSW, Australia
2 ACRF Image X Institute, the University of Sydney, Australia
3 Physical Sciences, Peter MacCallum Cancer Centre, Melbourne, Australia
4 Institute of Medical Physics, University of Sydney, School of Physics, Sydney, Australia
5 School of Mathematical and Physical Sciences, University of Newcastle, Newcastle, Australia
6 Department of Radiation Oncology, Calvary Mater Hospital, Newcastle, Australia
7 Department of Respiratory Medicine, Royal North Shore Hospital, Sydney, New South Wales, Australia
8 Faculty of Health Sciences, University of Sydney, Australia

Keywords: MLC tracking, lung tumor motion, LIGHT SABR, tumor tracking

Abstract

Purpose

The purpose of this work was to report on the geometric uncertainty for patients treated with multi-leaf collimator (MLC) tracking for lung SABR to verify the accuracy of the system.

Methods

Seventeen patients were treated as part of the MLC tracking for lung SABR clinical trial using electromagnetic beacons implanted around the tumor acting as a surrogate for target motion. Sources of uncertainties evaluated in the study included the surrogate-target positional uncertainty, the beam-surrogate tracking uncertainty, the surrogate localization uncertainty, and the target delineation uncertainty. Probability density functions (PDFs) for each source of uncertainty were constructed for the cohort and each patient. The total PDFs was computed using a convolution approach. The 95% confidence interval (CI) was used to quantify these uncertainties.

Results

For the cohort, the surrogate-target positional uncertainty 95% CIs were ±2.5 mm (−2.0/3.0 mm) in left-right (LR), ±3.0 mm (−1.6/4.5 mm) in superior–inferior (SI) and ±2.0 mm (−1.8/2.1 mm) in anterior–posterior (AP). The beam-surrogate tracking uncertainty 95% CIs were ±2.1 mm (−2.1/2.1 mm) in LR, ±2.8 mm (−2.8/2.7 mm) in SI and ±2.1 mm (−2.1/2.0 mm) in AP directions. The surrogate localization uncertainty minimally impacted the total PDF with a width of ±0.6 mm. The target delineation uncertainty distribution 95% CIs were ±5.4 mm. For the total PDF, the 95% CIs were ±5.9 mm (−5.8/6.0 mm) in LR, ±6.7 mm (−5.8/7.5 mm) in SI and ±6.0 mm (−5.5/6.5 mm) in AP.

Conclusion

This work reports the geometric uncertainty of MLC tracking for lung SABR by accounting for the main sources of uncertainties that occurred during treatment. The overall geometric uncertainty is within ±6.0 mm in LR and AP directions and ±6.7 mm in SI. The dominant uncertainty was the target delineation uncertainty. This geometric analysis helps put into context the range of uncertainties that may be expected during MLC tracking for lung SABR (ClinicalTrials.gov registration number: NCT02514512).

1. Introduction

The goal of radiation therapy is to provide adequate target coverage while limiting dose to adjacent critical organs. Tumors however are subject to motion from physiological processes such as respiration, which

© 2020 Institute of Physics and Engineering in Medicine

necessitates motion management strategies to ensure the goal of treatment is achieved (Brandner *et al* 2017, Molitoris *et al* 2018).

Dedicated radiation therapy linear accelerators that allow to track the tumor motion in real time have been used to treat patients. Among those, the CyberKnife system (Accuray Inc., Sunnyvale, USA), the Accuray Radixact (Accuray, Sunnyvale, CA), the Vero system (BrainLab AG, Feldkirchen, Germany) and multi-leaf collimator (MLC) tracking enable the treatment delivery to adapt to the target position and patient's internal dynamics in real time while the treatment is delivered.

The detailed geometric information recorded during MLC tracking treatment creates the opportunity to quantify the various sources of geometric uncertainties for the patient cohort, and each patient. The framework proposed by Stroom *et al* (1999) and Sawkey *et al* (2012) was adopted to quantify the geometric uncertainty, whereby individual and independent sources of uncertainties were computed as probability density functions (PDFs) and then convolved to obtain the total PDF. The key sources of uncertainties pertinent in MLC tracking for lung SABR include the surrogate-target positional uncertainty, the beam-surrogate tracking uncertainty, the surrogate localization uncertainty, and the target delineation uncertainty.

The purpose of this work is to report on the geometric uncertainties of MLC tracking for lung SABR patients to verify the accuracy of the system and inform margin requirements for future applications of MLC tracking in thoracic targets.

2. Methods

2.1. Patients, beacon insertion, planning and treatment

Seventeen patients diagnosed with stage I non-small cell lung cancer or lung metastases were recruited as part of the phase I/II clinical trial (LIGHTSABR, NCT02514512) and treated using SABR with MLC tracking between November 2015 and November 2018.

Three electromagnetic transponders (Varian Medical Systems, Palo Alto, USA) were bronchoscopically implanted for each patient in the airways surrounding the tumor using C-arm fluoroscopic image guidance.

Each patient received a 4D-CT simulation one week following the bronchoscopic implantation. For the 4D-CT simulation and the subsequent treatment, patients were lying supine ($N = 11$), prone ($N = 5$) or lateral decubitus ($N = 1$). The prone and lateral positions were used to meet the limitations imposed by the Calypso system (Varian Medical Systems, Palo Alto, USA) that electromagnetic beacons must be within 19 cm of the detector panel. Phase binning for 4D-CT imaging was performed for supine patients using the real-time position management infrared camera (Varian Medical Systems, Palo Alto, USA) and the pneumatic belt (bellows, Philips Medical Systems, Cleveland, USA) for prone and lateral decubitus patients. Ten phases were reconstructed with a slice thickness of 1.5 mm. Six patients out of seventeen were simulated with visual biofeedback using in-house software (Venkat *et al* 2008).

MLC tracking treatment planning was performed on the end-exhale phase to provide reliable tumor delineation (Thomas *et al* 2018), unless other phases were considered of higher quality. The gross tumor volume (GTV) was drawn by the treating oncologist. The clinical tumor volume (CTV) was assumed to equal the GTV. Isotropic margins of 5 mm were added to the CTV to define the planning target volume (PTV).

Patients were planned with volumetric modulated arc therapy (VMAT) using prescribed doses of 4×12 Gy or 5×10 Gy depending on the tumor location. The planning protocol prescribed 100% of the CTV to get more than 100% of the prescribed dose and at least 98% of the PTV to get 100% of the prescribed dose. There was no criteria specified for the maximum dose in the protocol. From a review of the treatment plans, the maximum dose to the GTV did not exceed 130% of the prescribed dose. The collimator angle was aligned along the most dominant tumor motion direction observed at 4D-CT, either in the superior–inferior (SI) direction ($N = 16$) or in the left–right (LR)/anterior–posterior (AP) direction ($N = 1$).

As shown in figure 1, treatments were delivered with a Varian Trilogy linear accelerator equipped with the Millennium MLC. The patient was placed on the table such that the Calypso-measured tumor position matched with the planned position. Cone beam computed tomography was then acquired to verify the tumor position at the end-of-exhale relative to the surrounding organs. The in-house MLC tracking software was initiated to take control of the leaves and the MLC tracking treatment was delivered similarly to a standard treatment. Further details about the software can be found in Keall *et al* (2014). A prediction algorithm (Ruan and Keall 2010) was used to account for the measured 230 ms system latency. The average beam-on time for two-arc VMAT was 5.03 min ($\pm$ 0.5 min) using 600 MU min^{-1} with an average of 1415 MU ($\pm$210 MU) per arc. Output logs from the MLC tracking software recorded the positions of the MLC, gantry angle and surrogate position. These were exported for analysis using MATLAB 2019 (MathWorks, USA).

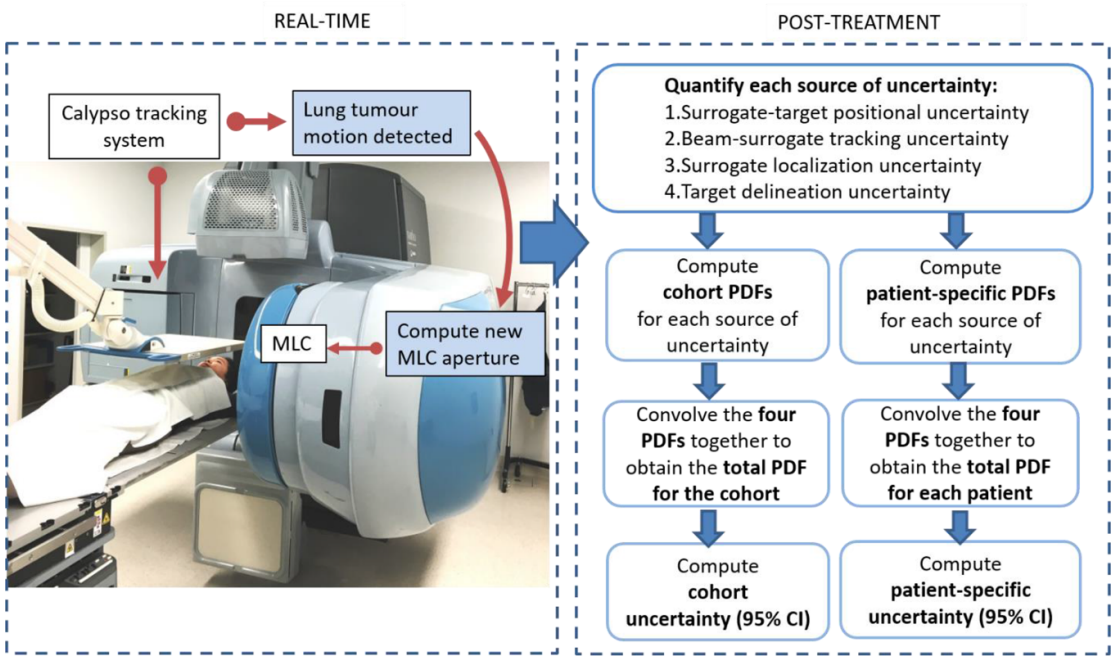

Figure 1. Schematic of the MLC tracking beam adaptation method using the Calypso tracking system. The output logs generated allowed a post-treatment analysis to quantify each source of uncertainty.

2.2. Methods for quantifying the geometric uncertainty

Using the output logs, the geometric uncertainty was computed for both the cohort and each patient. The geometric uncertainty refers to any geometric deviations at a given time that contributed to a misalignment between the centroid of the MLC aperture and the centroid of the target.

As shown in figure 1, following an MLC tracking treatment, four sources of uncertainty were quantified to construct four individual PDFs. Those four PDFs were then combined with a convolution method described in Stroom *et al* (1999) and Sawkey *et al* (2012) to obtain the total probability of geometric deviation. The method for building each PDF is described in the following sections. Using this total PDF, the geometric uncertainty for each patient was reported as being the 95% CI (2.5th and 97.5th percentile) (Cerviño *et al* 2009, Sawkey *et al* 2012). The 2.5th and the 97.5th percentile values were read directly from the PDF.

Each uncertainty was evaluated in the frame of reference of a static point located at the centroid of the GTV contoured in the planned 4D-CT phase. The LR, SI and AP directions correspond to a patient in the supine position. For prone and lateral patients, the uncertainties were transformed to match the same frame of reference.

2.2.1. Surrogate-target positional uncertainty.

The use of a surrogate to infer the target position introduces a geometric offset that needed to be accounted for. On each phase (10 phases per patient) of the 4D-CT, both the transponders and the target (GTV) were manually contoured and the position of the centroids in each phase computed. The differential motion relative to the end-of-exhale phase between the surrogate and the target constituted the surrogate-target position uncertainty.

The PDF for the surrogate-target positional uncertainties was built based on the aggregated uncertainties obtained from all 4D-CT while each patient-specific PDF was built using their individual 4D-CT.

2.2.2. Beam-surrogate tracking uncertainty.

In the context of MLC tracking, geometric deviations due to the system's latency, finite leaf width and leaf speed are known to introduce an offset between the position of the beam and the position of the surrogate. This differential position corresponds to the beam-surrogate tracking uncertainty.

The output logs were directly read from the linac in real-time using the MLC tracking software. Agnew *et al* (2012) assessed the accuracy of the logs in terms of MLC positions and found that the errors obtained from the linac were expected to range between 0.12 mm and 0.28 m.

To compute the beam-surrogate tracking uncertainty, the actual beam position relative to the planned beam position was obtained using the output logs containing both the actual and the planned leaf positions.

Table 1. List of uncertainties with their respective PDF functional form, uncertainty type and data source.

	Surrogate-target positional uncertainty	Beam-surrogate tracking uncertainty	Surrogate localization uncertainty	Target delineation uncertainty
PDF functional form				
Cohort	PDF built from entire cohort data	PDF built from entire cohort data	Step function from the literature	PDF built from two publications
Patient-specific	PDF built from patient-specific 4D-CT	PDF built from patient-specific data	Step function from the literature	PDF built from two publications
Uncertainty type	3D[a]	Beam's eye view	3D	3D
Data source	4D-CT manual segmentation	Position of surrogate and leaf positions in beam's-eye-view transformed to 3D	Literature (Balter *et al* 2005, Murphy *et al* 2008)	Literature (Peulen *et al* 2015, Mercieca *et al* 2017)

[a]3D refers to the static coordinate system in the planned 4D-CT phase.

The leaf positions were used to draw two binary images (set to zero outside the treatment field and one within the aperture) within the beam's-eye-view corresponding respectively to the actual aperture and the planned aperture. Using an image registration algorithm based on cross-correlation (Guizar-Sicairos *et al* 2008), the two-dimensional offset between the actual and planned aperture was computed for each data entry (25 Hz) to obtain the actual aperture shift relative to its planned position.

The surrogate position (centroid of the 2–3 beacons) relative to its planned position at the end-of-exhale was obtained directly from the output logs at the same frequency (25 Hz).

Transformation of the beam-surrogate tracking uncertainties from the two-dimensional beam's-eye-view into the three-dimensional reference coordinate system was calculated assuming that the dosimetric uncertainty directly along the therapeutic path was negligible as for photon beams the dose generally varies less with depth than laterally (Kry *et al* 2017).

The beam-surrogate tracking uncertainty was computed for each data entry at 25 Hz. The total PDF was built using the uncertainties from the 17 patients concatenated into one single matrix while the patient-specific PDF were built using their individual uncertainties.

2.2.3. Surrogate localization uncertainty.

The surrogate localization uncertainty relates to the accuracy and precision of the electromagnetic transponders' reported positions using the Calypso tracking system. This uncertainty was obtained based on published data that reported a standard deviation in the range of 0.2–0.6 mm for stationary (Balter *et al* 2005) and moving targets (Murphy *et al* 2008), respectively. For this analysis, the surrogate localization uncertainty PDF was modeled as a step function, with a mean of zero and width of 0.6 mm in each dimension.

2.2.4. Target delineation uncertainty.

Delineation of the tumor within the treatment planning system remains an important source of geometrical uncertainty. The delineation uncertainty was taken from measurements by Peulen *et al* (2015) and Mercieca *et al* (2017) who reported on the target delineation uncertainty for a cohort of lung cancer patients. GTVs obtained from 4D-CTs were contoured by several lung radiation oncologists onto the MIP (Peulen *et al*, Mercieca *et al*.), mid-ventilation phase (Mercieca *et al*) and the mid-position phase (Mercieca *et al*).

For Peulen *et al*, the collated data (in figure 2(a) of their manuscript) was chosen as it represents the distribution of standard deviation for the entire group of lung radiation oncologists. In Mercieca *et al*, the Mid-V data (figure 2, top left) was chosen as this most closely aligns with the current study of contouring on a single phase. We used these distributions to derive a PDF that was implemented in our model.

2.3. Quantifying the total uncertainty

For both the cohort and the patient-specific model, the total PDF was computed as the convolution of all PDFs. Kolmogorov–Smirnoff (KS) normality tests were ran for each cohort PDF. Table 1 summarizes the key points for each PDF.

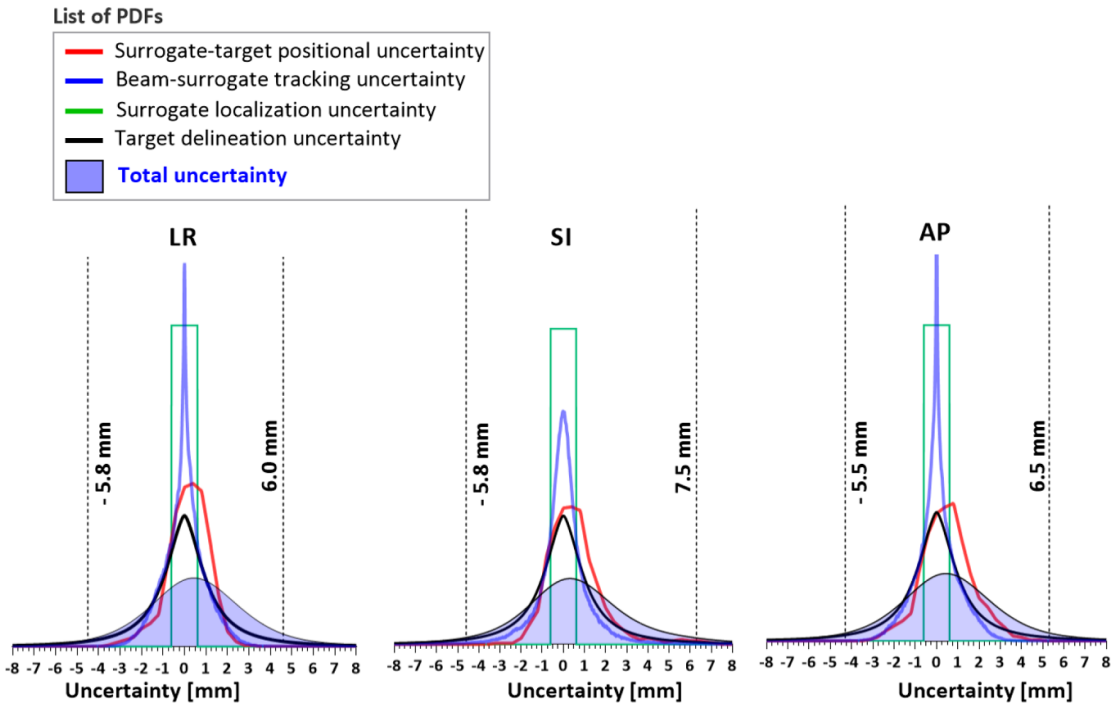

Figure 2. PDFs for the cohort in LR, SI and AP directions. PDFs for individual source of uncertainties are shown as curves and the total PDF as the shaded distribution. The uncertainties are represented as the 95% CIs (vertical lines). KS test showed that all PDF were significantly different than a normal distribution ($p < 0.01$).

2.3.1. Relationship between the beam-surrogate tracking uncertainties and the average surrogate peak-to-trough distance

Since the primary objective of MLC tracking is to compensate for the surrogate peak-to-trough distance, the relationship between the surrogate peak-to-trough distance and the beam-surrogate tracking uncertainty was investigated for each fraction ($N = 70$). The Pearson correlation was used to compute the degree of linearity between the two variables.

3. Results

Seventeen patients were treated with MLC tracking for lung SABR, totaling 70 fractions of treatment with dual-arc VMAT.

3.1. Uncertainties for the cohort

As seen in figure 2 with values summarized in table 2, the total PDF for the cohort (shaded distributions) shows that the uncertainties, the 95% CI (2.5th and 97.5th percentile, lie within ±5.9 mm (−5.8/6.0 mm) in LR, ±6.7 mm (−5.8/7.5 mm) in SI and ±6.0 mm (−5.5/6.5 mm) in AP directions.

The average surrogate peak-to-trough distance (± standard deviation) for the entire cohort is 3.2 ± 1.7 mm in LR, 8.6 ± 5.4 mm in SI and 4.8 ± 2.6 mm in AP directions.

The surrogate-target positional uncertainty computed from the 4D-CT shows that the uncertainties (2.5th/97.5th) are approximately ±2.5 mm (−2.0/3.0 mm) in LR, ±3.0 mm (−1.6/4.5 mm) in SI and ±2.0 mm (−1.8/2.1 mm) in AP directions. The asymmetric distribution in the SI direction showing the near-maximum uncertainty of 4.5 mm is likely due to one patient (table 3, Patient 10) with considerable visual 4D-CT artefacts.

The beam-surrogate uncertainty attributed to the MLC tracking technology contributed less or equal than 2.8 mm in all directions, with uncertainties of ±2.1 mm (−2.1/2.1 mm) in LR, ±2.8 mm (−2.8/2.7 mm) in SI and ±2.1 mm (−2.1/2.0 mm) in AP directions.

The surrogate localization uncertainty minimally impacted the total PDF with width of ±0.6 mm.

The PDF from Peulen et al provided 95% confidence intervals (CIs) of ±4.2 mm and Mercieca et al ±6.5 mm. The target delineation uncertainty, being the average PDF of Peulen et al and Mercieca et al, had a CI of ±5.4 mm. The target delineation uncertainty dominated the overall shape of the total PDF.

Table 2. Summary of the uncertainties for the entire cohort.

	Surrogate-target uncertainty [mm]			Beam-surrogate uncertainty [mm]			Surrogate localization uncertainty [mm]	Target delineation uncertainty [mm]	Total uncertainty [mm]		
	LR[a]	SI	AP	LR	SI	AP	LR/SI/AP	LR/SI/AP	LR	SI	AP
95% CI	±2.5	±3.0	±2.0	±2.1	±2.8	±2.0	±0.6	±5.4	±5.9	±6.6	±6.0
2.5th	−2.0	−1.6	−1.8	−2.1	−2.8	−2.1	−0.6	−5.4	−5.8	−5.8	−5.5
97.5th	3.0	4.5	2.1	2.1	2.7	2.0	0.6	5.4	6.0	7.5	6.5

[a]LR (+left, −right), SI (+superior, −inferior), AP (+anterior, −posterior).

Table 3. Summary of average surrogate peak-to-trough distance and uncertainties for each patient (95% CI). Bold text is used to highlight the patient with the largest uncertainty in each column.

	Average surrogate peak-to-trough distance [mm]			Surrogate-target positional uncertainty [mm]			Beam-surrogate tracking uncertainty [mm]			Surrogate localization uncertainty [mm]	Target delineation uncertainty [mm]	Total uncertainty		
Patient Id	LR	SI	AP	LR	SI	AP	LR	SI	AP	All directions	All directions	LR	SI	AP
1	2.6	6.4	6.5	±0.8	±2.4	±1.0	±1.7	±2.3	±2.3	±0.6	±5.4	±6.0	±6.4	±6.0
2	5.6	15.2	5.9	**±3.2**	±1.7	±3.1	**±2.3**	**±5.6**	±2.4	±0.6	±5.4	**±6.1**	**±9.2**	±6.0
3	2	4.6	1.2	±0.9	±1.5	±2.7	±1.0	±1.8	±0.8	±0.6	±5.4	±5.8	±6.3	±5.7
4	2.2	4.1	3.8	±2.5	±1.3	±2.1	±1.5	±1.6	±2.0	±0.6	±5.4	±5.9	±6.2	±5.9
5	**6.8**	5.5	7.5	±1.5	±1.1	±1.9	±1.6	±3.1	±2.3	±0.6	±5.4	±5.9	±6.9	±6.1
6	1.9	**18.3**	5.3	±1.6	±2.5	**±4.0**	±2.0	±3.6	±1.9	±0.6	±5.4	±6.1	±7.7	±6.0
7	2.3	4	3.1	±1.5	±1.5	±1.2	±1.4	±1.2	±1.6	±0.6	±5.4	±5.9	±6.1	±5.9
8	1.3	3.5	4.3	±1.0	±0.9	±1.1	±1.7	±1.3	±2.2	±0.6	±5.4	±5.9	±6.2	±6.0
9	4.5	12.9	2.3	±1.2	±1.2	±2.5	±2.1	±3.2	±1.5	±0.6	±5.4	±6.0	±6.7	±5.8
10[a]	5.3	11.5	5.2	±0.7	**±7.3**	±3.5	±2.0	±1.3	±2.0	±0.6	±5.4	±6.0	±7.5	±5.9
11	2.8	14.3	4.1	±0.6	±1.9	±1.2	±1.7	±3.5	±2.0	±0.6	±5.4	±6.1	±6.2	±5.9
12	0.9	12.1	3.8	±1.4	±0.7	±2.0	±1.1	±1.3	±1.7	±0.6	±5.4	±5.8	±6.2	±5.8
13	2.6	1.9	6.1	±0.5	±4.1	±2.5	±2.0	±0.7	±2.0	±0.6	±5.4	±6.0	±6.1	±5.9
14	4.1	6.3	3.7	±0.8	±0.5	±0.8	±2.1	±1.4	±2.2	±0.6	±5.4	±6.1	±6.2	±6.0
15	2.6	8.1	**10.4**	±1.5	±2.2	±1.0	±2.0	±2.2	**±2.5**	±0.6	±5.4	±6.0	±6.4	**±6.1**
16	1.1	2.7	3.4	±1.0	±1.5	±1.0	±1.2	±2.1	±1.6	±0.6	±5.4	±6.0	±6.4	±6.0
17	2.7	3.1	1.9	±1.1	±1.7	±1.2	±1.1	±2.2	±1.5	±0.6	±5.4	±6.0	±6.4	±6.0

[a]Patient 10's 4D-CT showed significant artefacts that may explain large surrogate-target positional uncertainty.

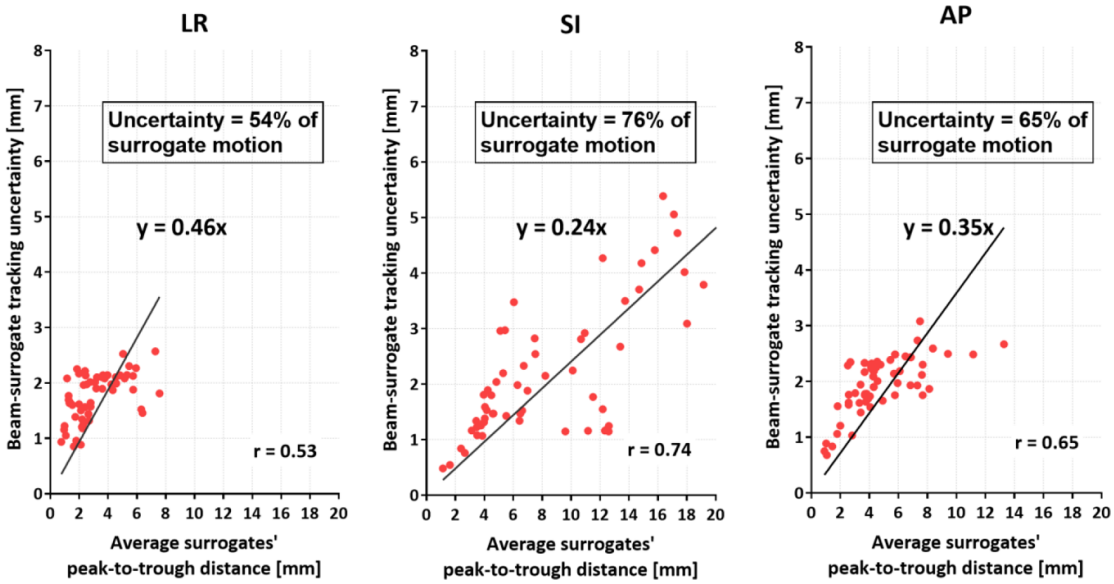

Figure 3. Beam-surrogate tracking uncertainty (95% CI) plotted against the average surrogate peak-to-trough distance for 17 patients (70 fractions). Line of best fit and the correlation factor *r* are shown in bold.

3.2. Uncertainties for each patient

Table 3 summarizes the magnitude of each source of uncertainty per patient. The first three columns show the average surrogate centroid peak-to-trough distance. Patients 2, 6, 10, 11 and 12 exhibited large (>10 mm) surrogate peak-to-trough distance in the SI direction, the largest being patient 6 with 18.3 mm. The dominant direction of motion was SI for all patients, excluding patients 5, 13 and 15 who had AP dominant motion. Largest AP motion was patient 15 with 10.4 mm. No patient exhibited LR dominant motion.

The surrogate-target positional uncertainty demonstrated that the average (± standard deviation) patient's CIs were 1.3 mm ± 0.7 mm in LR, 1.9 mm ± 1.0 mm in SI and 1.7 mm ± 0.8 mm in AP directions. Large uncertainties from patient 10 (±7.3 mm in SI) are believed to be due to 4D-CT under-sampling artefacts. For LR and AP, the largest uncertainty was traced to patient 2 (±3.2 mm in LR) and patient 6 (±4.0 mm in AP), both patients with large surrogate peak-to-trough distances.

For the beam-surrogate uncertainty, noticeable large uncertainties were observed for patient 2 (±5.6 mm in SI) that were mostly attributed to large and erratic surrogate motion that, due to the system's latency of 230 ms, impaired the accurate prediction of the surrogate position ahead of time. During their first fraction, patient 11 also exhibited erratic surrogate motion with large beam-surrogate tracking uncertainties.

3.3. Relationship between the beam-surrogate tracking uncertainties and the average surrogate peak-to-trough distance

Beam-surrogate tracking uncertainties during treatment were plotted against the average surrogate peak-to-trough distance, as shown in figure 3. Correlation using the Pearson coefficient *r* was found to be the lowest LR ($r = 0.53$) and AP ($r = 0.65$) directions and the highest in SI ($r = 0.74$) directions.

In the LR and AP directions, the line of best fit shows a slope of 0.46 and 0.35 respectively, meaning that the beam-surrogate tracking uncertainty represents 54% and 65% of the average surrogate peak-to-trough motion. It is worth noting that most of the error for the surrogate-target positional uncertainty in AP are plateauing at ~2.5 mm which corresponds to half a leaf width. This implies that the major contributor to the beam-surrogate tracking uncertainty is probably the leaf width, and this also explains the low Pearson correlation factor. This pattern is not as noticeable in the LR direction probably because most patient's average surrogate peak-to-trough distances were less than 2.5 mm.

In the SI direction, MLC tracking reduced by 76% the average surrogates' peak-to-trough distance. In the SI direction for patients with SI dominant motion, the magnitude of uncertainties is due to a combination of system's latency and leaf speed uncertainties, detailed further in the following section.

Previous work published by Steiner *et al* (2019) in our group compared the delivered and planned average surrogates' peak-to-trough and found that motion during 4D-CT consistently underestimates the true tumor motion during treatment.

4. Discussion

The purpose of this work was to compute the total geometric uncertainty for a cohort of patients treated with MLC tracking for lung SABR. Using the data collected from the clinical trial, the convolution approach developed by Stroom *et al* (1999) and Sawkey *et al* (2012) enabled the quantification of a set of uncertainties for the cohort and each patient. The overall geometric uncertainty is within ±6.0 mm in LR and AP directions and ±6.7 mm in SI. Individual analysis of uncertainties shows that the surrogate-target positional uncertainty was less than ±3.0 mm and the beam-surrogate tracking uncertainty was accountable for uncertainties equal to or less than ±2.8 mm. The largest uncertainty stemmed from the target delineation uncertainty (±5.4 mm) and the smallest from surrogate target localization uncertainty (±0.6 mm).

By treating the surrogate-target uncertainty and the beam-surrogate uncertainty without splitting the random and systematic error means that the random errors are potentially over-estimated. This means that the overall final margin is computed conservatively. However, we would like to emphasize that this study was designed to provide geometric uncertainty information for the GTV and does not deal with dosimetric margins. A finding from this study, which has been discussed in other studies (van Herk *et al* 2003, Sawkey *et al* 2012, Zhang *et al* 2012), is that the errors are not normally distributed as seen in figure 2 with the reported KS *p*-value. In these cases, to compute the dosimetric margins either an approximation needs to be made to assume normality, or the convolution approach used here would need to be used to incorporate other sources of uncertainty in order to create a margin, such as microscopic spread and beam penumbra required for GTV to CTV and CTV to PTV margins. With a convolution approach, the conventional concepts of a group mean, systematic error and random error do not apply.

Various studies have reported on the performance of other radiation therapy tracking devices comparable to the MLC tracking technology for lung treatment. (Floriano *et al* 2014) combined the uncertainties using summation in quadrature and found that 95% of the CTV is geometrically covered with ±5.0 mm. It is worth noting that substantial differences can be found in this work compared with ours. Floriano *et al* accounted for the deformation of the tumor in their analysis (margins ranging from 1.5 to 2.5 mm) but did not include the target delineation uncertainty that is responsible for the largest uncertainty in our model.

Similarly for the MHI Vero 4DRT (Depuydt *et al* 2014) calculated the 95% CI for the equivalent of the beam-surrogate tracking in the beam's-eye-view to be 3.9 mm on average. These uncertainties were larger than those from this study with calculated 95% CIs to be ±2.7 mm in the direction parallel to the MLC leaves and ±2.1 mm perpendicular to the leaves.

The uncertainties evaluated in this study were from an in-house developed version of MLC tracking that was an adaptation of existing technology and not a commercially designed system. Therefore, some of the geometric uncertainties measured here should be considered as upper bounds of those expected from a dedicated MLC tracking system.

The surrogate-target positional uncertainty could be reduced by tracking the target without implanted markers. Markerless tracking for lung treatment has been tested on fluoroscopic images on patients by Yang *et al* (2017) with the CyberKnife Xsight lung tracking software segmentation with reported segmentation errors of 0.38 ±0.54 mm, noticeably smaller than the surrogate-target positional uncertainty described in this paper (~2.5 mm). Mueller *et al* (2019) tested online real-time markerless tracking software on a Varian TrueBeam linear accelerator with a moving phantom and reported errors of 0.4–3.2 mm (LR), 0.7–1.6 mm (SI) and 0.8–1.5 mm (AP). A common issue described by both Yang *et al* and Mueller *et al* is that for patients with a tumor located adjacent to other organs, the lack of tumor contrast with fluoroscopic images increases the segmentation uncertainty and, in some cases, may restrict the patient selection for treatment. However, with the emergence of integrated MRI-linear accelerators (Raaymakers *et al* 2017) capable of MLC tracking as shown in a proof-of-concept in (Glitzner *et al* 2019), high-contrast images that could be used to track and adapt to the target position in real-time.

Improvement in the beam-surrogate uncertainty is achievable by reducing the latency of the system or using thinner leaves. Reduction in the system's latency would facilitate predicting the surrogate position ahead of time and in return reduce the beam-surrogate uncertainties. Faster leaf-fitting algorithms have been tested by Caillet *et al* (2019) and it was found that the speed of the calculation of the new leaf pattern has no effect on the overall system's latency. Reducing the system's latency could be achieved, similarly to the CyberKnife and Vero, by coupling the Calypso motion detection system with a faster input (e.g. thoracic belt, vest) and building a correlation model to help reduce the overall system's latency. Despite using fluoroscopic images for beacon segmentations sporadically (Yang *et al* reported on fluoroscopic images obtained every 40 s), CyberKnife studies (Pepin *et al* 2011) report latencies of 115 ms. The impact of system latencies may be reduced with improved motion prediction algorithms or biofeedback technology. The latter has been shown to reduce irregular motion with the ability to stabilize the patient's internal motion (Lee *et al* 2018). The

impact of latency may also be reduced with compression belt and CPAP devices (Goldstein *et al* 2015, Eade *et al* 2015) that dampen the magnitude of the target motion.

Previous work published by Steiner *et al* (2019) relied on ten patients from this cohort to compare the delivered and planned average surrogates' peak-to-trough and found that motion during 4D-CT consistently underestimates the true tumor motion during treatment.

Thinner leaves have been explored by Pommer *et al* (2013) showing that for prostate motion (i.e. small motion) the most limiting factor was the leaf width with consistently better dose distributions for treatments with thinner leaves. Pommer *et al* conclusion corroborate the data shown in figure 3 where the AP graphs show a cluster of errors plateauing at approximately 2.5 mm, corresponding to half of a leaf width. As an alternative to implementing thinner leaves, couch tracking (Jöhl *et al* 2019) could also help reduce residual uncertainties due to leaf width. Ehrbar *et al* (2017) showed that couch tracking alleviates the impact of the leaf width on the beam-surrogate tracking uncertainty.

The target delineation represents the largest uncertainty in this geometrical model. Studies have shown that this variability between observers can be reduced with adherence to contouring guidelines to harmonize the application of target delineation (Oar *et al* 2019). The use of multimodality imaging, such as PET/CT or PET/MRI (Pommer *et al* 2013), has been shown to improve delineation accuracy. The emergence of automatic or semi-automatic target segmentation (Pommer *et al* 2013, Ehrbar *et al* 2017, Jöhl *et al* 2019) is also showing promise to reduce the inter-observer variability while also potentially saving time for the clinician (Oar *et al* 2019).

5. Conclusion

This work reports on the geometric uncertainty of MLC tracking for lung SABR to be on average within $\pm$6.0 mm in LR and AP directions and $\pm$6.7 mm in SI and demonstrates the accuracy of the overall system by accounting for the main sources of uncertainties that occurred during treatment. This geometric analysis helps putting into context the range of uncertainties that may be expected during MLC tracking for lung SABR.

Acknowledgments

The authors thank the patient participants in this trial who entrusted their care to an emerging technology. Many additional radiation oncologists, medical physicists, radiation therapists, nurses and clinical trial coordinators were involved in and essential to the successful completion of the trial. Thanks to Dr. Helen Ball for reviewing the manuscript. Thanks to Prof Marcel van Herk, Dr. Eliana Vasquez Osorio and Dr. Susan Mercieca for their contribution to compute the delineation uncertainty and providing the data from Mercieca *et al.* Thanks to Prof Jan-Jakob Sonke for providing the data from Peulen *et al.*

Conflicts of interest

PJK is an inventor on the awarded US patents 7469035 and 8971489 that are related to MLC tracking. Patent #7469035 is unlicensed, patient #8971489 has been licensed by the University of Sydney to Leo Cancer Care. Paul J Keall and Jeremy Booth are investigators on one completed and two ongoing MLC tracking clinical trials that have been partially supported by Varian Medical Systems. Paul J Keall is an inventor on one licensed patent and one unlicensed patent related to MLC tracking. Paul J Keall acknowledges funding from an Australian Government NHMRC Senior Principal Research. Nicholas Hardcastle receives funding from Varian Medical Systems for unrelated research.

Ethical statement

Data presented in this work was collected as part of an ethics-approved clinical trial (ClinicalTrials.gov registration number: NCT02514512) and approved by the Northern Sydney Local Health District's Human Research Ethics Committee (reference number HREC/15/HAWKE/55). All patients provided informed consent for participation in the study and publication of the results. All investigations were conducted in accordance with the principles embodied in the Declaration of Helsinki and in accordance with the Australian Therapeutic Goods Administration (TGA).

References

Agnew C *et al* 2012 Implementation of phantom-less IMRT delivery verification using Varian DynaLog files and R/V output *Phys. Med. Biol.* **57** 6761

Balter J M *et al* 2005 Accuracy of a wireless localization system for radiotherapy *Int. J. Radiat. Oncol. Biol. Phys.* **61** 933–7

Brandner E D *et al* 2017 Motion management strategies and technical issues associated with stereotactic body radiotherapy of thoracic and upper abdominal tumors: a review from NRG oncology *Med. Phys.* **44** 2595–612

Caillet V *et al* 2019 In silico and experimental evaluation of two leaf-fitting algorithms for MLC tracking based on exposure error and plan complexity *Med. Phys.* **46** 1814–20

Cerviño L I *et al* 2009 The diaphragm as an anatomic surrogate for lung tumor motion *Phys. Med. Biol.* **54** 3529

Depuydt T *et al* 2014 Treating patients with real-time tumor tracking using the Vero gimbaled linac system: implementation and first review *Radiother. Oncol.* **112** 343–51

Eade T, Booth,J . and Keall P. *Lung cancer radiotherapy using realtime dynamic multileaf collimator (MLC) adaptation and radiofrequency tracking (LIGHTSABR)*. 2015; available from: https://clinicaltrials.gov/ct2/show/record/NCT02514512

Ehrbar S *et al* 2017 Validation of dynamic treatment-couch tracking for prostate SBRT *Med. Phys.* **44** 2466–77

Floriano A *et al* 2014 Retrospective evaluation of CTV to PTV margins using CyberKnife in patients with thoracic tumors *J. Appl. Clin. Med. Phys.* **15** 59–72

Glitzner M *et al* 2019 MLC-tracking performance on the Elekta unity MRI-linac *Phys. Med. Biol.*

Goldstein J D *et al* 2015 Continuous positive airway pressure for motion management in stereotactic body radiation therapy to the lung: a controlled pilot study *Int. J. Radiat. Oncol. Biol. Phys.* **93** 391–9

Guizar-Sicairos M, Thurman S T and Fienup J R 2008 Efficient subpixel image registration algorithms *Opt. Lett.* **33** 156–8

Jöhl A *et al* 2019 The ideal couch tracking system—requirements and evaluation of current systems *J. Appl. Clin. Med. Phys.*

Keall P J *et al* 2014 The first clinical implementation of electromagnetic transponder-guided MLC tracking *Med. Phys.* **41**

Kry S F *et al* 2017 AAPM TG 158: measurement and calculation of doses outside the treated volume from external-beam radiation therapy *Med. Phys.* **44** e391–e429

Lee D *et al* 2018 Audiovisual biofeedback improves the correlation between internal/external surrogate motion and lung tumor motion *Med. Phys.* **45** 1009–17

Mercieca S *et al* 2017 Interobserver variability in the delineation of the primary lung cancer and lymph nodes on different four-dimensional computed tomography reconstructions *Radiother. Oncol.*

Molitoris J K *et al* 2018 Advances in the use of motion management and image guidance in radiation therapy treatment for lung cancer *J. Thorac. Dis.* **10** S2437

Mueller M *et al* 2019 The first prospective implementation of markerless lung target tracking in an experimental quality assurance procedure on a standard linear accelerator *Phys. Med. Biol.*

Murphy M J *et al* 2008 The effect of transponder motion on the accuracy of the calypso electromagnetic localization system *Int. J. Radiat. Oncol. Biol. Phys.* **72** 295–9

Oar A *et al* 2019 Australasian gastrointestinal trials group (AGITG) and trans-tasman radiation oncology group (TROG) guidelines for pancreatic stereotactic body radiation therapy (SBRT) *Pract. Radiat. Oncol.*

Pepin E W *et al* 2011 Correlation and prediction uncertainties in the cyberknife synchrony respiratory tracking system *Med. Phys.* **38** 4036–44

Peulen H *et al* 2015 Target delineation variability and corresponding margins of peripheral early stage NSCLC treated with stereotactic body radiotherapy *Radiother. Oncol.* **114** 361–6

Pommer T *et al* 2013 The impact of leaf width and plan complexity on DMLC tracking of prostate intensity modulated arc therapy *Med. Phys.* **40** 111717

Raaymakers B *et al* 2017 First patients treated with a 1.5 T MRI-Linac: clinical proof of concept of a high-precision, high-field MRI guided radiotherapy treatment *Phys. Med. Biol.* **62** L41

Ruan D and Keall P 2010 Online prediction of respiratory motion: multidimensional processing with low-dimensional feature learning *Phys. Med. Biol.* **55** 3011

Sawkey D, Svatos M and Zankowski C 2012 Evaluation of motion management strategies based on required margins *Phys. Med. Biol.* **57** 6347

Steiner E *et al* 2019 Both four-dimensional computed tomography and four-dimensional cone beam computed tomography under-predict lung target motion during radiotherapy *Radiother. Oncol.* **135** 65–73

Stroom J C *et al* 1999 Inclusion of geometrical uncertainties in radiotherapy treatment planning by means of coverage probability *Int. J. Radiat. Oncol. Biol. Phys.* **43** 905–19

Thomas H M *et al* 2018 Impact of tumour motion compensation and delineation methods on FDG PET-based dose painting plan quality for NSCLC radiation therapy *J. Med. Imaging Radiat. Oncol.* **62** 81–90

van Herk M *et al* 2003 Biologic and physical fractionation effects of random geometric errors *Int. J. Radiat. Oncol. Biol. Phys.* **57** 1460–71

Venkat R B *et al* 2008 Development and preliminary evaluation of a prototype audiovisual biofeedback device incorporating a patient-specific guiding waveform *Phys. Med. Biol.* **53** N197

Yang Z-Y *et al* 2017 Target margin design for real-time lung tumor tracking stereotactic body radiation therapy using cyberknife xsight lung tracking system *Sci. Rep.* **7** 10826

Zhang Q, *et al, Three dimensional expansion of margins for single-fraction treatments: stereotactic radiosurgery brain cases* arXiv: 1205.1747

CHAPTER 06

Technical Note: In silico and experimental evaluation of two leaf-fitting algorithms for MLC tracking based on exposure error and plan complexity

This chapter is a technical note published in *Medical Physics* and written by me.

While the previous chapter computed the uncertainty of MLC tracking for patients treated with lung SABR, it also estimated the geometric impact of the MLC tracking technology alone to be less than 3 mm in all direction. It therefore raised the question of whether a faster MLC tracking leaf-fitting algorithm than the one use for the LIGHT SABR clinical trial would be more effective in a clinical situation.

This chapter answers this question by comparing two MLC tracking algorithms for thoracic and pelvic motion during radiotherapy. *In silico* and phantom experiments were performed for the clinically implemented MLC leaf-fitting algorithm and a novel, faster performing algorithm. The performances of the algorithms were compared based on the speed of calculation, and the quantification of fitted exposure errors attributed by the optimization algorithm.

Technical Note: *In silico* and experimental evaluation of two leaf-fitting algorithms for MLC tracking based on exposure error and plan complexity

Vincent Caillet[a)]
Northern Sydney Cancer Centre, Sydney, NSW, Australia
ACRF Image X Institute, Sydney Medical School, University of Sydney, Sydney, NSW, Australia

Ricky O'Brien
ACRF Image X Institute, Sydney Medical School, University of Sydney, Sydney, NSW, Australia

Douglas Moore
Beyond Center for Fundamental Concepts in Science, Arizona State University, Tempe, AZ, USA

Per Poulsen
Aarhus University, Aarhus, Denmark

Tobias Pommer
Unit of Radiotherapy Physics and Engineering, Karolinska University Hospital, Solna, Sweden

Emma Colvill
Northern Sydney Cancer Centre, Sydney, NSW, Australia
ACRF Image X Institute, Sydney Medical School, University of Sydney, Sydney, NSW, Australia

Amit Sawant
Department of Radiation Oncology, University of Maryland School of Medicine, Baltimore, MD 21201, USA

Jeremy Booth
Northern Sydney Cancer Centre, Sydney, NSW, Australia
ACRF Image X Institute, Sydney Medical School, University of Sydney, Sydney, NSW, Australia

Paul Keall
ACRF Image X Institute, Sydney Medical School, University of Sydney, Sydney, NSW, Australia

(Received 2 March 2018; revised 13 January 2019; accepted for publication 14 January 2019; published 4 March 2019)

Purpose: Multileaf collimator (MLC) tracking is being clinically pioneered to continuously compensate for thoracic and pelvic motion during radiotherapy. The purpose of this work was to characterize the performance of two MLC leaf-fitting algorithms, direct optimization and piecewise optimization, for real-time motion compensation with different plan complexity and tumor trajectories.
Methods: To test the algorithms, both *in silico* and phantom experiments were performed. The phantom experiments were performed on a Trilogy Varian linac and a HexaMotion programmable motion platform. High and low modulation VMAT plans for lung and prostate cancer cases were used along with eight patient-measured organ-specific trajectories. For both MLC leaf-fitting algorithms, the plans were run with their corresponding patient trajectories. To compare algorithms, the average exposure errors, i.e., the difference in shape between ideal and fitted MLC leaves by the algorithm, plan complexity and system latency of each experiment were calculated.
Results: Comparison of exposure errors for the *in silico* and phantom experiments showed minor differences between the two algorithms. The average exposure errors for *in silico* experiments with low/high plan complexity were 0.66/0.88 cm^2 for direct optimization and 0.66/0.88 cm^2 for piecewise optimization, respectively. The average exposure errors for the phantom experiments with low/high plan complexity were 0.73/1.02 cm^2 for direct and 0.73/1.02 cm^2 for piecewise optimization, respectively. The measured latency for the direct optimization was 226 $\pm$ 10 ms and for the piecewise algorithm was 228 $\pm$ 10 ms. *In silico* and phantom exposure errors quantified for each treatment plan demonstrated that the exposure errors from the high plan complexity (0.96 cm^2 mean, 2.88 cm^2 95% percentile) were all significantly different from the low plan complexity (0.70 cm^2 mean, 2.18 cm^2 95% percentile) ($P < 0.001$, two-tailed, Mann–Whitney statistical test).
Conclusions: The comparison between the two leaf-fitting algorithms demonstrated no significant differences in exposure errors, neither *in silico* nor with phantom experiments. This study revealed that plan complexity impacts the overall exposure errors significantly more than the difference between the algorithms. © *2019 American Association of Physicists in Medicine* [https://doi.org/10.1002/mp.13425]

Key words: fitting algorithm, MLC tracking, radiotherapy, real-time

1. INTRODUCTION

One of the main advantages of radiation therapy as opposed to other types of cancer treatment is that the treatment is noninvasive and highly targeted to the tumor. Despite strong evidence that the ITV-based planning technique (Internal Target Volume planning, ICRU 62[1]) provides safe radical treatment for stage I nonsmall cell lung carcinoma, there are no guarantees that the tumor will remain within the planned aperture throughout the entire treatment.[2,3]

New delivery approaches have been introduced to improve the targeting of the tumor during treatment. These techniques come in various forms, either by shifting the therapeutic beam to the tumor using a robotic arm CyberKnife,[4,5] a gimballed linear accelerator (Vero),[6,7] or the multileaf collimator (MLC)[8–10] or by adjusting the patient couch (couch tracking).[11]

Real-time MLC tracking is a novel technique that optimizes the leaf positions within the head of the linear accelerator to shift the radiation beam multileaf collimator leaves according to tumor motion. It has been implemented preclinically in several institutions on commercial linear accelerators[12–14] or developed into in-house control software and leaf-fitting algorithms.[8,10,12,15–17] Real-time MLC tracking has been clinically pioneered with three clinical trials leading to the first MLC tracking treatment for prostate[18–20] and stereotactic lung[21] with results reported in previous publications.[19,21]

The current clinically used version of MLC tracking relies on a leaf-fitting optimization algorithm (also known as "MLC tracking algorithm") named "direct optimization" algorithm.[22] A recent publication by Moore et al.[17] introduced an alternative MLC tracking algorithm named "piecewise optimization algorithm". With the current design of the piecewise algorithm, Moore et al. investigated its performances *in silico* using standard tumor motion (three patients) and intensity-modulated radiation therapy (IMRT) plans. However, *in silico* tests do not always reflect the real-life clinical situation. For that reason, their respective performances should be tested utilizing a linear accelerator with a broad range of tumor motions and MLC plan complexity.

To allow a thorough performance comparison between both algorithms in a clinical setting, the piecewise algorithm was implemented in the clinical version of the MLC tracking software. The aim of this work was to characterize the performance of two MLC leaf-fitting algorithms used in real-time motion compensation. This will be done both *in silico* and experimentally, spanning a range of tumor motions and treatment plans with varying degree of MLC modulation.

The significance of this paper is that it is the first to investigate and experimentally compare two MLC tracking algorithms in the identical clinical setting on a linear accelerator.

2. METHOD

2.A. Principle of multileaf collimator tracking algorithms

Multileaf collimator tracking is operated via an optimization algorithm tasked with finding the best-fitted leaf positions given a set of various constraints (finite leaf width and speed), or constraints setup by the user prior to treatment delivery, such as prescribing various tolerances or radiobiological properties to the organs-at-risk to avoid excessive overdosing.

The mechanism for managing these setup constraints differs between the direct and piecewise optimization algorithm. The different components of the direct optimization algorithm can be found in Ruan et al.[22], while more extensive explanations on the piecewise algorithm can be found in Moore et al.[17] Although both algorithms allow the MLC leaf positions to be optimized according to the radio-sensitivity factor attributed to different OAR (connoted as λ and σ constraints in the respective papers[17,22]), each algorithm deals with spatial variance differently. The optimization process is operated for the direct optimization on a pixel basis within the beam's eye view, therefore relying on a two-dimensional map of the organs.

The main difference between the two algorithms is that the piecewise algorithm deals with spatial variance by having an arbitrary number of volumetric ROI (Regions of Interest), hence accounting for the radio-sensitivity in three dimensions. In both cases, this implies that an *a priori* knowledge of the position and volume of OAR is available prior to treatment, or that each OAR is being localized in real-time during the treatment delivery.

The second difference is the way each algorithm deals with the quantification of exposure area that is sought to be minimized. For the direct optimization, the cost function is integrated both along and perpendicular to the leaf motion, as opposed to the piecewise algorithm where the algorithm resolves the integration linearly in one direction, solely along the leaf motion direction. Linear integral implicates that the algorithm is expected to converge faster toward a solution with the piecewise algorithm given equivalent set of constraints.

2.B. Experiments to assess and compare the algorithm performances

To characterize the performances of the algorithms, a series of *in silico* simulations and phantom experiments were performed. Both algorithms were tested under identical conditions assuming homogenous dose conditions: the target is considered as a rigid, nondeformable body and the underdose and overdose weights are set to be equal. Variables included the tumor motion, treatment site, and plan complexity. Comparison of algorithm performance was based on exposure errors, plan complexity, and the system latency. Figure 1 provides an overview of the method to

assess the performance of each algorithm both *in silico* and experimentally on a linear accelerator. Further details are provided below.

2.B.1. In silico *and phantom experiments*

The *in silico* experiments were performed on a Latitude E7450 i7 2.60 GHz Dell 16 Gb RAM using an MLC simulator.[23] The tumor motion traces were imported into the simulator as text files. The DICOM plan was read by the software and the treatment delivery was simulated. The simulator leaf speed was limited to 3.6 cm/s being the leaf speed of the actual linear accelerator.

The phantom experiments were performed on a Trilogy (Varian, Palo Alto, CA, USA) linear accelerator. Tumor motion traces were loaded into the HexaMotion programmable motion platform (Scandidos, Uppsala, Sweden) and triggered to start 10 s before the beginning of the beam delivery to allow training of the prediction algorithm. Calypso electromagnetic transponders (Varian Medical System, Palo Alto, CA, USA) were embedded into the HexaMotion platform, with a research version of the Calypso system sending the target position to the MLC tracking system. The kernel density estimation algorithm[24] currently used was clinically used for the lung trajectories.

2.B.2. Tumor motion

To span the type of tumor motion observed during radiation therapy, thoracic and pelvic tumor motion traces were selected from published databases to be characteristic three-dimensional (3D) motion patterns for those sites. Four types of motion were chosen for the lung[25] from a CyberKnife study, and four motion patterns for the prostate[26] obtained from a study with patients implanted with Calypso electromagnetic transponders. These tumor motion traces were categorized and named according to their characteristic pattern in previous study. Thoracic motion patterns were categorized as typical tumor motion, high-frequency breathing, a predominantly lateral motion, and characterized baseline shift. The represented prostate motion patterns were continuous drift, high-frequency excursions, erratic tumor motion, and stable tumor position.

2.B.3. Treatment plans

For each clinical site (lung and prostate), a selection of treatment plans used for previous MLC tracking experiments[27] were delivered that differed in MLC modulation to span the plan complexity expected during clinical practice. Two plans, low and highly modulated VMAT plan, were selected for each site, by varying the set of competitive objectives on the target and OARs. All arcs spanned a 358° revolution with the collimator set at 90° (i.e., with the leaves parallel to longitudinal target motion). All plans were prescribed to deliver 2 Gy to 95% of the Planning Target Volume.

2.B.4. Evaluation of plan complexity

With MLC tracking, the plan complexity is known to complicate the task of the algorithm for the leaves to reach the desired positions.[28,29] Therefore, for each of the four plans lung/prostate and modulation high/low modulations, their complexity needed to be quantified. The plan complexity was evaluated based on four parameters:

1. MU weighted Average adjacent Leaf Distance (ALDw[29]), previously shown to correlate with MLC tracking performance[28]
2. The average leaf travel for each plan, considering solely the leaves that contribute to the open leaves aperture.[28]

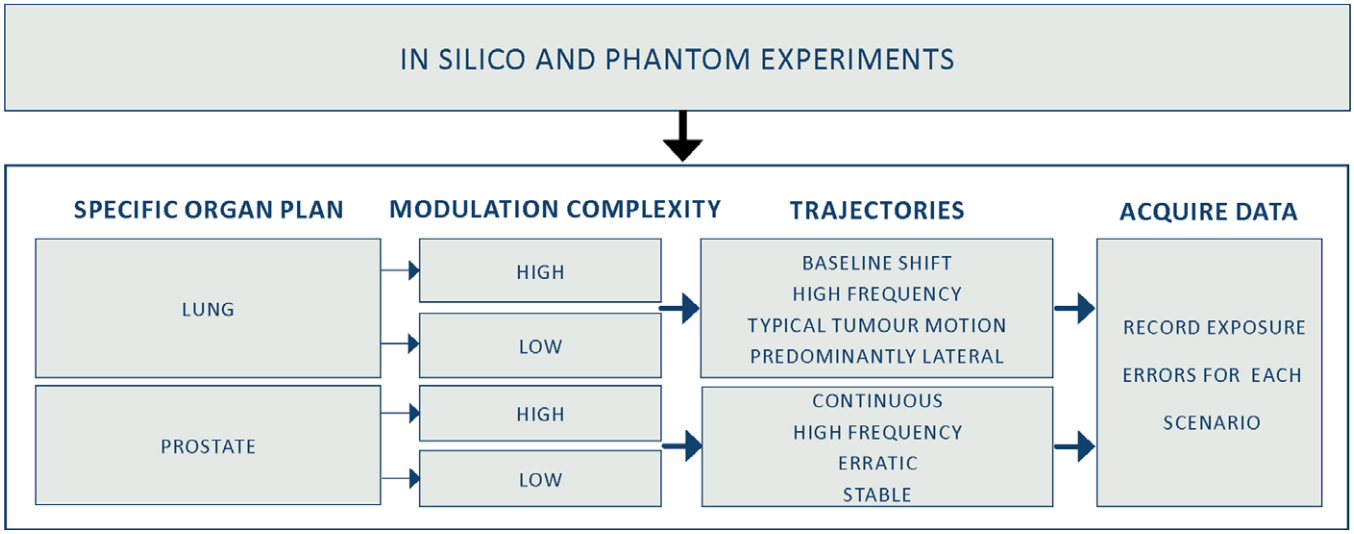

FIG. 1. Performance of each algorithm was characterized by two sets of experiments, *in silico* and phantom, conducted for two specific target scenarios (lung and prostate) combining different sets of plan complexities (high and low) and trajectories (baseline shift, high frequency, etc.). The exposure errors were calculated for each scenario. [Color figure can be viewed at wileyonlinelibrary.com]

3. The average area over circumference AoC[28] with formula $AoC = \frac{AreaofMLCaperture}{Circumference}$
4. The VMAT modulation score (MCs) by Masi et al.[30]

2.B.5. Measuring the system latency

Multileaf collimator tracking latency represents the inherent time delay between the tumor motion and the finished movement of the leaves to align the beam and the tumor. While execution of both MLC tracking algorithms possesses some inherent amount of latency, it is expected that a faster algorithm will be able to reduce the overall system latency.

The latency was evaluated using the setup described in Sawant et al.[31] A ball bearing was moving in a superior–inferior direction along the parallel motion of a circular shape radiation field during which EPID images were acquired at 15 Hz operated on the computer console equipped with a 2.27 GHz Intel Xeon E5520 processor and 4 GB RAM. The ball bearing was placed onto the HexaMotion platform embedded with the Calypso electromagnetic beacons. For each optimization algorithm, EPID projections were obtained over 10 periods. Since both the ball bearing and the leaves move in a sinusoidal motion, the two structures were segmented from the EPID and a sinusoidal fit was used to calculate the temporal offset between the centroid of the ball and the MLC aperture. The latency was then calculated as the time delay between the ball position and the segmented MLC aperture.

2.C. Comparing MLC tracking algorithm performances based on leaf-fitting exposure errors

To compare both performances, the exposure errors (overdose + underdose) were quantified in the beam's eye view using a framework developed by Poulsen et al.[32]

The mismatched area between the actual and planned MLC aperture represents the total amount of exposure errors which can be separated into individual sources of errors, namely the exposure errors due to width of the leaves, their speed and prediction algorithm errors when in use.

For each experiment, the exposure errors were computed using the fitted MLC positions obtained from the MLC tracking software. The fitted MLC positions corresponded to the given MLC positions fitted by the algorithm, thereby accounting for the width of the leaves but regardless of their physical speed. Focusing solely on the fitted MLC position dismisses any potential source of uncertainties allowing for a more direct comparison between the algorithms.

For each paired experiment, the exposure errors throughout the treatment arc were compared between each other using the Pearson correlation coefficient and root-mean-square error to evaluate the differences in exposure errors for each control point. Figure 2 provides an example of the exposure errors for a "paired experiment", representing identical experimental conditions (same plan and tumor). For each experiment, these exposure errors were computed using the resulting tumor tracking logs and fitted MLC position updated at 30 Hz into text files. Exposure error computation was achieved using MATLAB (R2017a, Math Works).

3. RESULTS

3.A. Quantification of exposure errors for each optimization algorithm

The average exposure errors for *in silico* low/high modulation were 0.66/0.88 cm^2 for direct optimization and 0.66/0.88 cm^2 for piecewise optimization. For the phantom experiment, it was 0.73/1.02 cm^2 for direct and 0.73/1.02 cm^2 for piecewise optimization. The side-by-side exposure errors displayed in Fig. 3 suggests that both algorithms performed equivalently spanning a large range of tumor motion, plan complexity, and treatment site.

The analysis of the *in silico* experiments demonstrated that the Pearson correlation coefficient for both algorithms is higher than r = 0.96 for all sets of organs and trajectories. The similar data obtained during linac experiments also showed strong correlation (r > 0.9) in most cases. The mean root-mean-square errors (RMSE) between paired algorithms were 0.10 cm^2 for the *in silico* and 0.18 cm^2 for the phantom experiments. High correlation and small RMSE error suggest

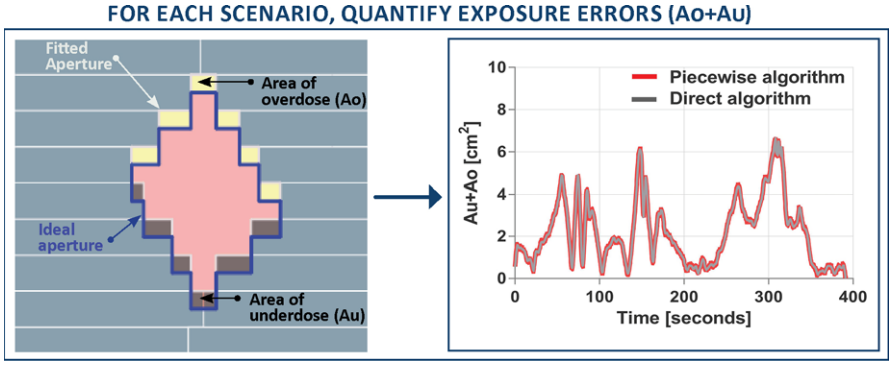

FIG. 2. For each scenario, the exposure errors were compared for each set of paired experiments to compare the piecewise algorithm against the direct optimization.

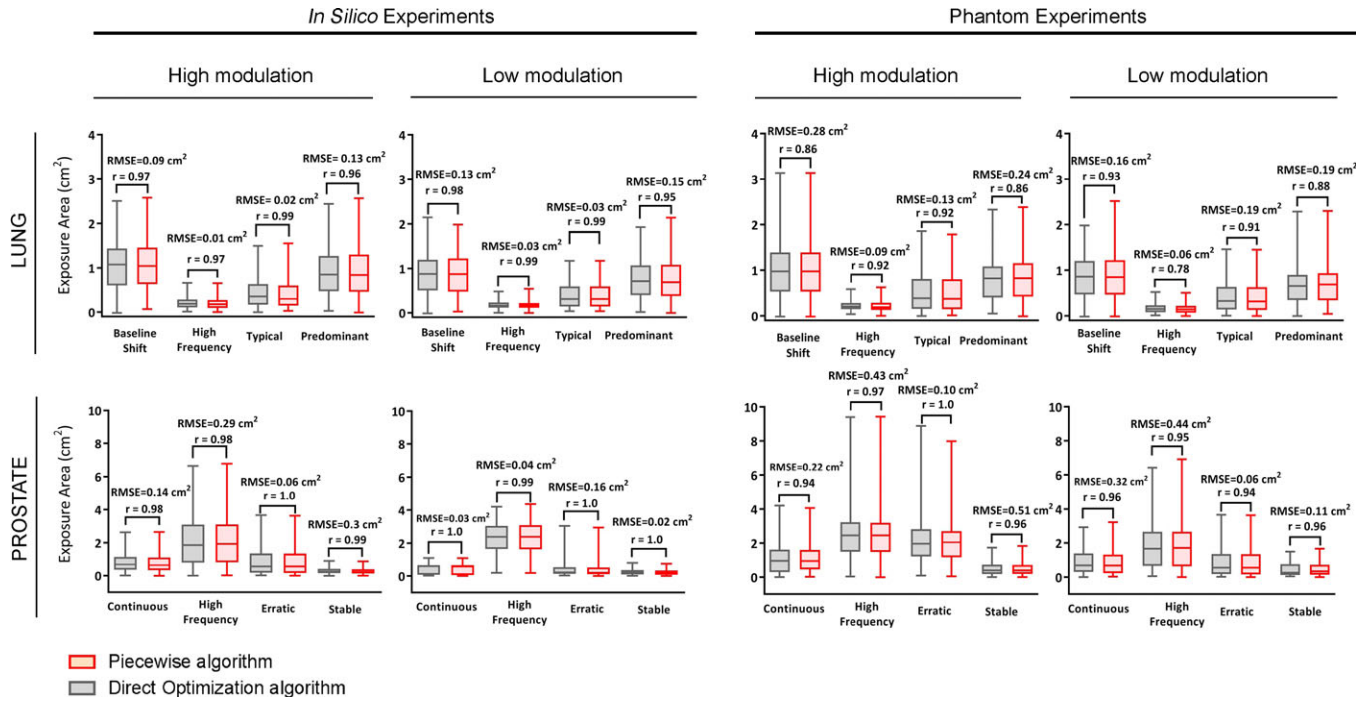

FIG. 3. Leaf-fitting exposure errors for the direct (gray) and piecewise (red) optimization for both *in silico* and phantom experiment (delivered). The Pearson correlation coefficient (r) and the root-mean-square error are provided for each paired experiment showing that the sum of exposure errors is equivalent given any tumor motion, organ, and plan complexity.

strong relationship between paired experiment results for all types of trajectory and plan complexity, indicating that both algorithms performed equivalently.

3.B. Relationship between plan complexity and exposure errors

The quantified simulated and phantom experiment exposure errors for each treatment plan established that the exposure errors from the high modulation plan (0.96 cm^2, 2.88 cm^2 95% percentile) were all significantly different from the low modulation (0.70 cm^2, 2.18 cm^2 95% percentile) ($P < 0.001$, two-tailed, Mann–Whitney statistical test). The descriptive metrics used to quantify the plan complexity are summarized in Table I.

The average distance to adjacent leaves and leaf travel distance was shown to increase with plan complexity while the modulation score (MCs) and relative area over circumference decreases with plan complexity. These results provide further evidence of the impact of treatment complexity on the exposure errors.

3.C. Latency

The latency for the direct optimization was 226 ± 10 ms and for the piecewise algorithm 228 ± 10 ms. These physical latencies can be compared with the fitting latency within the software. Across all the plans and tumor motion, the *in silico* fitting latency for the direct optimization algorithm was 12.2 ± 5 ms, compared with the piecewise algorithm computed as 3.1 ± 1 ms. Despite these differences, the fitting time between algorithms did not impact the overall latency of the experimental setup, only capable of detecting uncertainties within ±10 ms.

TABLE I. Summary of the plan metric to assess the plan complexity of each of the four plans.

	Lung		Prostate	
	High modulation	Low modulation	High modulation	Low modulation
Field MU	596	342	737	422
ALD_w	0.71 cm	0.20 cm	1.40 cm	0.70 cm
Leaf travel	0.19 cm	0.04 cm	0.30 cm	0.22 cm
AoC	0.34	0.75	0.49	0.92
MCS	0.07	0.17	0.15	0.28

AoC, Area over Circumference; ALD_w, Average adjacent Leaf Distance; MCs, modulation score; MU weighted.

4. DISCUSSION

The goal of this study was to characterize the performance of two MLC tracking algorithms for radiotherapy in a realistic simulated and clinical environment. Both algorithms were tested alternatively *in silico* and experimentally on a linear accelerator for the range of organ motion and plan complexity that may be expected during clinical practice.

This is the first time that two MLC tracking algorithms were experimentally compared in the identical clinical setting on a linear accelerator. Moore et al.[1] tested the

performances of the piecewise algorithm *in silico* with IMRT plans as a proof of concept. However, leaf-fitting is one part of the larger MLC tracking framework, and while *in silico* validation is a valuable tool to demonstrate proof of concept, the ultimate test is experimental investigation. Experimental investigation captures the impact of the leaf-fitting algorithm with other software and hardware subsystems (e.g., compatibility issues with the Calypso tracking system, error catching, beam-hold assertion, or constant rotating gantry during VMAT). For these reasons, this paper presents the first empirical comparison between the two algorithms.

We found that the plan complexity and tumor motion patterns have a much larger impact on dosimetric fidelity than the leaf-fitting algorithms. The implication is that there are bigger gains to be made by improved planning than developing more complex or faster algorithms.

The implementation and development of faster MLC tracking algorithms is therefore potentially marginalized by the prerequisite to reduce plan complexity or improve the hardware capabilities. Hardware enhancement has been investigated under diverse forms. Pommer et al.[28] investigated the dosimetric impact of finer leaves by testing alternatively a Varian Novalis Tx with Millennium MLC (5 mm leaf with) and High-Definition MLC (2.5 mm leaf width). Using reflective markers and the ExacTrac (Brainlab, Germany) to provide positional input to the tracking system, they found that finer leaves improved the tracking accuracy compared with 5 mm leaf width. The Varian TrueBeam system equipped with High-Definition MLC also provides MLC tracking capabilities in developer mode, but no performance analysis or dosimetric comparisons with other systems have been published to date.

Falk et al.[29] found that leaf position constraints can be setup within the treatment planning system during planning optimization to limit the movement of the leaves during planning. Other hardware enhancement, such as dynamic alignment of the collimator angle,[33] hybrid couch-MLC tracking strategies[34] improves MLC tracking accuracy by reducing the exposure errors for both prostate and lung.

Using a 2D time-resolved framework for performance analysis provides a fast and reliable comparison of exposure errors. This method offers a point-by-point analysis that conceptually facilitates the search of exposure errors and allows a straightforward comparison between multiple plan parameters within a single fixed analysis framework. Also, the analysis of exposure errors for MLC tracking has been shown to be correlated with dosimetric errors for lung and prostate[32,35] using gamma failure and root-mean-square errors.

An application where MLC tracking is uniquely capable of motion compensation is tracking deforming targets and deforming systems, e.g., a primary tumor and regional nodes for locally advanced lung and prostate cancer radiotherapy. Preliminary studies using the direct optimization algorithm have investigated experimental target deformation and multitarget tracking.[36] These experiments have been carried out on a linear accelerator using phantoms by mapping the deformation field in the linear accelerator beam's eye view and optimizing the fitting process accordingly.

The treatment plans and the tumor motion traces are included as supplementary materials (Data S1) to allow other groups to benchmark their algorithms against the results shown here.

5. CONCLUSION

The performance of two MLC tracking algorithms was characterized and compared using a 2D time-resolved framework in a clinical realistic scenario. The comparison was based on the quantification of fitted exposure errors attributed by the optimization algorithm solely, regardless of the speed of the leaves. Our results showed that the two algorithms performed similarly and provide equivalent quality-of-fit for the scenarios evaluated. The main source of error can be attributed to the complexity of the plan, quantified prior to plan delivery, which was shown to greatly impact on the MLC tracking accuracy.

ACKNOWLEDGMENT

Paul J Keall and Ricky O'Brien gratefully acknowledge funding from the Australian Cancer Research Foundation. Paul J Keall acknowledges funding from an Australian Government NHMRC Senior Principal Research Fellowship. Jeremy Booth thanks Varian Medical Systems for provision of research systems used in this study.

CONFLICTS OF INTERESTS

Paul J Keall and Jeremy Booth are investigators on one completed and two ongoing MLC tracking clinical trials that have been partially supported by Varian Medical Systems. Paul J Keall and Amit Sawant are inventors on one licensed patent and one unlicensed patent related to MLC tracking. Paul J Keall, Ricky O'Brien, and Vincent Caillet gratefully acknowledge funding from the Australian Cancer Research foundation. Paul J Keall acknowledges funding from an Australian Government NHMRC Senior Principal Research Fellowship.

[a)]Author to whom correspondence should be addressed. Electronic mail: vcai6204@uni.sydney.edu.au.

REFERENCES

1. ICRU. International Commission on Radiation Units and Measurements. Prescribing, recording and reporting photon beam therapy (Supplement to ICRU Report 50). ICRU Report 62. Oxford: Oxford University Press; 1999.
2. Wang L, Hayes S, Paskalev K, et al. Dosimetric comparison of stereotactic body radiotherapy using 4D CT and multiphase CT images for treatment planning of lung cancer: evaluation of the impact on daily dose coverage. *Radiother Oncol*. 2009;91:314–324.
3. Koto M, Takai Y, Ogawa Y, et al. A phase II study on stereotactic body radiotherapy for stage I non-small cell lung cancer. *Radiother Oncol*. 2007;85:429–434.

4. Adler JR Jr, Chang SD, Murphy MJ, et al. The Cyberknife: a frameless robotic system for radiosurgery. *Stereotact Funct Neurosurg*. 1997;69:124–128.
5. Prévost J-B, Hoogeman MS, Praag J, et al. Stereotactic radiotherapy with real-time tumor tracking for non-small cell lung cancer: clinical outcome. *Radiother Oncol*. 2009;91:296–300.
6. Depuydt T, Poels K, Verellen D, et al. Initial assessment of tumor tracking with a gimbaled linac system in clinical circumstances: a patient simulation study. *Radiother Oncol*. 2013;106:236–240.
7. Mukumoto N, Nakamura M, Yamada M, et al. Intrafractional tracking accuracy in infrared marker-based hybrid dynamic tumour-tracking irradiation with a gimballed linac. *Radiother Oncol*. 2014;111:301–305.
8. Fast MF, Nill S, Bedford JL, Oelfke U. Dynamic tumor tracking using the Elekta Agility MLC. *Med Phys*. 2014;41:111719.
9. Falk M, af Rosenschöld PM, Keall P, et al. Real-time dynamic MLC tracking for inversely optimized arc radiotherapy. *Radiother Oncol*. 2010;94:218–223.
10. Keall P, Kini VR, Vedam SS, Mohan R. Motion adaptive x-ray therapy: a feasibility study. *Phys Med Biol*. 2001;46:1.
11. Lang S, Zeimetz J, Ochsner G, Schmid Daners M, Riesterer O, Klöck S. Development and evaluation of a prototype tracking system using the treatment couch. *Med Phys*. 2014;41:021720.
12. Tacke MB, Nill S, Krauss A, et al. Real-time tumor tracking: automatic compensation of target motion using the Siemens 160 MLC. *Med Phys*. 2010;37:753–761.
13. Krauss A, Nill S, Tacke M, Oelfke U. Electromagnetic real-time tumor position monitoring and dynamic multileaf collimator tracking using a Siemens 160 MLC: geometric and dosimetric accuracy of an integrated system. *Int J Radiat Oncol Biol Phys*. 2011;79:579–587.
14. Hansen R, Ravkilde T, Worm ES, et al. Electromagnetic guided couch and multileaf collimator tracking on a TrueBeam accelerator. *Med Phys*. 2016;43:2387–2398.
15. Davies G, Poludniowski G, Webb S. MLC tracking for Elekta VMAT: a modelling study. *Phys Med Biol*. 2011;56:7541.
16. Davies G, Clowes P, Bedford JL, Evans PM, Webb G, Poludniowski G. An experimental evaluation of the Agility MLC for motion-compensated VMAT delivery. *Phys Med Biol*. 2013;58:4643.
17. Moore D, Ruan D, Sawant A. Fast leaf-fitting with generalized underdose/overdose constraints for real-time MLC tracking. *Med Phys*. 2016;43:465–474.
18. Keall PJ, Colvill E, O'Brien R, et al. The first clinical implementation of electromagnetic transponder-guided MLC tracking. *Med Phys*. 2014;41:020702.
19. Colvill E, Booth JT, O'Brien RT, et al. Multileaf collimator tracking improves dose delivery for prostate cancer radiation therapy: results of the first clinical trial. *Int J Radiat Oncol Biol Phys*. 2015;92:1141–1147.
20. Keall P, Nguyen DT, O'Brien R, et al. Stereotactic prostate adaptive radiotherapy utilising kilovoltage intrafraction monitoring: the TROG 15.01 SPARK trial. *BMC Cancer*. 2017;17(1):180.
21. Caillet V, Colvill E, Szymura K, Stevens M, Booth J, Keall P. SU-G-JeP1-05: Clinical Impact of MLC Tracking for Lung SABR. *Med Phys*. 2016;43:3648–3649.
22. Ruan D, Keall P. Dynamic multileaf collimator control for motion adaptive radiotherapy: An optimization approach. in Power Engineering and Automation Conference (PEAM), 2011 IEEE. 2011. IEEE.
23. Poulsen PR, Ravkilde T, O'Brien RT, Keall PJ. Experimentally validated simulator of dynamic MLC tracking treatments: a tool for tracking QA. *Int J Radiat Oncol Biol Phys*. 2013;87:S45.
24. Ruan D, Keall P. Online prediction of respiratory motion: multidimensional processing with low-dimensional feature learning. *Phys Med Biol*. 2010;55:3011.
25. Suh Y, Dieterich S, Cho B, Keall PJ. An analysis of thoracic and abdominal tumour motion for stereotactic body radiotherapy patients. *Phys Med Biol*. 2008;53:3623.
26. Langen KM, Willoughby TR, Meeks SL, et al. Observations on real-time prostate gland motion using electromagnetic tracking. *Int J Radiat Oncol Biol Phys*. 2008;71:1084–1090.
27. Keall PJ, Sawant A, Cho B, et al. Electromagnetic-guided dynamic multileaf collimator tracking enables motion management for intensity-modulated arc therapy. *Int J Radiat Oncol Biol Phys*. 2011;79:312–320.
28. Pommer T, Falk M, Poulsen PR, Keall PJ, O'Brien RT, af Rosenschöld PM. The impact of leaf width and plan complexity on DMLC tracking of prostate intensity modulated arc therapy. *Med Phys*. 2013;40:111717.
29. Falk M, Larsson T, Keall P, et al. The dosimetric impact of inversely optimized arc radiotherapy plan modulation for real-time dynamic MLC tracking delivery. *Med Phys*. 2012;39:1588–1594.
30. Masi L, Doro R, Favuzza V, Cipressi S, Livi L. Impact of plan parameters on the dosimetric accuracy of volumetric modulated arc therapy. *Med Phys*. 2013;40:071718.
31. Sawant A, Dieterich S, Svatos M, Keall P. Failure mode and effect analysis-based quality assurance for dynamic MLC tracking systems. *Med Phys*. 2010;37:6466–6479.
32. Poulsen PR, Fledelius W, Cho B, Keall P. Image-based dynamic multileaf collimator tracking of moving targets during intensity-modulated arc therapy. *Int J Radiat Oncol Biol Phys*. 2012;83:e265–e271.
33. Murtaza G, Toftegaard J, Ullah Khan E, Poulsen PR. Volumetric modulated arc therapy with dynamic collimator rotation for improved multileaf collimator tracking of the prostate. *Radiother Oncol*. 2017;122:109–115.
34. Toftegaard J, Hansen R, Ravkilde T, Macek K, Poulsen PR. An experimentally validated couch and MLC tracking simulator used to investigate hybrid couch-MLC tracking. *Med Phys*. 2017;44:798–809.
35. Ravkilde T, Keall PJ, Grau C, Høyer M, Poulsen PR. Time-resolved dose distributions to moving targets during volumetric modulated arc therapy with and without dynamic MLC tracking. *Med Phys*. 2013;40:111723.
36. Ge Y, O'Brien RT, Sheih C-C, Booth JT, Keall PJ. Toward the development of intrafraction tumor deformation tracking using a dynamic multileaf collimator. *Med Phys*, 2014;41:061703.

SUPPORTING INFORMATION

Additional supporting information may be found online in the Supporting Information section at the end of the article.

Data S1: All the treatment plans and tumor motion traces used in this manuscript can be downloaded from the following link: https://cloudstor.aarnet.edu.au/plus/s/cC7Jy0LrfH2SiAz

CHAPTER 07

Conclusion and Future work

This thesis presents the first-in-world implementation of the MLC tracking technology to correct for tumour motion during lung SABR.

This thesis initially focused on the feasibility of this novel technique by simulating patients' tumour motion in a real clinical scenario that provided confidence in the technology before moving to clinical trial. As this trial concluded, the geometric accuracy of the system was assessed for all seventeen patients. The results from this study showed that MLC tracking accuracy fell within clinically acceptable limits but suffered from both hardware and software limitations. Two MLC tracking algorithms were therefore comprehensively compared to understand the impact of leaf-fitting speed and exposure errors. It was determined that plan complexity and tumour prediction were large sources of error while algorithm speed was found to have little effect on MLC tracking performances. As such, the former two areas of research should be the focus of future MLC tracking development.

As a result of this thesis, MLC tracking has been shown to be able to deliver a safe and confident radiation treatment to the patient. The LIGHT SABR clinical trial provides the confidence that a tumour tracking technique can be implemented on a "standard" linear accelerator, enhancing its ability to account for tumour motion.

Future Directions

The current state of the art of MLC tracking still requires some developments to be clinically and widely available to ensure that the technology provides a safer and higher standard of treatment than current standard of care.

A very interesting and promising area of research is markerless tumour tracking that would not require any physical insertions of beacons and would rely solely on external devices to track the internal position of the tumour or surrogate. Markerless tracking has been used with the CyberKnife Xsight lung tracking software or the carbon-ion pencil beam system [1, 2], but the combination of markerless tracking with MLC tracking remains yet to be implemented in a clinical setting.

There is increasing evidence that correcting for tumour motion during radiotherapy should

account for both tumour translation and tumour rotation. Much of the clinical focus has been on tumour translation, but the implementation of tumour tracking to account for rotation is on its way as such rotations have shown to be significant for both prostate and lung tumours [3, 4]. Kim *et al.* [5] use the KIM technology to successfully estimate, in real-time, the 6 degrees-of-freedom motion during prostate treatment. This method could be further enhanced using external respiratory sensors, as investigated by Nguyen *et al.* [6]. An exciting study from Wu *et al.* [7] investigated MLC tracking adaptation of rotational target motion limited for rotation perpendicular to the beam direction. The author, however, mentioned that adaptation of rotation parallel to the beam direction would require further investigation.

Along with tumour rotation, the deformation of the surrounding internal anatomy is being investigated. The feasibility of MLC tracking to account for deforming systems has been investigated *in silico* by Ge *et al.* [8], a study that gave confidence to set up the very exciting KOALA clinical trial. The purpose of the KOALA (NCT02588846) clinical trial is to offer the first multi-target tracking in prostate radiotherapy using MLC and KIM to account for the relative motion of the moving prostate tumour target and the static pelvic nodal target for high-risk prostate cancer patients.

As stated in **Chapter 2**, hardware could be improved to provide thinner and faster leaves, as well as minimizing the leakage between the leaves. Additional software improvements to provide a faster response time between the detection of tumour position and the dynamic re-alignment of the MLC leaves would potentially help reduce the latency of the system.

And last, but not least, is the advent of MRI-linac that has garnered enormous interest over the last few years. Hybrid on-line magnetic resonance imaging (MRI)-guidance have enabled intra-fraction imaging for real-time tumour tracking with incomparable image quality. Recently, Glitzner *et al.* [9] demonstrated the feasibility of implementing MLC tracking on a commercially available MRI-linac system. MRI-linac potentially hold the key toward fast, safe and markerless MLC tracking that may elevate the standard of care to a widely available tumour tracking for all moving organs during radiotherapy.

References

1. Mori, S., et al., *Carbon-ion pencil beam scanning treatment with gated markerless tumor tracking: an analysis of positional accuracy.* International Journal of Radiation Oncology* Biology* Physics, 2016. **95**(1): p. 258-266.
2. Fu, D., et al., *Xsight lung tracking system: A fiducial-less method for respiratory motion tracking*, in *Treating Tumors that Move with Respiration*. 2007, Springer. p. 265-282.
3. Amro, H., et al., *The dosimetric impact of prostate rotations during electromagnetically guided external-beam radiation therapy.* International Journal of Radiation Oncology* Biology* Physics, 2013. **85**(1): p. 230-236.
4. Aubry, J.-F., et al., *Measurements of intrafraction motion and interfraction and intrafraction rotation of prostate by three-dimensional analysis of daily portal imaging with radiopaque markers.* International Journal of Radiation Oncology* Biology* Physics, 2004. **60**(1): p. 30-39.
5. Kim, J., et al., *Quantifying the accuracy and precision of a novel real-time 6 degree-of-freedom kilovoltage intrafraction monitoring (KIM) target tracking system.* Physics in Medicine & Biology, 2017. **62**(14): p. 5744.
6. Nguyen, D.T., et al., *An augmented correlation framework for the estimation of tumour translational and rotational motion during external beam radiotherapy treatments using intermittent monoscopic x-ray imaging and an external respiratory signal.* Physics in Medicine & Biology, 2018. **63**(20): p. 205003.
7. Wu, J., et al., *Electromagnetic detection and real-time DMLC adaptation to target rotation during radiotherapy.* International Journal of Radiation Oncology* Biology* Physics, 2012. **82**(3): p. e545-e553.
8. Ge, Y., et al., *Toward the development of intrafraction tumor deformation tracking using a dynamic multi-leaf collimator.* Medical physics, 2014. **41**(6Part1): p. 061703.
9. Glitzner, M., et al., *MLC-tracking performance on the Elekta unity MRI-linac.* Physics in Medicine & Biology, 2019. **64**(15): p. 15NT02.

APPENDIX 01

The first patient treatment of electromagnetic-guided real time adaptive radiotherapy using MLC tracking for lung SABR

This chapter was published in *Radiotherapy and Oncology* and written by Jeremy Booth. I, Vincent Caillet, contributed to software and interface development and performed the quality assurance procedures, data collection and analysis for the clinical trial detailed in the manuscript.

This chapter details the clinical process and quality assurance procedures put into place during the LIGHT SABR clinical trial for the first in-world patient to be treated with this technique. The manuscript reports on the tumour motion and the dosimetric results using a dose reconstruction algorithm that compares the planned and delivered treatment dose to the patient.

Radiotherapy and Oncology 121 (2016) 19–25

Contents lists available at ScienceDirect

Radiotherapy and Oncology

journal homepage: www.thegreenjournal.com

First in man

The first patient treatment of electromagnetic-guided real time adaptive radiotherapy using MLC tracking for lung SABR

Jeremy T. Booth [a,b,*], Vincent Caillet [a,b], Nicholas Hardcastle [a,c], Ricky O'Brien [b], Kathryn Szymura [a], Charlene Crasta [a], Benjamin Harris [a], Carol Haddad [a], Thomas Eade [a], Paul J. Keall [b]

[a] Northern Sydney Cancer Centre, Level 1 Royal North Shore Hospital; [b] University of Sydney, Schools of Physics or Medicine, Sydney; and [c] Centre for Medical Radiation Physics, University of Wollongong, Wollongong, Australia

ARTICLE INFO

Article history:
Received 26 April 2016
Received in revised form 18 August 2016
Accepted 22 August 2016
Available online 17 September 2016

Keywords:
Lung cancer
Real time adaptive radiotherapy
MLC tracking
Radiation pneumonitis

ABSTRACT

Background and purpose: Real time adaptive radiotherapy that enables smaller irradiated volumes may reduce pulmonary toxicity. We report on the first patient treatment of electromagnetic-guided real time adaptive radiotherapy delivered with MLC tracking for lung stereotactic ablative body radiotherapy.

Materials and methods: A clinical trial was developed to investigate the safety and feasibility of MLC tracking in lung. The first patient was an 80-year old man with a single left lower lobe lung metastasis to be treated with SABR to 48 Gy in 4 fractions. In–house software was integrated with a standard linear accelerator to adapt the treatment beam shape and position based on electromagnetic transponders implanted in the lung. MLC tracking plans were compared against standard ITV-based treatment planning. MLC tracking plan delivery was reconstructed in the patient to confirm safe delivery.

Results: Real time adaptive radiotherapy delivered with MLC tracking compared to standard ITV-based planning reduced the PTV by 41% (18.7–11 cm^3) and the mean lung dose by 30% (202–140 cGy), V20 by 35% (2.6–1.5%) and V5 by 9% (8.9–8%).

Conclusion: An emerging technology, MLC tracking, has been translated into the clinic and used to treat lung SABR patients for the first time. This milestone represents an important first step for clinical real-time adaptive radiotherapy that could reduce pulmonary toxicity in lung radiotherapy.

© 2016 Elsevier Ireland Ltd. All rights reserved. Radiotherapy and Oncology 121 (2016) 19–25

Stereotactic Ablative Body Radiotherapy (SABR) for lesions in the lung has shown substantially improved 5 year survival compared to conventionally fractionated treatments [1–3]. Comparison with surgery outcomes is favourable in weighted cohorts [4]. However, further application of lung SABR based on lesion size, proximity to central structures and dose level/fractionation has been limited by toxicity [5,6]. Legitimate reduction of margins with utilisation of more accurate, real-time motion adaptive, treatment delivery will directly reduce the irradiated volume and potentially toxicity.

For lung lesions, treatment delivery ideally needs to localise and adapt in real-time to account for variable inter- and intra-fraction tumour motion, to remove interplay for dynamic treatment, and to permit high efficiency. Critically, lung SABR planning is typically generated from 4DCT; growing evidence suggests motion at this single time point may not be representative of motion experienced during the short course treatment [7,8].

Real time guidance and adaptation has been clinically applied on specialised robotic and gimballed linear accelerators for lung SABR and both techniques have demonstrated significant reductions in treated volumes [9,10]. Another real-time image guidance and adaption technique, electromagnetic (EM) guided MLC tracking, is expected to match reductions in treated volumes to robotic and gimbal modalities [11,12]. MLC tracking began treating prostate cancer patients in 2013 [13] and demonstrated high fidelity of delivered dose, including dose painting, to moving targets. [14] However, to date MLC tracking has only been used clinically to treat prostate cancer, which exhibits occasional slow motion. In this work we apply MLC tracking to lung cancer, which exhibits constant and complex motion.

We present the first-in-human study to clinically realise the benefits of real time adaptation on a standard linac for lung SABR. We describe our experience with the first patient.

* Corresponding author at: Northern Sydney Cancer Centre, Level 1 Royal North Shore Hospital, Reserve Rd, St Leonards, NSW 2065, Australia.
E-mail address: Jeremy.Booth@health.nsw.gov.au (J.T. Booth).

http://dx.doi.org/10.1016/j.radonc.2016.08.025
0167-8140/© 2016 Elsevier Ireland Ltd. All rights reserved.

Materials and methods

Clinical trial protocol and patients

The Lung Intensity Guided Hypofractionated Tumour tracking SABR (LIGHT SABR) study is a single institution investigator-led Phase I/II clinical trial with full local ethics approval and registration (NCT02514512). The primary endpoint is that 90% of treatments are delivered without MLC tracking related software failures, isolated as failure to deliver treatment with MLC tracking treatment caused directly by malfunction of the MLC tracking software. The trial will recruit 20 patients with stage I NSCLC or 1–3 oligometastases. Patients will be treated with electromagnetic-guided real-time adaptation with MLC tracking utilising Calypso lung transponders (Varian Medical Systems, Palo Alto) to provide the real-time motion signal. The workflow is shown in Fig. 1. The use of in-house MLC tracking software was registered with the Therapeutic Goods Administration in Australia utilising the Clinical Trial Notification system.

MLC tracking with electromagnetic-guidance

Three Calypso lung transponders were implanted one week prior to simulation using standard fiberoptic bronchoscopy with radial endobronchial ultrasound and X-ray image guidance. Transponders were placed as close as possible to the target lesion. Beacon migration and accuracy as a surrogate of lesion position were evaluated prior to treatment in 4DCT and during treatment with CBCT and fluoroscopic imaging. Beacon centroid to lesion centroid in each phase of the 4DCT was measured to describe the relative motion normalised to end of exhale. Surrogacy error was defined as the difference in beacon centroid and tumour centroid position in each phase. Prior to treatment, planning contours for PTV and transponders were overlayed on the CBCT to assess potential migration and alignment. Additionally, fluoroscopic imaging with a field encompassing lesion and transponders was acquired over three breathing cycles at two orthogonal angles prior to treatment for retrospective assessment of tumour/beacon motion with respiration; and fluoroscopic imaging was acquired during treatment for retrospective assessment of tumour motion during treatment.

The planning 4DCT scan was performed using an external surrogate for respiratory motion, Philips bellows (Philips Medical Systems, Cleveland) for 4DCT, with the patient free-breathing and positioned in a BodyFix™ device with arms above head.

Treatment plans were created in the Eclipse planning system (v. 11, Varian Medical Systems, Palo Alto) for a 6 MV dual RapidArc delivery utilising the AAA algorithm. The collimator was angled to align with the major motion axis of the lesion (superior–inferior) and the arcs rotated between 90 and 270 degrees (Varian IEC). Plan complexity was recorded using the modulation complexity score (MCS) which has been shown to correlate with delivery accuracy and can affect tracking performance above a 0.8 threshold [15,16]. Treatment planning was performed for MLC tracking, and for comparison (and back-up in case of MLC tracking failure) a 'conventional' ITV-based plan was also created. MLC tracking plans utilised the end-of-exhale phase as a reference phase to define the $GTV_{Tracking}$, with the CTV defined as being equal to the GTV and a 5 mm CTV to PTV margin. The end-of-exhale phase assures a proper localisation and delineation of the tumour [17–19] while the 5 mm margin has been described in the literature to be sufficient to account for tracking system latency up to 500 ms [20] and differences in tumour sizes and shape during respiration [21]. The exhale phase CT scan is likely to have the fewest imaging artefacts, and having the smallest lung volume, is likely to over- rather than under-estimate the actual lung dose. The conventional plan was established for an ITV derived from the 4DCT which included the GTV in each breathing phase. The ITV was expanded by 5 mm to create the PTV. The conventional plan was calculated on a mean CT image from 4DCT. Both plans met the dose volume criteria of RTOG 0915 [22]. The fractionation scheme was 48 Gy in four fractions delivered to greater than 95% of the PTV.

At treatment sessions the patient was aligned to lasers in the BodyFix device and Philips bellows were attached to record the breathing signal during treatment. For each fraction, CBCT was acquired and a best-fit alignment to the transponders was performed. The PTV structure was then overlaid to confirm tumour coverage based on beacon localisation. The patient was treated with Calypso-guided MLC tracking [23]. We utilise the kernel density estimation prediction algorithm [24] to account for the system's 220 ms latency [13].

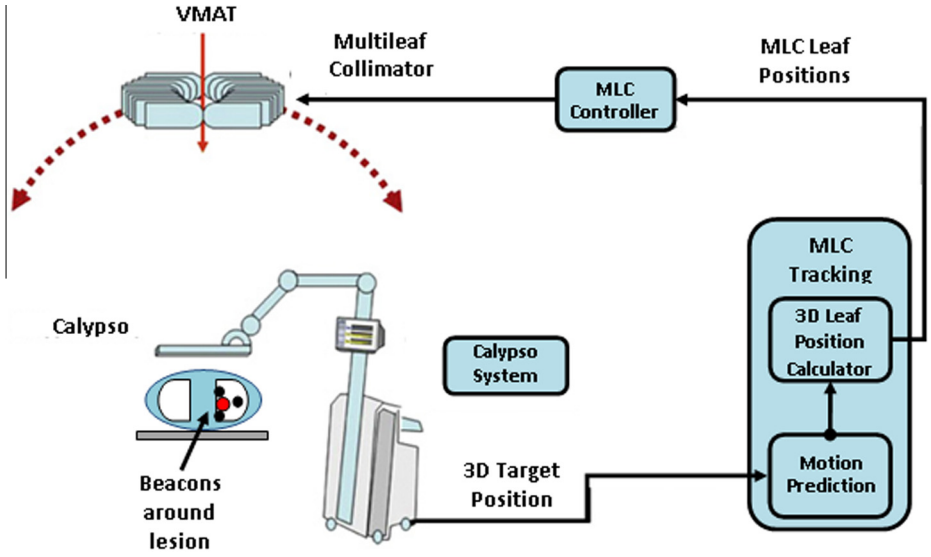

Fig. 1. Schematic of the MLC tracking control system used for the clinical trial. Electromagnetic transponders send real-time localisation to the MLC tracking system which updates the MLC pattern and sends these new leaf positions to the MLC controller for treatment at the linac.

Quality assurance (QA) regime

Quality assurance before, during and after treatment is essential, particularly with research software controlling the treatment unit. Standard quality assurance measures for SABR treatment were utilised including secondary monitor units check and fluence delivery [25]. Further quality measures, based on Failure Mode and Effects Analysis [26] and broad discussion with international thought leaders on MLC tracking safety, were implemented. These extra measures included:

- MLC tracking patient-specific QA incorporating review of over- and under-dose areas of patient plan with patient-specific motion [27],
- Checklist applied to additional MLC tracking-specific workflow steps,
- Pre-treatment delivery to a Delta4 phantom (ScandiDos, Sweden) with and without motion (patient-specific with HexaMotion (Scandidos, Sweden)),
- Pre-treatment fluoroscopy to interrogate Calypso beacon motion migration and surrogacy to tumour, and post-treatment dose reconstruction [28,29].

MLC tracking errors were reported using the areas of under- and over-dose (A_u and A_o respectively) between the plan and delivery, as developed by Poulsen[29]. The under- and over-dose areas have been shown to correlate with dose delivery errors and clearly articulate the contribution of leaf adjustment error, leaf fitting, and target localisation to the MLC tracking performance. Treatment log files including MLC motion, Calypso trajectories, kV and MV images and Philips bellows motion were recorded.

Dose reconstruction is a critical step as delivered dose for real-time adaptation will ultimately depend on the motion encountered. An isocentre shift method was utilised for volumes assumed to move with transponders (GTV and lung). The isocentre shift method considers each arc as many sub arcs each with isocentre shifted (in 2 mm bins) to mimic the motion. Treatment log files and the transponder trajectories were utilised to create a motion encoded treatment plan that was calculated in the planning system. Dose reconstruction was performed for spine and heart volumes assuming they were static. Reconstruction of the delivered conventional plan was performed for comparison. Delivery of the conventional plan assumed pre-treatment patient alignment and utilised treatment log files acquired in a dummy delivery and transponder motion from treatment sessions. The tracking plan was reconstructed on the end exhale phase CT while the conventional plan was reconstructed on the average CT. End-exhale GTV is used for both cases. For the reconstruction of the conventional plan, use of an average CT had <1% difference to calculation on the end exhale scan for this plan, which agrees with previous reports justifying dose calculation on average CT from 4DCT [30].

Results

We present data from the first patient treatment on 30th October 2015; an 80 y/o male with a single metastasis in the left lower lobe. He was positioned on his right side in a BodyFix bag due to the posterior distance to transponders from anterior chest wall preventing supine treatment (our normal setup) and patient performance preventing prone treatment. The internal peak to peak motion of the lesion at 4DCT was 10.8 mm, 4.8 mm, and 3.2 mm in the superior–inferior (SI), left–right (LR) and anterior–posterior (AP) directions, respectively. The surrogate accuracy of the transponder centroid to the GTV centre determined in each phase of the 4DCT showed mean discrepancies of 1.2 mm, 0.6 mm and 0.94 mm in the superior–inferior, lateral and anterior–posterior directions, respectively. Image artefacts in the 4DCT contributed to uncertainty in the determination of the surrogacy error; the beacon and GTV shape and size varied across the 10 breathing phases.

The plan complexity for each plan was within acceptable range (<0.8) with MCS of 0.06 for the MLC tracking plan and 0.21–0.28 for the conventional ITV-based plan. The MLC tracking errors were minimal for delivery of the MLC tracking plan with mean A_uA_o of

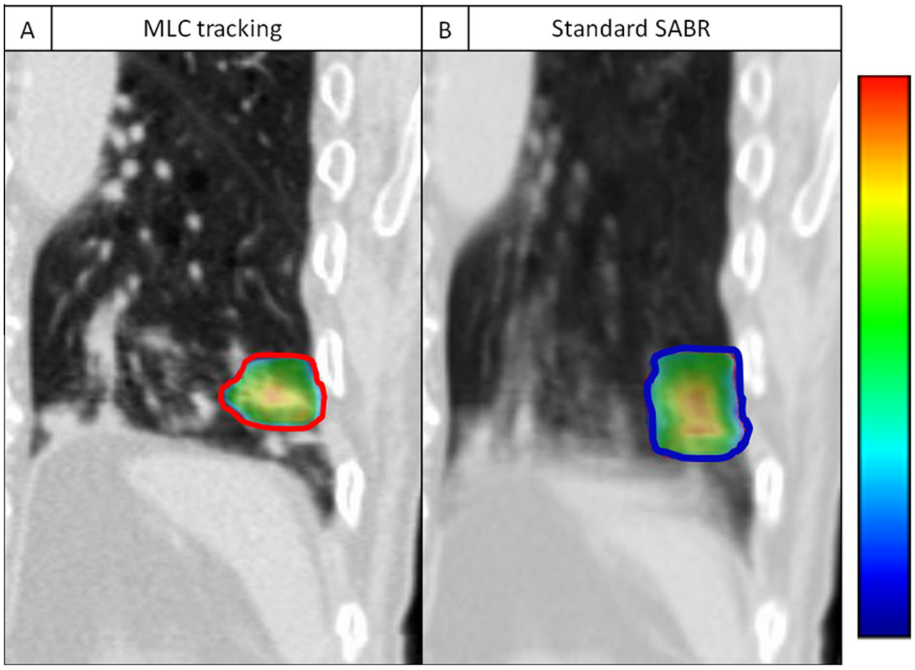

Fig. 2. Comparison of Planning Target Volumes shows a significant reduction (41%) in the volume with MLC tracking delivery (A) compared to standard ITV-based planning (B). The red contour indicates the PTV on end exhale phase of 4DCT used for MLC tracking and the blue contour indicates the PTV on mean of 4DCT used for the ITV-based plan. Coronal view.

2.26 cm^2 attributed to leaf adjustment (2.09cm^2), leaf-fitting (0.43cm^2 for arc 1 and 0.62cm^2 for arc2) and target localisation error (0.62cm^2 for arc 1 and 0.93cm^2 for arc2).

The $PTV_{Tracking}$ was 18.7 cc, 41% smaller than the PTV for standard planning (29.8 cc) (Fig. 2). Targeting a smaller PTV translated to lower normal lung doses for this patient, with mean lung dose reduced by 31% or 0.6 Gy, V20 reduced by 35% or 48 cm^3 and V5 reduced by 9% or 50 cm^3. Dose maximum (D2%) reported to the spine was reduced from 5.1 to 3.8 Gy (33%). Plans had equivalent dose coverage for their respective PTV volumes.

Treatments had an average appointment time of 90 min. A significant proportion of time was allocated to ensuring correct patient rotation due to the beacon centroid being offset from tumour and patient being positioned in the lateral decubitus position. Transponders were located 2.5, 2.1 and 2.5 cm from the lesion edge, all anterior and lateral. Through the four treatment fractions, the internal motion of the transponders ranged between 15.0–16.5 mm, 3.4–3.7 mm, and 3.1–3.3 mm, in the SI, LR, and AP directions respectively, demonstrating substantially larger superior–inferior motion extent compared to simulation (Fig. 3). Fig. 3 shows motion of the transponders during treatment to be larger than the ITV (motion observed during 4DCT) 22%, 32% and 31% of the time, in the SI, LR and AP directions respectively. Motion extending outside the PTV, a 5 mm expansion of the ITV, occurred during treatment 2%, 1% and 2% of the time, in the CC, LR and AP directions respectively. Critically, this infers that a geometric miss would have occurred if ITV-based treatment would have been delivered with only pre-treatment imaging. Furthermore, the components of the PTV margin expansion to account for inter-observer contouring variability, surrogacy accuracy and sub-clinical tumour growth, were utilised in full to account for tumour motion variation. Conventionally, SABR delivery does not deploy intra-treatment tumour monitoring so any geometric miss would have been undiscovered.

The motion of the lesion and transponders with respiration captured in kV and MV images is shown in Fig. 4. A video of the kV and MV images acquired during treatment is provided as Supplementary material.

Fig. 5 shows the delivered dose reconstructed onto the respective planning CT datasets over the four days of treatment for MLC tracking delivery and the conventional ITV-based plan. The planned dose to the GTV is equivalent between MLC tracking and no tracking. However the delivered doses for no tracking are lower than that planned: the mean GTV D95 across fractions is 106 ± 2% (range 103–108%) compared to 110% planned. This difference occurred due to the systematically larger motion experienced with this patient during treatment compared to simulation. The MLC tracking delivery provided mean GTV D95 doses of 110 ± 0.5% (range 109–110%) compared to 111% planned. Fig. 5 demonstrates modest decreases in lung and heart doses and improved target coverage relative to the conventional plan. The MLC tracking delivery was also more reproducible (lower range of mean GTV D95 values) than the standard SABR delivery across fractions.

Discussion

This paper reports on the first patient treatment with real-time adaptive treatment for lung cancer with MLC tracking. MLC tracking radiotherapy has previously been delivered to 28 prostate patients with 858 successful treatment fractions. MLC tracking for lung SABR is more complicated than prostate MLC tracking: respiratory motion is larger, more frequent and faster than prostate motion, SABR delivering larger dose per fraction, and there is an increased importance of system latency mitigation with the use

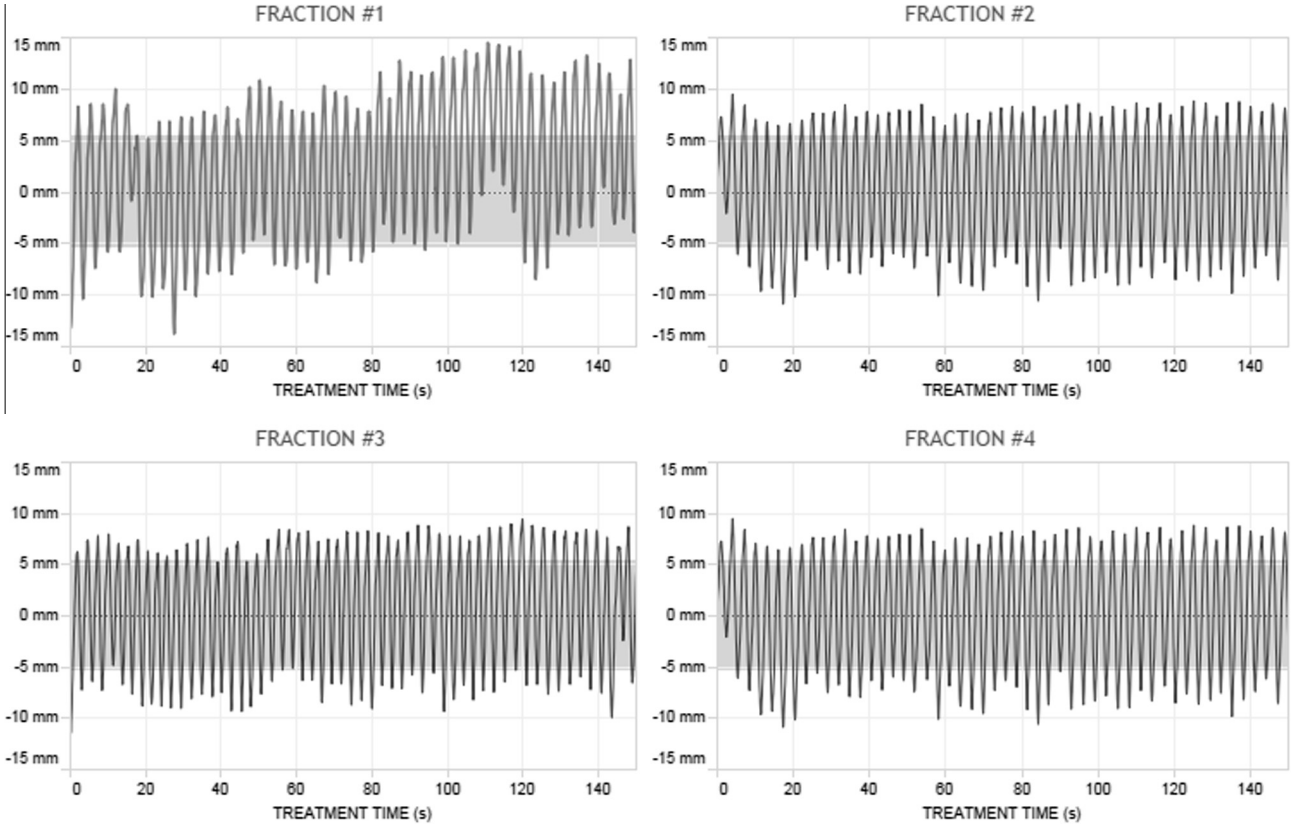

Fig. 3. Superior–inferior motion of the lung tumour (positive values represent motion in superior direction) for each of the four treatment fractions. The motion during 4DCT used to create the ITV of 10.8 mm is shown as a grey band in each plot. The tumour motion for all fractions was larger than that than expected from planning.

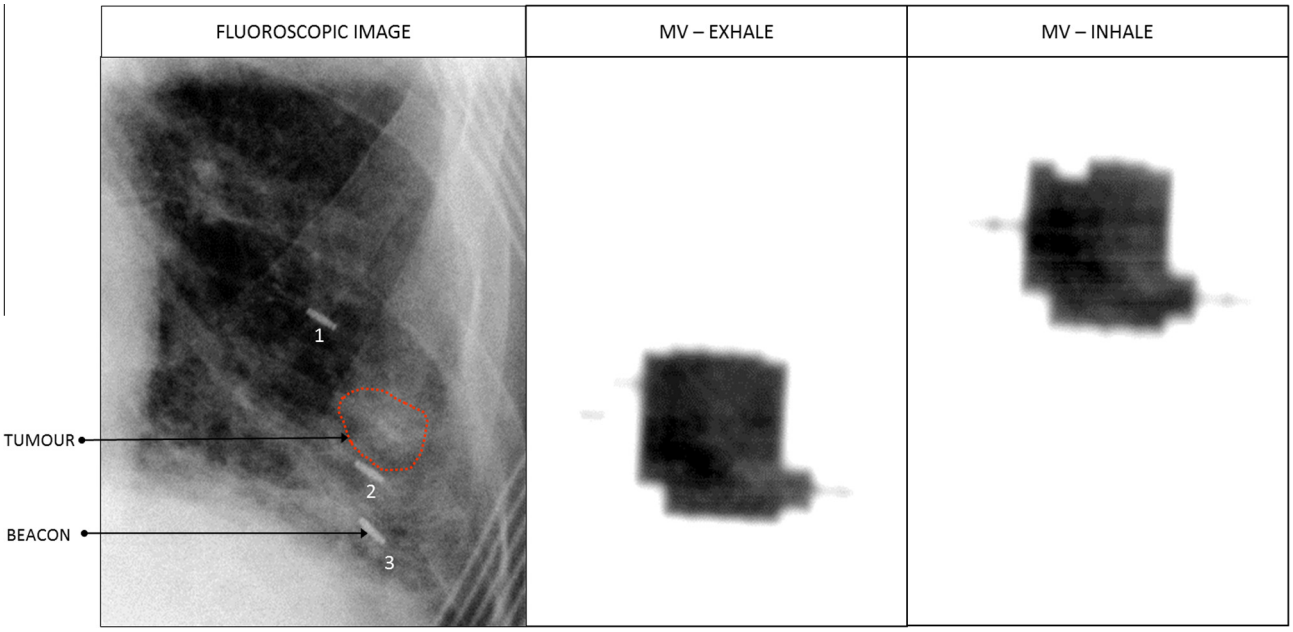

Fig. 4. Fluoroscopic image (left) showing three electromagnetic transponders and the tumour contour, and corresponding MV treatment images at inhale and exhale (right). A movie of the kV and MV images acquired during the treatment delivery is attached as supplementary material.

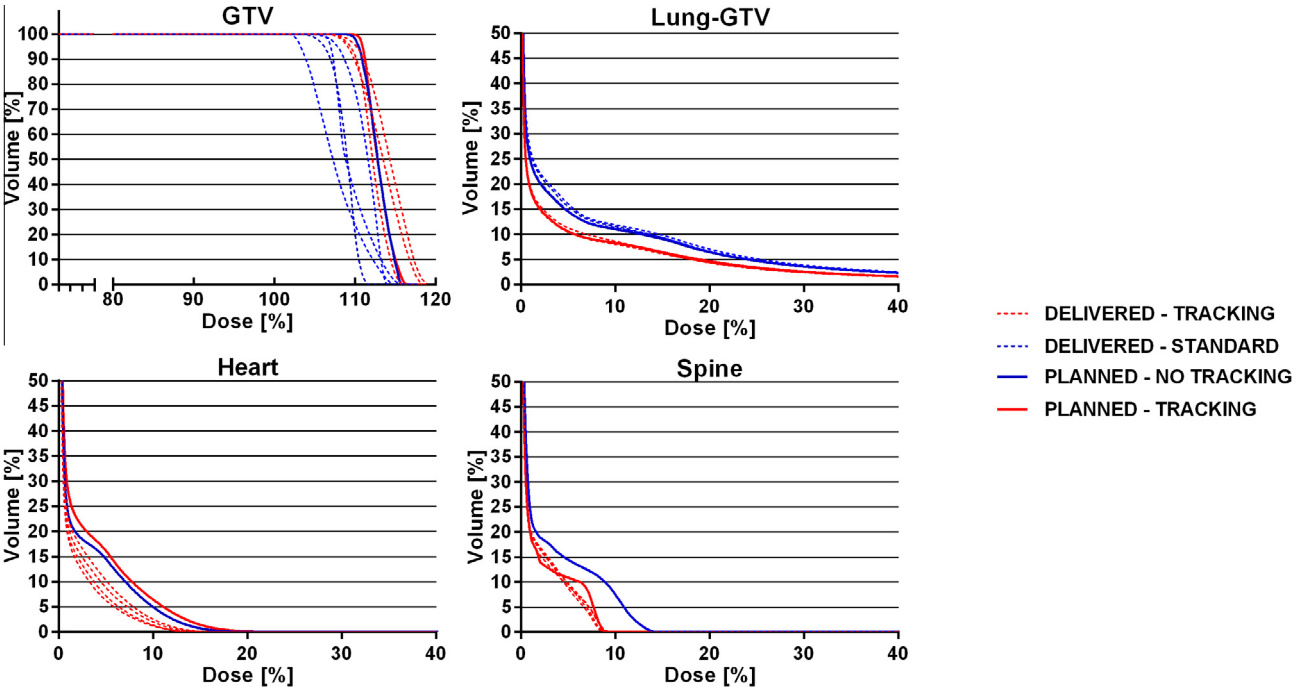

Fig. 5. Reconstructed delivered dose for the all fractions of the MLC tracking lung SABR patient showing delivered dose to target is maintained from planning and OAR dose is reduced for this patient. Dashed lines = dose for individual fractions; solid lines = planned dose for the treatment course.

of a prediction algorithm. The clinical issues are also different for lung SABR compared to prostate radiotherapy, with use of ITV based planning, baseline shifts of tumour position during respiration, irregular internal motion and inhomogeneity.

The patient in this study benefited from real-time adaptive treatment with a 41% smaller target volume, which is comparable to that reported for adaptive delivery with robotic and gimbal devices [11,12]. The extent of motion was significantly larger at treatment compared to that seen during 4DCT acquisition. For the conventional ITV-based plan, motion exceeded the ITV ~30% of the time. For this case the PTV expansion of 5 mm has ensured coverage of the target is retained ~98% of the time. However, the PTV expansion of 5 mm is derived to account for up to 5 mm inter-observer contouring variability, sub-clinical tumour extension and the measured 1-3 mm of surrogacy uncertainty with the beacon transponders.

Internal peak to peak transponder motion for this patient was significantly larger than the motion amplitude determined from simulation 4DCT. We believe that this is due to the sampling that occurs with standard 4DCT reconstruction, which score peak

exhale and inhale minimally based on the short time in these positions, compared to the transponder locations during treatment which are reported 20 times per second.

The impact of MLC tracking will depend on the extent of tumour motion and patients with larger tumour motion will benefit from larger reductions in target volume and subsequent reductions in organ at risk doses. Even modest reduction of lung dose in absolute terms will benefit planning to isotoxic tolerances in the oligometastatic setting or for subsequent lesions. Furthermore, all patients potentially benefit if a baseline shift occurs from the gating enacted when the tumour moves outside the motion limits obtained from simulation. A similar level of dose coverage would have been achieved with a pure gating strategy; however, the efficiency of MLC tracking delivery is superior to gating strategies where a duty cycle of 30% is not uncommon. It should be noted however that introduction of flattening filter free delivery has reduced irradiation times, potentially improving the efficiency of gated treatments.

MLC tracking is highly accessible as it requires only two key components; real-time target guidance and a multi-leaf collimator. The great majority of linear accelerators currently sold now have the MLC. This study utilised real time target guidance from electromagnetic transponders as they are a proven robust position signal, but localisation could equally be derived from other methods such as X-ray fluoroscopy, real-time magnetic resonance imaging, or external surrogates. The electromagnetic transponders provide an internal surrogate of the tumour and their location will affect the accuracy of their surrogate motion. Further research is directed towards markerless MLC tracking that would not require implantation of transponders, a potential source of toxicity, replaced with direct (image-based) tracking [31–34].

Reporting delivered dose poses some challenges to classical application of the ICRU volumes for MLC tracking. In real-time adaptive radiotherapy, the $PTV_{Tracking}$ can be considered time-resolved with its components defined in each respiratory phase to account for treatment uncertainty; in our implementation the PTV is equivalent across respiratory phases. This is contrasted to the PTV for conventional ITV-based planning, which should be defined in the classical way and is difficult to compare directly to $PTV_{Tracking}$. The more important metric is GTV coverage, which is maintained in this case. The PTV is a geometric tool to ensure GTV coverage, and for meaningful application with real-time adaptive treatment will require further data to development tolerances.

Clinical translational relevance

An emerging treatment delivery technology, MLC tracking has been translated in the clinic and used for real time adaptive radiotherapy with lung SABR for the first time. MLC tracking for real time adaptation with a standard linear accelerator improves target dose coverage, reduces organ at risk doses and is potentially highly accessible requiring only software change to be implemented on a modern linear accelerator.

Conflicts of interest

PJK is an inventor on the awarded US patents 7,469,035 and 8,971,489 that are related to MLC tracking. This work is supported by a Varian Medical Systems Collaborative Research Grant.

Acknowledgements

This work is supported by a Varian Medical Systems Collaborative Research Grant. PJK is supported by an NHMRC Senior Professorial Research Fellowship.

Appendix A. Supplementary data

Supplementary data associated with this article can be found, in the online version, at http://dx.doi.org/10.1016/j.radonc.2016.08.025.

References

[1] Borst GR, Ishikawa M, Nijkamp J, Hauptmann M, Shirato H, Bengua G, et al. Radiation pneumonitis after hypofractionated radiotherapy: evaluation of the LQ (L) model and different dose parameters. Int J Radiat Oncol Biol Phys 2010;77:1596–603.
[2] Guckenberger M, Baier K, Polat B, Richter A, Krieger T, Wilbert J, et al. Dose–response relationship for radiation-induced pneumonitis after pulmonary stereotactic body radiotherapy. Radiother Oncol 2010;97:65–70.
[3] Timmerman R, Paulus R, Galvin J, Michalski J, Straube W, Bradley J, et al. Stereotactic body radiation therapy for inoperable early stage lung cancer. JAMA 2010;303:1070–6.
[4] Chang JY, Senan S, Paul MA, Mehran RJ, Louie AV, Balter P, et al. Stereotactic ablative radiotherapy versus lobectomy for operable stage I non-small-cell lung cancer: a pooled analysis of two randomised trials. Lancet Oncol 2015;16:630–7.
[5] Lo S, Sahgal A, Chang E, Mayr N, Teh B, Huang Z, et al. Serious complications associated with stereotactic ablative radiotherapy and strategies to mitigate the risk. Clin Oncol 2013;25:378–87.
[6] Lagerwaard FJ, Verstegen NE, Haasbeek CJ, Slotman BJ, Paul MA, Smit EF, et al. Outcomes of stereotactic ablative radiotherapy in patients with potentially operable stage I non-small cell lung cancer. Int J Radiat Oncol Biol Phys 2012;83:348–53.
[7] Purdie TG, Moseley DJ, Bissonnette J-P, Sharpe MB, Franks K, Bezjak A, et al. Respiration correlated cone-beam computed tomography and 4DCT for evaluating target motion in stereotactic lung radiation therapy. Acta Oncol 2006;45:915–22.
[8] Rietzel E, Chen GT, Choi NC, Willet CG. Four-dimensional image-based treatment planning: target volume segmentation and dose calculation in the presence of respiratory motion. Int J Radiat Oncol Biol Phys 2005;61:1535–50.
[9] Matsuo Y, Shibuya K, Nakamura M, Narabayashi M, Sakanaka K, Ueki N, et al. Dose–volume metrics associated with radiation pneumonitis after stereotactic body radiation therapy for lung cancer. Int J Radiat Oncol Biol Phys 2012;83:e545–9.
[10] Hoogeman M, Prévost J-B, Nuyttens J, Pöll J, Levendag P, Heijmen B. Clinical accuracy of the respiratory tumor tracking system of the cyberknife: assessment by analysis of log files. Int J Radiat Oncol Biol Phys 2009;74:297–303.
[11] Calliet V, Hardcastle N, Szymura K, Haddad C, Keall PJ, Booth JT. Justification of MLC tracking for lung SABR. Wellington, New Zealand: Engineering and Physical Sciences in Medicine; 2015.
[12] Suh Y, Sawant A, Venkat R, Keall PJ. Four-dimensional IMRT treatment planning using a DMLC motion-tracking algorithm. Phys Med Biol 2009;54:3821.
[13] Keall PJ, Colvill E, O'Brien R, Ng JA, Poulsen PR, Eade T, et al. The first clinical implementation of electromagnetic transponder-guided MLC tracking. Med Phys 2014;41:020702.
[14] Colvill E, Booth JT, O'Brien R, Eade TN, Kneebone AB, Poulsen PR, et al. MLC tracking improves dose delivery for prostate cancer radiotherapy: results of the first clinical trial. Int J Radiat Oncol Biol Phys 2015.
[15] Pommer T, Falk M, Poulsen PR, Keall PJ, O'Brien RT, Rosenschöld PM. The impact of leaf width and plan complexity on DMLC tracking of prostate intensity modulated arc therapy. Med Phys 2013;40:111717.
[16] McGarry CK, Agnew CE, Hussein M, Tsang Y, McWilliam A, Hounsell AR, et al. The role of complexity metrics in a multi-institutional dosimetry audit of VMAT. Br J Radiol 2016;89:20150445.
[17] Berbeco RI, Nishioka S, Shirato H, Chen GT, Jiang SB. Residual motion of lung tumours in gated radiotherapy with external respiratory surrogates. Phys Med Biol 2005;50:3655.
[18] Depuydt T, Poels K, Verellen D, Engels B, Collen C, Buleteanu M, et al. Treating patients with real-time tumor tracking using the Vero gimbaled linac system: implementation and first review. Radiother Oncol 2014;112:343–51.
[19] Persson GF, Nygaard DE, Hollensen C, Rosenschöld PM, Mouritsen LS, Due AK, et al. Interobserver delineation variation in lung tumour stereotactic body radiotherapy. Br J Radiol 2014;85:e654–60.
[20] Bedford JL, Fast MF, Nill S, McDonald FM, Ahmed M, Hansen VN, et al. Effect of MLC tracking latency on conformal volumetric modulated arc therapy (VMAT) plans in 4D stereotactic lung treatment. Radiother Oncol 2015;117:491–5.
[21] Senthi S, Dahele M, Slotman BJ, Senan S. Investigating strategies to reduce toxicity in stereotactic ablative radiotherapy for central lung tumors. Acta Oncol 2014;53:330–5.
[22] Group RTO. RTOG 0915. A Randomized Phase II Study Comparing 2 Stereotactic Body Radiation Therapy (SBRT) Schedules for Medically Inoperable Patients with Stage I Peripheral Non-Small Cell Lung Cancer. Philadelphia (PA): RTOG; 2009.
[23] Keall PJ, Sawant A, Cho B, Ruan D, Wu J, Poulsen P, et al. Electromagnetic-guided dynamic multileaf collimator tracking enables motion management for intensity-modulated arc therapy. Int J Radiat Oncol Biol Phys 2011;79:312–20.

[24] Ruan D, Keall P. Online prediction of respiratory motion: multidimensional processing with low-dimensional feature learning. Phys Med Biol 2010;55:3011.
[25] Siva S, Kirby K, Caine H, Pham D, Kron T, Te Marvelde L, et al. Comparison of single-fraction and multi-fraction stereotactic radiotherapy for patients with 18 F-fluorodeoxyglucose positron emission tomography-staged pulmonary oligometastases. Clin Oncol 2015;27:353–61.
[26] Sawant A, Dieterich S, Svatos M, Keall P. Failure mode and effect analysis-based quality assurance for dynamic MLC tracking systems. Med Phys 2010;37:6466–79.
[27] Poulsen PR, Fledelius W, Cho B, Keall P. Image-based dynamic multileaf collimator tracking of moving targets during intensity-modulated arc therapy. Int J Radiat Oncol Biol Phys 2012;83:e265–71.
[28] Schmidt ML, Hoffmann L, Kandi M, Møller DS, Poulsen PR. Dosimetric impact of respiratory motion, interfraction baseline shifts, and anatomical changes in radiotherapy of non-small cell lung cancer. Acta Oncol 2013;52:1490–6.
[29] Poulsen PR, Schmidt ML, Keall P, Worm ES, Fledelius W, Hoffmann L. A method of dose reconstruction for moving targets compatible with dynamic treatments. Med Phys 2012;39:6237–46.
[30] Glide-Hurst CK, Hugo GD, Liang J, Yan D. A simplified method of four-dimensional dose accumulation using the mean patient density representation. Med Phys 2008;35:5269–77.
[31] Shieh C-C, Keall PJ, Kuncic Z, Huang C-Y, Feain I. Markerless tumor tracking using short kilovoltage imaging arcs for lung image-guided radiotherapy. Phys Med Biol 2015;60:9437.
[32] Rottmann J, Keall P, Berbeco R. Markerless EPID image guided dynamic multi-leaf collimator tracking for lung tumors. Phys Med Biol 2013;58:4195.
[33] Poulsen PR, Cho B, Sawant A, Ruan D, Keall PJ. Dynamic MLC tracking of moving targets with a single kV imager for 3D conformal and IMRT treatments. Acta Oncol 2010;49:1092–100.
[34] Cho B, Poulsen PR, Sloutsky A, Sawant A, Keall PJ. First demonstration of combined kV/MV image-guided real-time dynamic multileaf-collimator target tracking. Int J Radiat Oncol Biol Phys 2009;74:859–67.

APPENDIX 02

Statement of Authors' contribution

Chapter 3 is a review article for which I am the primary author and is published as:
Caillet, Vincent, Jeremy T. Booth, and Paul Keall. "IGRT and motion management during lung SBRT delivery." *Physica Medica* 44 (2017): 113-122.

Review of the literature, drafting of the manuscript and revisions were conducted by V. Caillet. J. Booth and P. Keall provided input and feedback into the preparation of the manuscript and revisions for submission to the editors.

As supervisor for the candidature upon which this thesis is based, I can confirm that the authorship attribution statements above are correct.

Paul Keall 29/09/2020

Chapter 4 is a peer-reviewed paper for which I am the primary author and is published as:
Caillet, Vincent, Paul J. Keall, Emma Colvill, Nicholas Hardcastle, Ricky O'Brien, Kathryn Szymura, and Jeremy T. Booth. "MLC tracking for lung SABR reduces planning target volumes and dose to organs at risk." *Radiotherapy and Oncology* 124, no. 1 (2017): 18-24.

V. Caillet, J. Booth and P. Keall designed the study. V. Caillet performed the data creation and analysis. R. O'Brien supplied code and expert input into design of the study and software development. E. Colvill helped directing the experiments. N. Hardcastle and K. Szymura provided expert clinical input. The drafting of the manuscript and revisions were conducted by V. Caillet. All authors provided input and feedback into the preparation of the manuscript and revisions for journal submission.

In addition to the statements above, since I am not the corresponding author of this publication, permission to include the published material has been granted by the corresponding author J. Booth.

Vincent Caillet, 28th of September 2020

As supervisor for the candidature upon which this thesis is based, I can confirm that the authorship attribution statements above are correct.

Paul Keall 29/09/2020

Chapter 5 is a peer-reviewed paper for which I am the primary author and is published as:
Caillet, Vincent, Benjamin Zwan, Adam Briggs, Nicholas Hardcastle, Kathryn Szymura, Alexander Podreka, Ricky T O'Brien et al. "Geometric uncertainty analysis of MLC tracking for lung SABR." *Physics in Medicine & Biology* (2020).

Clinical trial design was conducted by P. Keall, J. Booth, T. Eade, V. Caillet, R. O'Brien, N. Hardcastle, A. Briggs, D. Jayamanne, C. Haddad and B. Harris. R. O'Brien supplied code and expert input into software development. V. Caillet, A. Briggs and N. Hardcastle contributed to software and interface development and performed the quality assurance procedures, data collection and analysis for the clinical trial. B. Swan and P. Greer provided input into the algorithm used to compute beam-to-target uncertainty. A. Prodreka, N. Hardcastle and K. Szymura provided expert clinical input.

The drafting of the manuscript and revisions were conducted by V. Caillet, P. Keall and J. Booth. All authors provided input and feedback into the preparation of the manuscript and revisions for journal submission.

As supervisor for the candidature upon which this thesis is based, I can confirm that the authorship attribution statements above are correct.

Paul Keall 29/09/2020

Chapter 6 is a peer-reviewed paper for which I am the primary author and is published as:
Caillet, Vincent, Ricky O'Brien, Douglas Moore, Per Poulsen, Tobias Pommer, Emma Colvill, Amit Sawant, Jeremy Booth, and Paul Keall. "*In silico* and experimental evaluation of two leaf-fitting algorithms for MLC tracking based on exposure error and plan complexity." *Medical physics* 46, no. 4 (2019): 1814-1820.

V. Caillet, J. Booth and P. Keall designed the study. V. Caillet performed the data creation and analysis using a modified code supplied by P. Poulsen. R. O'Brien supplied code and expert input into software development. A. Sawant and D. Moore supplied the second MLC tracking algorithm tested in the platform. T. Pommer supplied a code used to compute plan complexity. The drafting of the manuscript and revisions were conducted by V. Caillet. All authors provided input and feedback into the preparation of the manuscript and revisions for journal submission.

As supervisor for the candidature upon which this thesis is based, I can confirm that the authorship attribution statements above are correct.

Paul Keall 29/09/2020

Appendix 1 is a peer-reviewed paper for which I am the secondary author and is published as:
Booth, Jeremy, **Vincent Caillet**, Nicholas Hardcastle, Ricky O'Brien, Kathryn Szymura, Charlene Crasta, Benjamin Harris, Carol Haddad, Thomas Eade, and Paul J. Keall. "The first patient treatment of electromagnetic-guided real time adaptive radiotherapy using MLC tracking for lung SABR." *Radiotherapy and Oncology* 121, no. 1 (2016): 19-25.

P. Keall, J. Booth, T. Eade, V. Caillet, C. Haddad, B. Harris designed the study. V. Caillet performed the data creation and analysis. R. O'Brien supplied code and expert input into design of the study and software development. C. Crasta, N. Hardcastle and K. Szymura provided expert clinical input. The drafting of the manuscript and revisions were conducted by J. Booth. All authors provided input and feedback into the preparation of the manuscript and revisions for journal submission.

In addition to the statements above, since I am not the corresponding author of this publication, permission to include the published material has been granted by the corresponding author J. Booth

Vincent Caillet, 28th of September 2020

As supervisor for the candidature upon which this thesis is based, I can confirm that the authorship attribution statements above are correct.

Paul Keall 29/09/2020

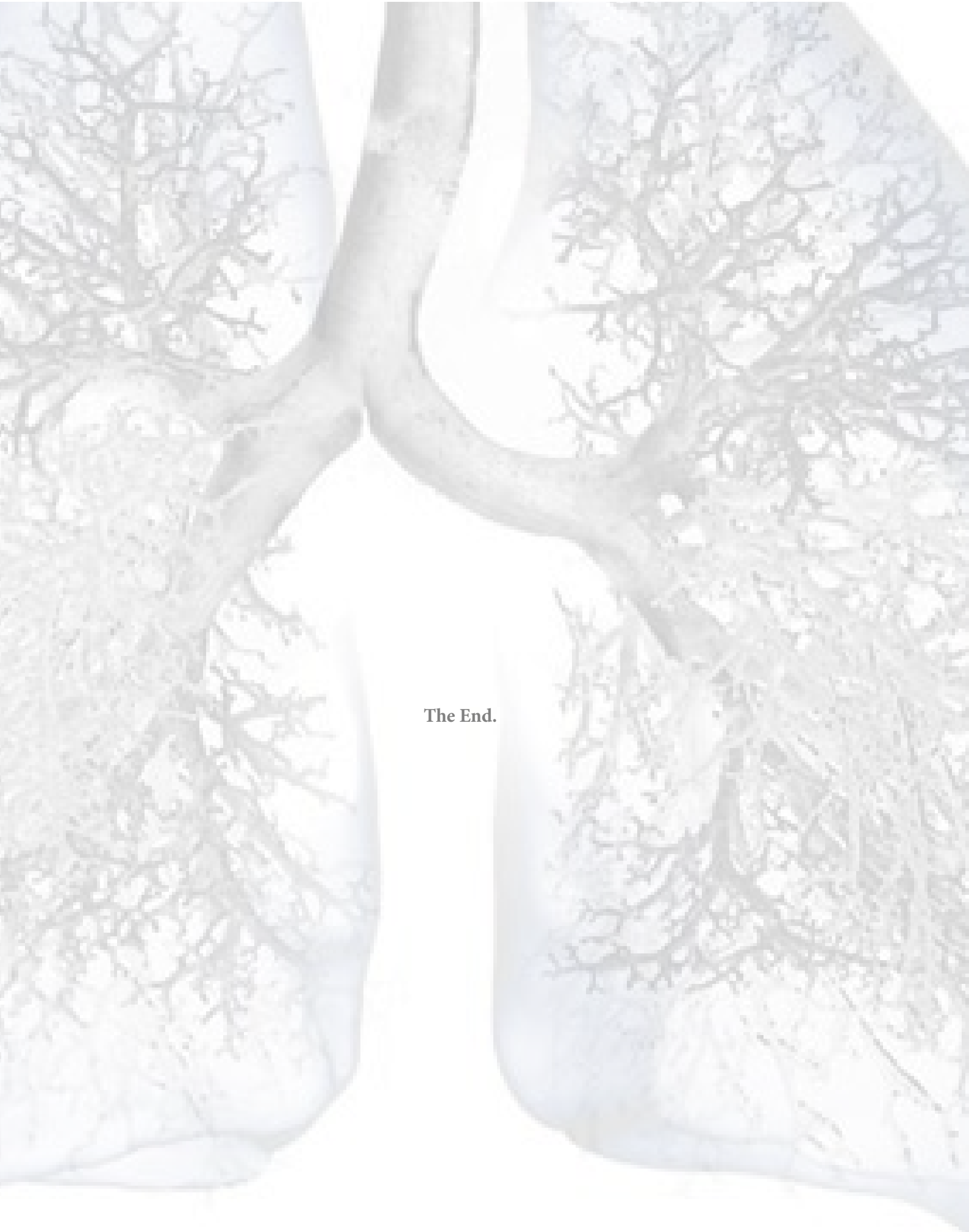

The End.